Evanescent Electromagnetic Fields

Evanescent fields can be observed, when electromagnetic fields, impinging onto the surface of an optically thinner medium, are totally reflected into the optically thicker medium (total internal reflection). The evanescent fields are penetrating into the thinner medium with exponentially decreasing intensity. It will be demonstrated in this circular that a complete description of the evanescent fields can be achieved within the framework of Maxwell's theory. No "new physics" are required. Furthermore Snellius' law of refraction, the Fresnel-coefficients, and the phase shifts of all fields for arbitrary under- and overcritical angles of incidence will be derived. Using the Stokes relations, explicit formulas for the frustrated total internal reflection (FTIR) are computed.

Contents

1. Introduction 2
2. Observations of evanescent fields 4
3. Law of refraction, and critical angle 7
4. Fresnel-coefficients and phase angles 24
5. Multilayer stacks and FTIR 57
References 84

1. Introduction

When electromagnetic radiation, coming in from a transparent medium with refractive index n_a, is impinging under the angle ϑ_e onto the plain surface of another medium with refractive index n_b, then it will in general be partly refracted under the angle ϑ_b into the medium b, and partly reflected under the angle ϑ_r into the medium a, see fig. 1.

Snellius' law of refraction, which is stating the relation between the angles and the refractive indices, is well-known since the early 17$^{\text{th}}$ century:

$$\vartheta_r = \vartheta_e \tag{1a}$$

$$n_a \sin\vartheta_e = n_b \sin\vartheta_b \tag{1b}$$

Two centuries later, Fresnel presented precise formulas for the amplitudes of the refracted and the reflected radiation. In sections 3 and 4 we will derive both Snellius' law of refraction and Fresnel's formulas from Maxwell's equations.

Real solutions of Snellius' law of refraction are existing only for

$$\frac{n_a}{n_b} \sin\vartheta_e = \sin\vartheta_b \leq 1 \ . \tag{2}$$

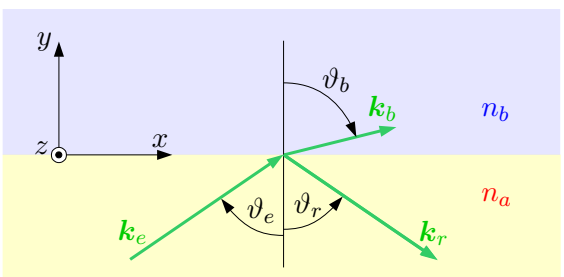

Fig. 1 : Angles and coordinates

If $n_a > n_b$, then this condition is not met for sufficiently large incoming angles $\vartheta_e < \pi/2$. The angle

$$\vartheta_{e,\text{critical}} = \arcsin\left(\frac{n_b}{n_a}\right) \tag{3}$$

is called the critical angle. If radiation is coming in under an angle $\vartheta_e > \vartheta_{e,\text{critical}}$, then — according to experience — it is reflected totally back into the medium a.

Surprisingly, even in case of over-critical incoming angles, the electromagnetic fields in medium b are not zero. Instead their intensity is decreasing only exponentially with the distance from the boundary surface. These exponentially decreasing fields in medium b are called "evanescent fields". Experimental evidence for the existence of evanescent fields will be presented in section 2.

From fig. 1 one can read $k_{b,y} = k_b \cos\vartheta_b$. That sketch, however, is a description of the case of under-critical incoming angles only. It's impossible to display the angle ϑ_b in a similar sketch for the case $\vartheta_e > \vartheta_{e,\text{critical}}$. The derivations of the theoretical description of evanescent fields in the two leading textbooks on classical optics and electrodynamics, namely Born and Wolf [1], and Jackson [2], and — following them — the derivations in all other textbooks known to me are — without proof! — based on the assumption, that both the relation $k_{b,y} = k_b \cos\vartheta_b$ and the law of refraction (1b) are valid for over-critical incoming angles as well. Then, because of $\sin\vartheta_b > 1$, the angle $\vartheta_b \in \mathbb{C}$ must be complex, and consequently $k_{b,y}$ must be complex.

While the law of refraction for under-critical incoming angles is derived from Maxwell's equations, the complex angles of refraction are introduced at this point in the literature ad-hoc and with no theoretical justification, and therefore are quite mysterious. The results are of cause confirmed by experimental observations, but it is remaining unclear whether the theory of evanescent fields can

be completely accomplished within the framework of Maxwell's electrodynamics, or whether at some point "new physics" are required.

To me it seems much more "natural", first to prove that the ansatz

$$\boldsymbol{E}(t,\boldsymbol{r}) = \hat{\boldsymbol{E}} e^{i(\boldsymbol{k}\cdot\boldsymbol{r}-\omega t+\varphi_E)} \tag{4a}$$

$$\boldsymbol{B}(t,\boldsymbol{r}) = \hat{\boldsymbol{B}} e^{i(\boldsymbol{k}\cdot\boldsymbol{r}-\omega t+\varphi_B)} \tag{4b}$$

can describe both plain waves and evanescent fields, provided that the wave-vector $\boldsymbol{k}$ may be complex. Then one *can* in a second step introduce complex angles, to achieve a most simple formalism. But the complex angles are not essential for our description; only the complex wave-vectors are indispensable. Waves with complex wave-vectors are well known as exponentially damped waves, and can easily be visualized — in contrast to complex angles.

2. Observations of evanescent fields

If an electromagnetic wave, coming in from an optically thicker medium a, is impinging under the angle $\vartheta_e > \vartheta_{e,\text{critical}}$ onto the surface of an optically thinner medium b, then it is totally reflected. Still that wave penetrates a little bit (quantitative statements will follow immediately) into the medium b, before it returns into the medium a. This fact is proofed mainly by two types of observations: The "frustrated total internal reflection"(FTIR), and the Goos-Hänchen shift.

FTIR is known since centuries, already Newton mentioned it in the "Opticks" [3, Second Book, Part I, Observation 1]. To observe FTIR, often an experimental setup as displayed in the left sketch of fig. 2 on the following page is used. An electromagnetic wave is impinging under an angle of 45° from inside onto the hypotenuse

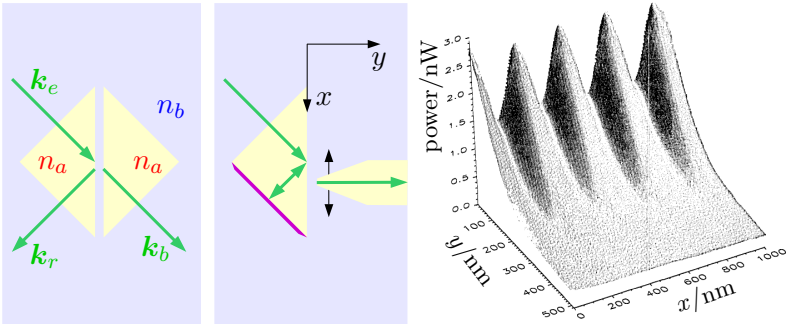

Fig. 2 : Frustrated total internal reflection

of an isosceles prism. The wave is totally reflected, if $n_a > n_b$ and $\vartheta_{e,\text{critical}} < 45°$. But if a second prism is placed at a distance of less than approximately one wavelength between the two hypotenuses, then a small part of the incoming power can be detected as a transmitted wave with wave-number $\boldsymbol{k}_b = \boldsymbol{k}_e$ at the opposite side of the apparatus.

A modern experiment of Meixner et. al. [4] for the observation of this effect is sketched in the middle picture of fig. 2. The incoming electromagnetic wave is the radiation of an argon laser (wavelength 514.5 nm in air). The material b is air ($n_b = 1.000$), and the prism is made of a glass with $n_a = 1.520$. The surface of one side of the prism is coated by a reflecting metal. Thus a standing wave evolves in the prism. The distance K from knot to knot of the standing wave along the hypotenuse is

$$K = \frac{1}{2} \cdot \frac{514.5\,\text{nm}}{1.520 \cdot \sin 45°} = 239.3\,\text{nm} \ . \tag{5}$$

The second prism is replaced by a glass-fiber wave-guide, whose tip (effective aperture about 80 nm) is moved along the x-axis at

the distance y from the prism's hypotenuse. The optical power coupled into the detector has been displayed by Meixner et. al. [4] as a function of x and y in the diagram reprinted on the right side of fig. 2. The distance 239 nm in x-direction between the knots of the standing wave is easily discernible. The observed reduction of the detected power I in y-direction can be approximated [4] by

$$I = I_0 e^{-2y/\gamma} \quad \text{with } \gamma = 207.8\text{nm} \pm 0.6\text{nm} \; . \tag{6}$$

Will the totally reflected wave still penetrate into the medium b and create an evanescent field, if there is no prism and no other detector, which could verify the evanescent field? The exploration of quantum phenomena in the twentieth century has taught us that this question is not trivial. There exists an effect, however, namely the Goos-Hänchen shift, which is suggesting the answer "yes".

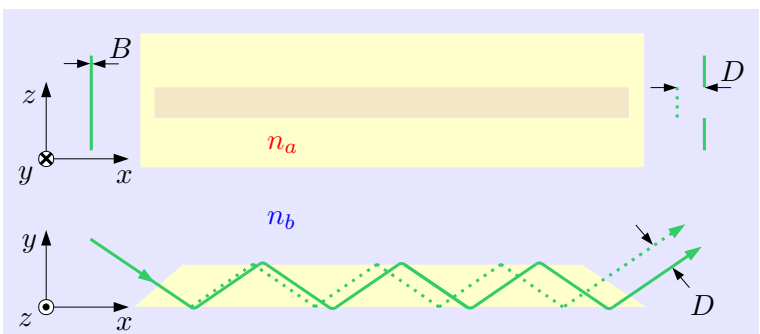

Fig. 3 : Goos-Hänchen shift

Goos and Hänchen [5,6] performed their experiment in multiple variants. One of the variants is sketched in fig. 3 : A bundle of light, whose cross-section is about $B \approx 0.3\,\text{mm}$, is coupled into a prism, and after about 60 to 70 total reflections eventually coupled out at the opposite side of the prism. In the middle of the prism's

top and bottom sides, reflecting silver layers are applied. At each reflection, the radiation bundle penetrates a little bit into the optically thinner medium b, before it returns into the medium a. Only at the silver stripes the radiation bundle is reflected immediately, without intruding into the medium b. Thereby that part of the light-bundle, which is reflected by medium b (continuous line in the sketch), is shifted upon each reflection a little bit in x-direction versus that part of the light-bundle, which is reflected by the silver stripe (dotted line in the sketch).

The effect is displayed in the sketch highly exaggerated. Goos and Hänchen worked with the green line of a mercury lamp, and observed after sixty to seventy reflections shifts of about $D = 50\,\mu$m to $D = 100\,\mu$m, i. e. about one third of the width $B \approx 0.3\,$mm of the light-bundle. D does depend sensitively on the incoming angle ϑ_e, and is largest if ϑ_e is only slightly larger than $\vartheta_{e,\text{critical}}$.

3. Law of refraction, and critical angle

Starting point for all theoretical considerations in this article are Maxwell's equations

$$\boldsymbol{\nabla} \times \boldsymbol{E} = -\dot{\boldsymbol{B}} \tag{7a}$$

$$\boldsymbol{\nabla} \times \boldsymbol{H} = \boldsymbol{\jmath} + \dot{\boldsymbol{D}} \tag{7b}$$

$$\boldsymbol{\nabla} \cdot \boldsymbol{D} = \rho \tag{7c}$$

$$\boldsymbol{\nabla} \cdot \boldsymbol{B} = 0 \tag{7d}$$

and the material equations

$$\boldsymbol{D} = \epsilon_0 \boldsymbol{E} + \boldsymbol{P} = \epsilon \boldsymbol{E} \qquad \text{with } \epsilon = \epsilon_r \epsilon_0 \tag{7e}$$

$$\boldsymbol{H} = \boldsymbol{B}/\mu_0 - \boldsymbol{M} = \boldsymbol{B}/\mu \qquad \text{with } \mu = \mu_r \mu_0\ . \tag{7f}$$

We emphasize

$$\boldsymbol{E} \in \mathbb{R},\ \boldsymbol{B} \in \mathbb{R},\ \boldsymbol{H} \in \mathbb{R},\ \boldsymbol{D} \in \mathbb{R},\ \boldsymbol{\jmath} \in \mathbb{R},\ \rho \in \mathbb{R},\ \epsilon_0 \in \mathbb{R},\ \mu_0 \in \mathbb{R}\,, \tag{7g}$$

i. e. all components of the three-dimensional field-strengths always are real in Maxwell's theory.

As we are assuming both media to be isotropic, the relative dielectric constants $\epsilon_{r,a}$ and $\epsilon_{r,b}$, and the relative magnetic permeabilities $\mu_{r,a}$ and $\mu_{r,b}$, can be described by numbers, and don't need to be represented by 3×3-component tensors. Furthermore we assume both media, and the boundary surface between them, to be free of macroscopic charges and current densities:

$$\rho = 0 \qquad , \qquad \boldsymbol{\jmath} = 0 \tag{7h}$$

This assumption implies that both media are good electrical isolators, in which no macroscopic currents are induced by the electromagnetic waves.

In the sequel we will use for vectors $\boldsymbol{F}$ the notation

$$\begin{aligned} \boldsymbol{F} \equiv \underbrace{\boldsymbol{u}_x F_x}_{\equiv \boldsymbol{F}_x} + \underbrace{\boldsymbol{u}_y F_y}_{\equiv \boldsymbol{F}_y} + \underbrace{\boldsymbol{u}_z F_z}_{\equiv \boldsymbol{F}_z} \equiv \underbrace{\boldsymbol{u}_x F_x + \boldsymbol{u}_z F_z}_{\equiv \boldsymbol{F}_{xz}} + \underbrace{\boldsymbol{u}_y F_y}_{\equiv \boldsymbol{F}_y} \end{aligned} \tag{8}$$

$$F \equiv |\boldsymbol{F}| \qquad , \qquad F_{xz} \equiv |\boldsymbol{F}_{xz}| \ , \tag{9}$$

with $\boldsymbol{u}_x$, $\boldsymbol{u}_y$, and $\boldsymbol{u}_z$ being unit vectors in the directions of the three cartesian coordinates. The electric and magnetic fields can thereby be described as the sum of fields $\boldsymbol{F}_{xz}$ in the plane of the boundary surface between the two media, and the fields $\boldsymbol{F}_y$ perpendicular to that plane. Alternatively, we will often sub-divide the fields into fields $\boldsymbol{F}_{xy}$, which are polarized in the plane spanned by the wave-vectors $\boldsymbol{k}$, and the fields $\boldsymbol{F}_z$, which are polarized perpendicular to that plane.

Note that the thin printed moduli F and F_{xz} with zero or two indices always are ≥ 0, while the thin printed vector components with exactly one component-index (like e. g. F_x) may be greater, or equal, or less than zero.

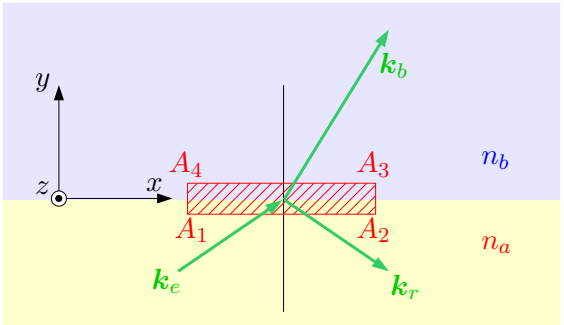

Fig. 4 : The surface A of integration

We integrate the Maxwell-equations (7a) and (7b) over the red-hatched area A depicted in fig. 4 . The corner points of A are A_1, A_2, A_3, A_4, and it's normal unit vector is $\boldsymbol{u}_A = \boldsymbol{u}_z$.

$$\int_A \mathrm{d}\boldsymbol{u}_z \cdot (\boldsymbol{\nabla} \times \boldsymbol{E}) = \oint_A \mathrm{d}\boldsymbol{l}_A \cdot \boldsymbol{E}_{xy} = -\int_A \mathrm{d}\boldsymbol{u}_z \cdot \dot{\boldsymbol{B}}_z \tag{10a}$$

$$\int_A \mathrm{d}\boldsymbol{u}_z \cdot (\boldsymbol{\nabla} \times \boldsymbol{H}) = \oint_A \mathrm{d}\boldsymbol{l}_A \cdot \boldsymbol{H}_{xy} = \int_A \mathrm{d}\boldsymbol{u}_z \cdot \dot{\boldsymbol{D}}_z \tag{10b}$$

By means of Stokes' theorem, the surface integrals over the rotation have been converted into path integrals along the surface's boundary l_A. Furthermore we have considered that only certain components of the vectors are contributing to the integral due to multiplication by the differentials $\mathrm{d}\boldsymbol{u}_z$ resp. $\mathrm{d}\boldsymbol{l}_A$.

Now the area A is vertically shrunk such that the points A_1 and A_2 become situated infinitesimal close to the boundary surface in medium a, and the points A_3 and A_4 infinitesimal close to that surface in medium b. Thereby the integrals over $\dot{\boldsymbol{B}}$ and $\dot{\boldsymbol{D}}$ become zero, because the area A becomes infinitesimal small. The path integrals from A_2 to A_3 and from A_4 to A_1 disappear as well. We

choose the distances from A_1 to A_2 and from A_3 to A_4 finite, but so small that the fields don't change appreciably along the way from A_1 to A_2 resp. from A_3 to A_4. This leads to the following integrals:

$$\int_{A_1}^{A_2} \mathrm{d}\boldsymbol{l}_A \cdot \boldsymbol{E}_x + \int_{A_3}^{A_4} \mathrm{d}\boldsymbol{l}_A \cdot \boldsymbol{E}_x = 0 \approx$$
$$\approx E_x(y=-0) \cdot \overline{A_2A_1} - E_x(y=+0) \cdot \overline{A_3A_4} \tag{11a}$$
$$\int_{A_1}^{A_2} \mathrm{d}\boldsymbol{l}_A \cdot \boldsymbol{H}_x + \int_{A_3}^{A_4} \mathrm{d}\boldsymbol{l}_A \cdot \boldsymbol{H}_x = 0 \approx$$
$$\approx H_x(y=-0) \cdot \overline{A_2A_1} - H_x(y=+0) \cdot \overline{A_3A_4} \tag{11b}$$

There is a negative sign for the path from A_3 to A_4, because the integration along that path is done in direction opposite to the x-coordinate. Using

$$\overline{A_2A_1} = \overline{A_3A_4} \ , \tag{12}$$

we get

$$E_{a,x} = E_{b,x} \qquad , \qquad H_{a,x} = H_{b,x} \ , \tag{13a}$$

with $\boldsymbol{E}_a$ resp. $\boldsymbol{H}_a$ being the fields in material a, and $\boldsymbol{E}_b$ resp. $\boldsymbol{H}_b$ being the fields in material b.

Next we want to demonstrate that similar equations hold for E_z and H_z. For that purpose the area A in figure 4 is rotated by $\pi/2$ around the y-axis, such that the normal vector of the area is pointing into x-direction. Thereby one gets instead of (11) the equations

$$-E_z(y=-0) \cdot \overline{A_2A_1} + E_z(y=+0) \cdot \overline{A_3A_4} = 0$$
$$-H_z(y=-0) \cdot \overline{A_2A_1} + H_z(y=+0) \cdot \overline{A_3A_4} = 0 \ ,$$

because now the path integrals are running parallel to the z-axis in medium b, but antiparallel to the z-axis in medium a. With $\overline{A_2A_1} = \overline{A_3A_4}$ we get

$$E_{a,z} = E_{b,z} \quad , \quad H_{a,z} = H_{b,z} \; . \tag{13b}$$

The physical meaning of equations (13a) and (13b) is obvious: Those components of the fields $\boldsymbol{E}$ and $\boldsymbol{H}$, which are tangential to the boundary surface between the two media, are continuous at the boundary surface.

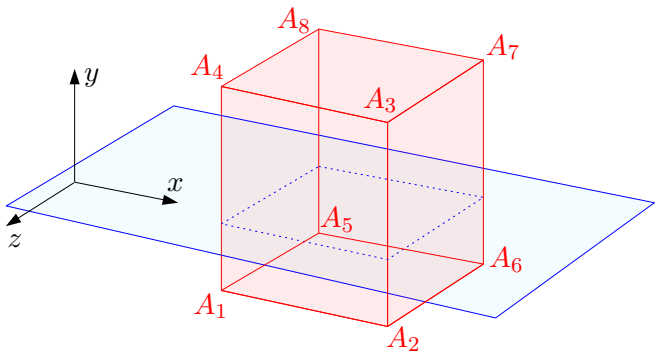

Fig. 5 : The integration volume V

Now we integrate Maxwell's equations (7c) and (7d) over the volume V with corner points A_1 through A_8, which is sketched in figure 5 . The boundary surface between the media is indicated in blue. Points A_1, A_2, A_6, A_5 are below that surface in medium a, points A_4, A_3, A_7, A_8 are above it in medium b. If the volume's y-components are chosen infinitesimal small, and it's x- and z-components are chosen finite, but so small that the fields don't change significantly on the integration surfaces, then one gets with (7h), and by means of Gauß' theorem,

$$0 \overset{(7c)}{=} \int_V \mathrm{d}V\, \boldsymbol{\nabla} \cdot \boldsymbol{D} = \int_{O(V)} \mathrm{d}\boldsymbol{f} \cdot \boldsymbol{D} = \overline{A_7 A_8} \cdot \overline{A_3 A_7} \cdot$$
$$\cdot \Big(D_{b,y}(y = +0) - D_{a,y}(y = -0) \Big) \,.$$

Thus at the boundary surface

$$D_{a,y} = D_{b,y} \tag{13c}$$

holds. By the same method, from (7d)

$$B_{a,y} = B_{b,y} \tag{13d}$$

is derived. The equations (13) are indicating that those components of $\boldsymbol{E}$ and $\boldsymbol{H}$ which are tangential to the boundary surface, and those components of $\boldsymbol{D}$ and $\boldsymbol{B}$ which are perpendicular to the boundary surface, are continuous at the boundary surface.

In the sequel, we will mark incoming fields in the medium a by the index $_e$, reflected fields in the medium a by the index $_r$, and fields in the medium b by the index $_b$. Furthermore we define a right-handed system of cartesian coordinates x, y, z as depicted in fig. 1 on page 2: The boundary surface between the media a and b is the xz plane ($y = 0$), i. e. the positive y-axis is perpendicular to the boundary surface, and is pointing into the medium b. The coordinate system is rotated around the y-axis such that the wave-vector of the incoming wave is in the xy plane ($k_{e,z} = 0$), and that $k_{e,x} \geq 0$ holds.

As we are assuming both media a and b to be isotropic, the z-components of the wave-vectors of the reflected fields and the fields in medium b must as well be zero ($k_{r,z} = k_{b,z} = 0$) for symmetry reasons, because the arguments for $k_{r,z} > 0$ wouldn't be better or worse in isotropic media than the arguments for $k_{r,z} < 0$. Corresponding considerations hold for $k_{b,z}$:

$$k_{e,z} = k_{r,z} = k_{b,z} = 0 \tag{14}$$

In (19) we will formally define the notion "plane wave". If the incoming fields are plane waves, then — according to experience — all fields in both media can be described completely by those solutions of Maxwell's equations, which have the form

$$\boldsymbol{E}(t,\boldsymbol{r}) = \hat{\boldsymbol{E}} e^{i(\boldsymbol{k}\cdot\boldsymbol{r}-\omega t+\varphi_E)} \tag{15a}$$

$$\boldsymbol{B}(t,\boldsymbol{r}) = \hat{\boldsymbol{B}} e^{i(\boldsymbol{k}\cdot\boldsymbol{r}-\omega t+\varphi_B)}\ , \tag{15b}$$

even in case of over-critical incoming angles, provided that we allow that the y-component of the wave-vector may be complex:

$$\boldsymbol{k} = \boldsymbol{u}_x k_x + \boldsymbol{u}_y k_y \quad \text{with } k_x \in \mathbb{R},\ k_y \in \mathbb{C},\ k_z \overset{(14)}{=} 0 \tag{15c}$$

t is the time, $\boldsymbol{r}$ the location in three-dimensional space, ω is a frequency, φ is a constant phase angle.

The fields of course must be real, see (7g). Therefore equations (15a) and (15b) are to be interpreted as

$$\boldsymbol{E} = \mathrm{Re}\Big[\hat{\boldsymbol{E}} e^{i(\boldsymbol{k}\cdot\boldsymbol{r}-\omega t+\varphi_E)}\Big] = \hat{\boldsymbol{E}}\cos(\boldsymbol{k}\cdot\boldsymbol{r}-\omega t+\varphi_E) \tag{16a}$$

$$\boldsymbol{B} = \mathrm{Re}\Big[\hat{\boldsymbol{B}} e^{i(\boldsymbol{k}\cdot\boldsymbol{r}-\omega t+\varphi_B)}\Big] = \hat{\boldsymbol{B}}\cos(\boldsymbol{k}\cdot\boldsymbol{r}-\omega t+\varphi_B)\ . \tag{16b}$$

Only for convenience we skip in most of our formulas the explicit notation $\mathrm{Re}[\ldots]$.

For the reminder of this article we will exclusively consider fields of the form (15), and statements like "all fields have this or that property" are to be understood as "all fields of the form (15) have this or that property".

Insertion of (15) and (7h) into Maxwell's equations (7a) and (7b) results into

$$\begin{aligned}\boldsymbol{\nabla}\times\boldsymbol{E} &= \boldsymbol{u}_x\Big(\frac{\partial E_z}{\partial y}-\frac{\partial E_y}{\partial z}\Big)+\boldsymbol{u}_y\Big(\frac{\partial E_x}{\partial z}-\frac{\partial E_z}{\partial x}\Big)+\\ &+\boldsymbol{u}_z\Big(\frac{\partial E_y}{\partial x}-\frac{\partial E_x}{\partial y}\Big)=i\boldsymbol{u}_x(k_yE_z-k_zE_y)+\\ &+i\boldsymbol{u}_y(k_zE_x-k_xE_z)+i\boldsymbol{u}_z(k_xE_y-k_yE_x)\;=\\ &=i\boldsymbol{k}\times\boldsymbol{E}=-\dot{\boldsymbol{B}}=+i\omega\boldsymbol{B} \qquad (17a)\\ \boldsymbol{\nabla}\times\boldsymbol{H} &= i\boldsymbol{k}\times\boldsymbol{H}=-i\omega\boldsymbol{D}\;. \qquad (17b)\end{aligned}$$

The wave-vectors and field-vectors thus meet the conditions

$$\boldsymbol{k}\times\boldsymbol{E}=\omega\boldsymbol{B} \qquad (18a)$$

$$\boldsymbol{k}\times\boldsymbol{B}=\mu\boldsymbol{k}\times\boldsymbol{H}=-\omega\mu\boldsymbol{D}=-\omega\epsilon\mu\boldsymbol{E}\;. \qquad (18b)$$

Electromagnetic fields are called "plane waves", if they have the form (15) and if k_y is real:

$$\begin{aligned}&\text{p. w.}\equiv\text{plane wave}\iff\\ &\iff \boldsymbol{k}\in\mathbb{R}\iff k_x\in\mathbb{R},\,k_y\in\mathbb{R},\,k_z\in\mathbb{R}\end{aligned} \qquad (19)$$

In case of plain waves, according to (18)

$$\text{p. w.}: \qquad \boldsymbol{k}\perp\boldsymbol{E}\perp\boldsymbol{B}\perp\boldsymbol{k}\;, \qquad (20)$$

with the three vectors $\boldsymbol{k},\boldsymbol{E},\boldsymbol{B}$ according to (18a) forming a right-handed system.

If in a plane wave $\boldsymbol{E}(t,\boldsymbol{r})=0$, then according to (18a) $\boldsymbol{B}(t,\boldsymbol{r})=0$. Thus for the phase factors

$$\text{p. w.}: \quad \varphi_E=\varphi_B \quad \text{or} \quad \varphi_E=\varphi_B+\pi \qquad (21)$$

must hold. For the moduli, in case of a plane wave

$$\text{p. w.}: \quad E=\frac{\omega}{k}B=\frac{c}{n}B=\frac{1}{\sqrt{\epsilon\mu}}B \qquad (22)$$

holds, with the

$$\text{index of refraction:} \quad n = \sqrt{\epsilon_r \mu_r} \tag{23}$$

and the

$$\text{velocity of light in vacuum:} \quad c = \frac{1}{\sqrt{\epsilon_0 \mu_0}} \ . \tag{24}$$

We exclusively consider "conventional" materials with the properties

$$\epsilon_r > 0 \quad , \quad \mu_r > 0 \quad , \quad n > 0 \ , \tag{25}$$

and ignore the "modified" materials with negative index of refraction, which are known since 2001.

By taking the derivatives of Maxwell's equations (7a) and (7b) with respect to time, inserting them mutually, and considering (7h), we get the wave-equations

$$\boldsymbol{\nabla} \times \boldsymbol{\nabla} \times \boldsymbol{E} = -\epsilon\mu \ddot{\boldsymbol{E}} \tag{26a}$$

$$\boldsymbol{\nabla} \times \boldsymbol{\nabla} \times \boldsymbol{B} = -\epsilon\mu \ddot{\boldsymbol{B}} \ . \tag{26b}$$

As the equations for the magnetic field and the electric field are formally identical, we only consider the electric field. For fields of the form (15), we get

$$\begin{aligned} &\boldsymbol{\nabla} \times \boldsymbol{\nabla} \times \boldsymbol{E} = \\ &= -\boldsymbol{u}_x \Big(k_y (k_x E_y - k_y E_x) - k_z (k_z E_x - k_x E_z) \Big) - \\ &\quad - \boldsymbol{u}_y \Big(k_z (k_y E_z - k_z E_y) - k_x (k_x E_y - k_y E_x) \Big) - \\ &\quad - \boldsymbol{u}_z \Big(k_x (k_z E_x - k_x E_z) - k_y (k_y E_z - k_z E_y) \Big) \ = \\ &= -\boldsymbol{k} \times \boldsymbol{k} \times \boldsymbol{E} = +\omega^2 \epsilon\mu \boldsymbol{E} \end{aligned} \tag{27a}$$

Due to $k_z \overset{(14)}{=} 0$, these equations simplify significantly:

$$-k_x k_y E_y + k_y^2 E_x = \omega^2 \epsilon\mu E_x \tag{28a}$$
$$k_x^2 E_y - k_x k_y E_x = \omega^2 \epsilon\mu E_y \tag{28b}$$
$$k_x^2 E_z + k_y^2 E_z = \omega^2 \epsilon\mu E_z \tag{28c}$$

As always $\omega^2\epsilon\mu \neq 0$, we get from the first and the second equation

$$\begin{aligned}
&\text{if } k_y = 0: \quad E_x = 0 \text{ and } k_x^2 E_y = \omega^2 \epsilon\mu E_y \\
&\text{if } k_x = 0: \quad E_y = 0 \text{ and } k_y^2 E_x = \omega^2 \epsilon\mu E_x \\
&\text{if } k_x \neq 0 \text{ and } k_y \neq 0: \\
&\qquad (k_x^2 + k_y^2) E_y = \omega^2 \epsilon\mu E_y \\
&\qquad (k_x^2 + k_y^2) E_x = \omega^2 \epsilon\mu E_x \ .
\end{aligned}$$

Thus in either case, even if the wave vectors are complex, the simple equation

$$\sqrt{k_x^2 + k_y^2} = \omega\sqrt{\epsilon\mu} \tag{29}$$

holds. We compare this result with

$$\text{p. w.}: \quad k \overset{(22)}{=} \omega\sqrt{\epsilon\mu}\ , \tag{30}$$

which we derived for the modulus of the real wave-vector of a plane wave. From the comparison we deduce this somewhat surprising

rule: If $\boldsymbol{V}$ is a vector with one imaginary and two real components, then it's modulus must be computed by

$$V \equiv |\boldsymbol{V}| = {}_{+}\sqrt{V_x^2 + V_y^2 + V_z^2} \neq {}_{+}\sqrt{|V_x|^2 + |V_y|^2 + |V_z|^2}\ . \tag{31}$$

Even though we will repeatedly encounter examples for this rule in course of our evaluation, we will avoid to apply it, as we see no

obvious way to justify it mathematically and/or physically. Instead we will always work around the issue like we have done in derivation of (29), even if this sometimes is a quite tedious task.

We insert the general ansatz (15) into an arbitrary one of the relations (13):

$$\hat{E}_{e,x} e^{i(k_{e,x}x - \omega_e t + \varphi_{e,E})} + \\ + \hat{E}_{r,x} e^{i(k_{r,x}x - \omega_r t + \varphi_{r,E})} \overset{(13a)}{=} \hat{E}_{b,x} e^{i(k_{b,x}x - \omega_b t + \varphi_{b,E})} \tag{32}$$

This condition must be met at any point of the boundary surface between the two media. Note that only $k_x x$ is showing up in the exponents, because on the boundary surface $y \overset{\text{fig. 1}}{=} 0$, and $k_z \overset{(14)}{=} 0$ everywhere. Equation (32) must hold at any time t. That's possible only if

$$\omega \equiv \omega_e = \omega_r = \omega_b \ , \tag{33}$$

meaning that the radiation's frequency does not change upon reflection or refraction.

Furthermore (32) must hold at any position x. That's possible only if

$$k_x \equiv k_{e,x} = k_{r,x} = k_{b,x} \qquad , \qquad k_x \overset{(15c)}{\in} \mathbb{R} \ . \tag{34}$$

In this article we exclusively consider the case that the incoming fields are plane waves. Then $k_{e,y} \in \mathbb{R}$ according to (19), and $k_{r,y}$ as well must be real due to

$$\sqrt{k_x^2 + k_{r,y}^2} \overset{(29)}{=} \omega \sqrt{\epsilon_a \mu_a} \overset{(29)}{=} \sqrt{k_x^2 + k_{e,y}^2} > \sqrt{k_x^2} \ , \tag{35}$$

meaning that the reflected fields are forming a plane wave[1] accord-

[1] Of course we have "proved" this fact only under the precondition that the general formula (15) is indeed a correct description of the reflected fields.

ing to (19) as well. As

$$k_r \overset{(35)}{=} k_e \ , \tag{36}$$

we can read from fig. 1 on page 2:

$$k_x = k_e \sin\vartheta_e = k_e \sin\vartheta_r \implies \vartheta_r = \vartheta_e \tag{37}$$

$$k_{r,y} = -k_e \cos\vartheta_e = -k_{e,y} \tag{38}$$

For the field in medium b, we can conclude from (29):

$$\sqrt{k_x^2 + k_{b,y}^2} = \omega\sqrt{\epsilon_b\mu_b} = \frac{\sqrt{\epsilon_b\mu_b}}{\sqrt{\epsilon_a\mu_a}}\, k_e \overset{(23)}{=} \frac{n_b}{n_a}\, k_e \tag{39}$$

If the field in medium b is a plane wave, then $k_{b,y} \in \mathbb{R}$, and then

$$\text{p. w. :} \quad k_b \overset{(39)}{=} \frac{n_b}{n_a}\, k_e \ . \tag{40}$$

Then we can read from fig. 1:

$$\begin{aligned} \text{p. w. :} \quad k_x &\overset{(34)}{=} k_{b,x} = k_b \sin\vartheta_b \overset{(34)}{=} k_e \sin\vartheta_e \\ &\implies n_b \sin\vartheta_b \overset{(40)}{=} n_a \sin\vartheta_e \end{aligned} \tag{41}$$

$$\begin{aligned} k_{b,y} = k_b \cos\vartheta_b &= {}_+\sqrt{k_b^2 - k_x^2} = \\ &\overset{(39),(34)}{=} k_e \, {}_+\sqrt{(n_b/n_a)^2 - \sin^2\vartheta_e} \in \mathbb{R} \end{aligned} \tag{42}$$

(41) is Snellius' law of refraction. We emphasize, that this relation was found by reading the angles off from fig. 1. That was only possible, because all wave-vectors and their respective angles versus the $(y = 0)$-plane, including $\boldsymbol{k}_b$ and ϑ_b, have been considered real.

The reverse conclusion is valid as well: The plane waves (15) with $k_{b,y} \in \mathbb{R}$ are a correct description of the fields in medium b

only if the angle ϑ_b in Snellius's law of refraction (41) is real, i. e. only if

$$\sin\vartheta_e \overset{(42)}{\leq} \frac{n_b}{n_a} = \sin\vartheta_{e,\text{critical}} \ . \tag{43}$$

If $k_{b,y}$ would have a finite real part and a finite imaginary part, then the fields in medium b would be damped plane waves: The energy of the waves penetrating into medium b would be partly absorbed and converted into heat. In this article we are not interested in that case, instead we assume perfect transparency of both media.

Therefore we consider as third and last alternative a purely imaginary $k_{b,y}$. We define the

$$\text{penetration depth} \equiv \gamma \equiv \frac{i}{k_{b,y}} \in \mathbb{R} \ , \tag{44}$$

and combine it with the always valid relation

$$-k_{b,y}^2 \overset{(29)}{=} k_x^2 - \omega^2\epsilon_b\mu_b \overset{(37),(39)}{=} k_e^2\sin^2\vartheta_e - \frac{n_b^2}{n_a^2}k_e^2 = \gamma^{-2} \ . \tag{45}$$

Thereby the fields in medium b become

$$\boldsymbol{E}_b \overset{(15a)}{=} \hat{\boldsymbol{E}}_b e^{-y/\gamma + i(k_x x - \omega t + \varphi_{b,E})} \tag{46a}$$

$$\boldsymbol{B}_b \overset{(15b)}{=} \hat{\boldsymbol{B}}_b e^{-y/\gamma + i(k_x x - \omega t + \varphi_{b,B})} \tag{46b}$$

$$\gamma \overset{(45)}{=} \frac{1}{k_{e_+}\sqrt{\sin^2\vartheta_e - (n_b/n_a)^2}} \overset{(43)}{=} \frac{1}{k_{e_+}\sqrt{\sin^2\vartheta_e - \sin^2\vartheta_{e,\text{critical}}}} > 0 \ . \tag{46c}$$

We constrain the penetration depth to the positive root, because y is always zero or positive in medium b. Therefore only a positive

$\gamma > 0$ is resulting into exponentially damped fields. The negative root is considered "unphysical", and is discarded. Note that neither $\gamma = 0$ nor $\gamma = \infty$ can happen for $\vartheta_e > \vartheta_{e,\text{critical}}$. γ can however assume arbitrarily high finite values for $\vartheta_e \gtrsim \vartheta_{e,\text{critical}}$.

(46c) implies $\vartheta_e > \vartheta_{e,\text{critical}}$. While the fields (15a) and (15b) with real $k_{b,y} \in \mathbb{R}$ are correct descriptions of the fields in medium b exclusively for angles $\vartheta_e \leq \vartheta_{e,\text{critical}}$ according to (43), the solution (46) is valid exclusively for over-critical incoming angles.

It will turn out convenient in the sequel, to define an angle ϑ_b such that for arbitrary incoming angles ϑ_e, including $(n_a/n_b)\sin\vartheta_e > 1$, formally the law of refraction

$$n_b \sin\vartheta_b \overset{(41)}{=} n_a \sin\vartheta_e \tag{47}$$

holds. If $(n_a/n_b)\sin\vartheta_e > 1$, then $\sin\vartheta_b$ must be greater than one. That is possible only if $\vartheta_b \in \mathbb{C}$ is complex:

$$\begin{aligned} \vartheta_b &= \vartheta' + i\vartheta'' \quad \text{with } \vartheta' \in \mathbb{R}\,,\ \vartheta'' \in \mathbb{R} \\ \frac{n_a}{n_b}\sin\vartheta_e &\overset{(47)}{=} \sin\vartheta_b = \frac{e^{i\vartheta'}e^{-\vartheta''} - e^{-i\vartheta'}e^{+\vartheta''}}{2i} = \\ &= \frac{(e^{-\vartheta''} - e^{+\vartheta''})\cos\vartheta'}{2i} + \frac{(e^{-\vartheta''} + e^{+\vartheta''})\sin\vartheta'}{2} \end{aligned} \tag{48}$$

As the left side of (48) is real, the right side must be real as well. Consequently the first term in the bottom line must vanish, implying $\vartheta'' = 0$ and/or $\vartheta' = \pm\pi/2$. With $\vartheta'' = 0$, (48) reduces to $\sin\vartheta_b = \sin\vartheta'$. This is a solution of the law of refraction in the case $\vartheta_e \leq \vartheta_{e,\text{critical}}$. But a solution for over-critical angles does exist only with $\vartheta' = \pm\pi/2$. We decide for $\vartheta' = +\pi/2$:

$$\begin{aligned} &\text{if } \vartheta_e > \vartheta_{e,\text{critical}} : \\ &\frac{n_a}{n_b}\sin\vartheta_e = \sin\vartheta_b = +\frac{e^{-\vartheta''} + e^{+\vartheta''}}{2} = +\operatorname{ch}\vartheta''\,. \end{aligned} \tag{49}$$

With $\vartheta' = -\pi/2$ the exotic "modified materials" with negative index of refraction could be handled. We always will assume $\vartheta' = +\pi/2$, because we occupy ourselves exclusively with conventional materials, for which $n_a > 0$ and $n_b > 0$ holds.

The sign of ϑ'', however, is not fixed by (49) due to $\mathrm{ch}(+\vartheta'') = \mathrm{ch}(-\vartheta'')$. Thus we define the following complex angle:

$$\vartheta_b \equiv \vartheta' + i\vartheta'' \quad \text{with } \vartheta' \in \mathbb{R}\,,\ \vartheta'' \in \mathbb{R}$$

$$\sin\vartheta_b \equiv \frac{n_a}{n_b}\,\sin\vartheta_e \tag{50a}$$

$$\text{if } \vartheta_e \le \vartheta_{e,\text{critical}}\ :$$

$$\vartheta_b \equiv \vartheta' \quad , \quad \vartheta'' = 0 \tag{50b}$$

$$\text{if } \vartheta_e > \vartheta_{e,\text{critical}}\ :$$

$$\vartheta_b \equiv +\pi/2 + i\vartheta''\,. \tag{50c}$$

Eventually we compute $\cos\vartheta_b$:

$$\text{if } \vartheta_e > \vartheta_{e,\text{critical}}\ :$$

$$\begin{aligned}\cos\vartheta_b &= \frac{e^{i\pi/2-\vartheta''} + e^{-i\pi/2+\vartheta''}}{2} = i\,\frac{e^{-\vartheta''} - e^{+\vartheta''}}{2} = \\ &= -i\,\mathrm{sh}\,\vartheta'' = -i\,{}_{\pm}\sqrt{\mathrm{ch}^2\vartheta'' - 1} \overset{(49)}{=} \\ &= -i\,{}_{\pm}\sqrt{\sin^2\vartheta_b - 1} \overset{(50a)}{=} -i\,{}_{\pm}\sqrt{(n_a/n_b)^2\sin^2\vartheta_e - 1}\end{aligned} \tag{51}$$

While $\sin\vartheta_b$ is real, $\cos\vartheta_b$ is purely imaginary. The well-known formula $\sin^2\vartheta_b + \cos^2\vartheta_b = 1$ holds as well for $\vartheta_e > \vartheta_{e,\text{critical}}$.

We emphasize that ϑ_b can be interpreted geometrically only if $\vartheta_e \le \vartheta_{e,\text{critical}}$ (and therefore $\vartheta_b \in \mathbb{R}$), as drawn in fig. 1. If $\vartheta_e > \vartheta_{e,\text{critical}}$, then (50a) is not a physical statement, but nothing than a purely formal mathematical *definition* of the complex angle ϑ_b.

If $\cos\vartheta_b$ is constrained to

$$\text{if } \vartheta_e > \vartheta_{e,\text{critical}} :$$
$$\cos\vartheta_b \overset{(51)}{=} +i\sqrt{\sin^2\vartheta_b - 1} = +i\sqrt{(n_a/n_b)^2\sin^2\vartheta_e - 1}\ , \tag{52}$$

then the penetration depth of the evanescent field can be written in this form:

$$\text{if } \vartheta_e > \vartheta_{e,\text{critical}} :$$
$$\gamma \overset{(44)}{=} \frac{i}{k_{b,y}} \overset{(46c)}{=} \frac{1}{k_e(n_b/n_a)\sqrt{(n_a/n_b)^2\sin^2\vartheta_e - 1}} =$$
$$\overset{(52)}{=} \frac{i}{k_e(n_b/n_a)\cos\vartheta_b} \tag{53a}$$
$$\Longrightarrow \quad k_{b,y} = \frac{k_e n_b}{n_a}\cos\vartheta_b \tag{53b}$$

We already know

$$k_{b,x} \overset{(34)}{=} k_x \overset{(37)}{=} k_e\sin\vartheta_e \overset{(50a)}{=} \frac{k_e n_b}{n_a}\sin\vartheta_b\ . \tag{54}$$

Thereby the evanescent fields (46) can be written as

$$\text{if } \vartheta_e > \vartheta_{e,\text{critical}} :$$
$$\boldsymbol{E}_b \overset{(44)}{=} \hat{\boldsymbol{E}}_b e^{i(\boldsymbol{k}_b\cdot\boldsymbol{r}-\omega t+\varphi_{b,E})} \tag{55a}$$
$$\boldsymbol{B}_b \overset{(44)}{=} \hat{\boldsymbol{B}}_b e^{i(\boldsymbol{k}_b\cdot\boldsymbol{r}-\omega t+\varphi_{b,B})} \tag{55b}$$
$$\boldsymbol{k}_b = \boldsymbol{u}_x\Big(\frac{k_e n_b}{n_a}\sin\vartheta_b\Big) + \boldsymbol{u}_y\Big(\frac{k_e n_b}{n_a}\cos\vartheta_b\Big)\ . \tag{55c}$$

Note that this is the notation of the fields stated in (15). $\boldsymbol{u}_x$ and $\boldsymbol{u}_y$ are unit-vectors in x- and y-direction. As $\sin\vartheta_b$ is real, and

$\cos\vartheta_b$ is imaginary, the x-component of the wave-vector $\boldsymbol{k}_b$ is real, and it's y-component is imaginary.

Let's compare (55c) with the wave-vector $\boldsymbol{k}_b$ at under-critical incoming angles:

$$\text{if } \vartheta_e \le \vartheta_{e,\text{critical}} :$$

$$\boldsymbol{k}_b \overset{(41),(42)}{=} \boldsymbol{u}_x k_b \sin\vartheta_b + \boldsymbol{u}_y k_b \cos\vartheta_b \tag{56a}$$

$$k_b = |\boldsymbol{k}_b| \overset{(40)}{=} \frac{n_b}{n_a}\, k_e \overset{(41)}{=} \frac{\sin\vartheta_e}{\sin\vartheta_b}\, k_e \tag{56b}$$

Thus the wave-vectors at under- and over-critical incoming angles are formally identical, if the complex angle $\vartheta_b = (50)$ is inserted, *and* if the strange rule (31) is applied, stating

$$\text{if } \vartheta_e > \vartheta_{e,\text{critical}} :$$

$$\begin{aligned} |\boldsymbol{k}_b| &\overset{(31)}{=} {}_+\sqrt{k_{b,x}^2 + k_{b,y}^2 + k_{b,z}^2} = k_e \frac{n_b}{n_a} \neq \\ &\neq {}_+\sqrt{|k_{b,x}|^2 + |k_{b,y}|^2 + |k_{b,z}|^2} = \\ &= {}_+\sqrt{2\,(n_a/n_b)^2 \sin^2\vartheta_e - 1}\ . \end{aligned} \tag{57}$$

We emphasize, that (55) has been derived with no reference whatsoever to (31). Thus this result does not depend on the soundness of that dubious rule.

The formulas (46) for the evanescent fields are checked by the experiment of Meixner et. al. [4]. The setup and results of that experiment have been sketched in fig. 2 on page 5. According to (46), the evanescent field is in x-direction a wave with wave-number $k_x = k_e \sin\vartheta_e$. This is confirmed by the measurements. The exponential damping in y-direction is determined by the penetration depth γ. In the experiment of Meixner et. al. [4], the value

$$\gamma = \Big(\frac{2\pi \cdot 1.520}{514.5\,\text{nm}} \sqrt{\sin^2 45^\circ - 1.520^{-2}}\Big)^{-1} = 207.9\,\text{nm} \tag{58}$$

is expected. In sufficient distance from the prism, Meixner et. al. achieved with $\gamma = 207.8\text{nm} \pm 0.6\text{nm}$ a good fit to their measured values, thereby impressively confirming the solution (46). We will discuss their observations at small distance between tip and prism in section 5.

4. Fresnel-coefficients and phase angles

Any electromagnetic field can be described as the sum of "perpendicular polarized" and "parallel polarized" fields:

$$\boldsymbol{E} = \underbrace{\boldsymbol{E}_\perp}_{\boldsymbol{E}_z} + \underbrace{\boldsymbol{E}_\parallel}_{\boldsymbol{E}_{xy}} \quad , \quad \boldsymbol{B} = \underbrace{\boldsymbol{B}_\perp}_{\boldsymbol{B}_{xy}} + \underbrace{\boldsymbol{B}_\parallel}_{\boldsymbol{B}_z} \tag{59}$$

Perpendicular polarization is meaning that the electric field is polarized perpendicular to that plane which is spanned by the wave-vectors, i. e. perpendicular to the xy-plane, see figure 1 on page 2. Engineers name this a TE-wave, i. e. a wave with transversal electric field. At perpendicular polarization, only $E_z \neq 0$, while $E_x = E_y = 0$. At parallel polarization $E_z = 0$, while $\boldsymbol{E}_{xy} \neq 0$. Engineers name this a TM-wave, i. e. a wave with transversal magnetic field. In case of plain waves ($\boldsymbol{k} \in \mathbb{R}$), the vectors $\boldsymbol{k}, \boldsymbol{E}, \boldsymbol{B}$ form a right-handed orthogonal system because of (18a) This is the reason for the breakdown (59) of $\boldsymbol{B}$ into $\boldsymbol{B}_\parallel$ and $\boldsymbol{B}_\perp$. The marks $\perp$ and $\parallel$ thus are always referring to the polarization of the electric field, not the magnetic field, relative to the xy-plane.

In (13) we stated, that — at arbitrary incoming angles of the radiation — those components of the fields $\boldsymbol{E}$ and $\boldsymbol{H}$ which are tangential to the boundary surface of the media, and those components of the fields $\boldsymbol{D}$ and $\boldsymbol{B}$ which are perpendicular to the boundary surface, are continuous at the boundary surface. We

insert the fields (15) into (13):

at perpendicular polarization ($\boldsymbol{E}_z = \boldsymbol{E}$) :

$$\hat{E}_{b,z} e^{i\varphi_{b,E}} = \hat{E}_{e,z} e^{i\varphi_{e,E}} + \hat{E}_{r,z} e^{i\varphi_{r,E}} \tag{60a}$$

$$\hat{B}_{b,x} e^{i\varphi_{b,B}} = \frac{\mu_b}{\mu_a}\Big(\hat{B}_{e,x} e^{i\varphi_{e,B}} + \hat{B}_{r,x} e^{i\varphi_{r,B}}\Big) \tag{60b}$$

$$\hat{B}_{b,y} e^{i\varphi_{b,B}} = \hat{B}_{e,y} e^{i\varphi_{e,B}} + \hat{B}_{r,y} e^{i\varphi_{r,B}} \tag{60c}$$

at parallel polarization ($\boldsymbol{B}_z = \boldsymbol{B}$) :

$$\hat{E}_{b,x} e^{i\varphi_{b,E}} = \hat{E}_{e,x} e^{i\varphi_{e,E}} + \hat{E}_{r,x} e^{i\varphi_{r,E}} \tag{60d}$$

$$\hat{B}_{b,z} e^{i\varphi_{b,B}} = \frac{\mu_b}{\mu_a}\Big(\hat{B}_{e,z} e^{i\varphi_{e,B}} + \hat{B}_{r,z} e^{i\varphi_{r,B}}\Big) \tag{60e}$$

$$\hat{E}_{b,y} e^{i\varphi_{b,E}} = \frac{\epsilon_a}{\epsilon_b}\Big(\hat{E}_{e,y} e^{i\varphi_{e,E}} + \hat{E}_{r,y} e^{i\varphi_{r,E}}\Big) \tag{60f}$$

Two trivial equations $0 = 0$ have been skipped. By definition, we always choose the six amplitudes

$$\begin{aligned} &0 \le \hat{E}_e \in \mathbb{R} \quad , \quad 0 \le \hat{E}_r \in \mathbb{R} \quad , \quad 0 \le \hat{E}_b \in \mathbb{R} \ , \\ &0 \le \hat{B}_e \in \mathbb{R} \quad , \quad 0 \le \hat{B}_r \in \mathbb{R} \quad , \quad 0 \le \hat{B}_b \in \mathbb{R} \end{aligned} \tag{61}$$

real and positive. Their components can be found by means of the formulas

$$\boldsymbol{B} \overset{(18a)}{=} \frac{1}{\omega}\, \boldsymbol{k} \times \boldsymbol{E} \tag{62a}$$

$$\boldsymbol{E} \overset{(18b)}{=} -\frac{1}{\omega\epsilon\mu}\, \boldsymbol{k} \times \boldsymbol{B} \ , \tag{62b}$$

which are valid for arbitrary under- and over-critical incoming angles. We cancel common factors, and make use of $k_z = 0$:

$$\hat{B}_x e^{i\varphi_B} = +\frac{1}{\omega}\, k_y \hat{E}_z e^{i\varphi_E} \overset{(63f)}{=} -\frac{1}{\omega^2\epsilon\mu}\, k_y (k_x \hat{B}_y - k_y \hat{B}_x) e^{i\varphi_B} \tag{63a}$$

$$\hat{B}_y e^{i\varphi_B} = -\frac{1}{\omega}\, k_x \hat{E}_z e^{i\varphi_E} \overset{(63f)}{=} +\frac{1}{\omega^2\epsilon\mu}\, k_x (k_x \hat{B}_y - k_y \hat{B}_x) e^{i\varphi_B} \quad (63b)$$

$$\hat{B}_z e^{i\varphi_B} = +\frac{1}{\omega}\, (k_x \hat{E}_y - k_y \hat{E}_x) e^{i\varphi_E} \quad (63c)$$

$$\hat{E}_x e^{i\varphi_E} = -\frac{1}{\omega\epsilon\mu}\, k_y \hat{B}_z e^{i\varphi_B} \overset{(63c)}{=} -\frac{1}{\omega^2\epsilon\mu}\, k_y (k_x \hat{E}_y - k_y \hat{E}_x) e^{i\varphi_E} \quad (63d)$$

$$\hat{E}_y e^{i\varphi_E} = +\frac{1}{\omega\epsilon\mu}\, k_x \hat{B}_z e^{i\varphi_B} \overset{(63c)}{=} +\frac{1}{\omega^2\epsilon\mu}\, k_x (k_x \hat{E}_y - k_y \hat{E}_x) e^{i\varphi_E} \quad (63e)$$

$$\hat{E}_z e^{i\varphi_E} = -\frac{1}{\omega\epsilon\mu}\, (k_x \hat{B}_y - k_y \hat{B}_x) e^{i\varphi_B} \quad (63f)$$

Remember that we only for convenience skipped the explicit notation Re[...] for the fields and their components, see (16). All wave-vector components are real, with the exception of $k_{b,y}$ at overcritical incoming angles:

at arbitrary ϑ_e :

$$k_x \overset{(34)}{=} k_{e,x} = k_{r,x} \overset{(37)}{=} k_e \sin\vartheta_e \overset{(34)}{=} k_{b,x} \overset{(54)}{=} \frac{k_e n_b}{n_a} \sin\vartheta_b \quad (64a)$$

$$k_{e,y} \overset{(38)}{=} -k_{r,y} \overset{(38)}{=} k_e \cos\vartheta_e \quad (64b)$$

at $\vartheta_e \le \vartheta_{e,\text{critical}}$:

$$k_{b,y} \overset{(40),(42)}{=} \frac{k_e n_b}{n_a} \cos\vartheta_b \quad , \quad \cos\vartheta_b \in \mathbb{R} \quad (64c)$$

at $\vartheta_e > \vartheta_{e,\text{critical}}$:

$$k_{b,y} \overset{(44)}{=} \frac{i}{\gamma} \overset{(53b)}{=} \frac{k_e n_b}{n_a} \cos\vartheta_b \quad , \quad \gamma \in \mathbb{R} \quad , \quad i\cos\vartheta_b \in \mathbb{R} \quad (64d)$$

Thus we can conclude from (63)

at arbitrary ϑ_e :

$$\varphi_{e,B} = \varphi_{e,E} \quad \text{OR} \quad \varphi_{e,B} = \varphi_{e,E} + \pi \quad (65a)$$

$$\varphi_{r,B} = \varphi_{r,E} \quad \text{OR} \quad \varphi_{r,B} = \varphi_{r,E} + \pi \tag{65b}$$

at $\vartheta_e \leq \vartheta_{e,\text{critical}}$:

$$\varphi_{b,B} = \varphi_{b,E} \quad \text{OR} \quad \varphi_{b,B} = \varphi_{b,E} + \pi \tag{65c}$$

at $\vartheta_e > \vartheta_{e,\text{critical}}$:

$$\varphi_{b,B_x} = \varphi_{b,E_z} + \pi/2 \quad \text{OR} \quad \varphi_{b,B_x} = \varphi_{b,E_z} - \pi/2 \tag{65d}$$

$$\varphi_{b,B_y} = \varphi_{b,E_z} \quad \text{OR} \quad \varphi_{b,B_y} = \varphi_{b,E_z} + \pi \tag{65e}$$

$$\varphi_{b,E_x} = \varphi_{b,B_z} + \pi/2 \quad \text{OR} \quad \varphi_{b,E_x} = \varphi_{b,B_z} - \pi/2 \tag{65f}$$

$$\varphi_{b,E_y} = \varphi_{b,B_z} \quad \text{OR} \quad \varphi_{b,E_y} = \varphi_{b,B_z} + \pi \ . \tag{65g}$$

This result — though quite complicated — is very reasonable: The flow of energy of the evanescent electromagnetic field is described by the Poynting vector

at $\vartheta_e > \vartheta_{e,\text{critical}}$:

$$\boldsymbol{S}_b = \boldsymbol{E}_b \times \boldsymbol{B}_b \, / \mu_b \tag{66a}$$

$$\mu_b S_{b,x} = E_{b,y} B_{b,z} - E_{b,z} B_{b,y} \tag{66b}$$

$$\mu_b S_{b,y} = E_{b,z} B_{b,x} - E_{b,x} B_{b,z} \tag{66c}$$

$$\mu_b S_{b,z} = E_{b,x} B_{b,y} - E_{b,y} B_{b,x} = 0 \ . \tag{66d}$$

At perpendicular polarization $E_x = E_y = B_z = 0$, and at parallel polarization $B_x = B_y = E_z = 0$. Thus $S_{b,z} = 0$ at any polarization. Because of the phase conditions (65d) through (65g), $S_{b,y}$ is changing signs for each quarter wavelength. Consequently there is for one quarter of a wavelength a finite flow of energy in positive y-direction, and then the same amount of energy is flowing back in negative y-direction for the next quarter wavelength. Thus the mean energy flow in y-direction during each half wavelength is zero. But there is no change of signs in $S_{b,x}$, and consequently there is a net energy flow of the evanescent field in x-direction. This result is confirmed by the experimentally observed Goos-Hänchen shift (described in section 2).

The change of a phase-angle by π is equivalent to the inversion of the respective amplitude's direction. As we did not yet fix the directions of amplitudes, we are free to decide the alternatives (65) *by definition*. We decide for these assignments:

$$\begin{aligned}
&\text{at arbitrary } \vartheta_e : \\
&\quad \varphi_{e,B} = \varphi_{e,E} && \text{(67a)} \\
&\quad \varphi_{r,B} = \varphi_{r,E} + \pi && \text{(67b)} \\
&\text{at } \vartheta_e \leq \vartheta_{e,\text{critical}} : \\
&\quad \varphi_{b,B} = \varphi_{b,E} && \text{(67c)} \\
&\text{at } \vartheta_e > \vartheta_{e,\text{critical}} : \\
&\quad \varphi_{b,B_x} = \varphi_{b,E_z} - \pi/2 && \text{(67d)} \\
&\quad \varphi_{b,B_y} = \varphi_{b,E_z} && \text{(67e)} \\
&\quad \varphi_{b,E_x} = \varphi_{b,B_z} - \pi/2 && \text{(67f)} \\
&\quad \varphi_{b,E_y} = \varphi_{b,B_z} && \text{(67g)}
\end{aligned}$$

Note that the assignments (67e) and (67g) are unique, because $S_{b,x} =$ (66b) must be positive for either polarization, to match the Goos-Hänchen shift. All other assignments are arbitrary. We just must take care to stay consistent in the sequel. As only the relative values of the various phase-angles matter, we may choose one of the phase-angles arbitrarily. We decide for

$$\varphi_{e,E} = 0 \ . \qquad \text{(67h)}$$

Furthermore we choose by definition for all fields

$$\begin{aligned}
\text{at perpendicular polarization:} \quad & \hat{E}_z = \hat{E} \geq 0 && \text{(67i)} \\
\text{at parallel polarization:} \quad & \hat{B}_z = \hat{B} \geq 0 \ , && \text{(67j)}
\end{aligned}$$

i. e. these amplitudes are oriented in positive z-direction.

Inserting (64) and (67) into (63), we get

at perpendicular polarization and arbitrary ϑ_e :

$$\hat{B}_{e,x} = +\frac{1}{\omega}\, k_e \cos\vartheta_e\, \hat{E}_{e,z} \tag{68a}$$

$$\hat{B}_{e,y} = -\frac{1}{\omega}\, k_e \sin\vartheta_e\, \hat{E}_{e,z} \tag{68b}$$

$$\hat{B}_{r,x} = +\frac{1}{\omega}\, k_e \cos\vartheta_e\, \hat{E}_{r,z} \tag{68c}$$

$$\hat{B}_{r,y} = +\frac{1}{\omega}\, k_e \sin\vartheta_e\, \hat{E}_{r,z} \tag{68d}$$

at perpendicular polarization and $\vartheta_e \le \vartheta_{e,\mathrm{critical}}$:

$$\hat{B}_{b,x} = +\frac{1}{\omega}\, \frac{k_e n_b}{n_a}\, \cos\vartheta_b\, \hat{E}_{b,z} \tag{68e}$$

$$\hat{B}_{b,y} = -\frac{1}{\omega}\, \frac{k_e n_b}{n_a}\, \sin\vartheta_b\, \hat{E}_{b,z} \tag{68f}$$

at perpendicular polarization and $\vartheta_e > \vartheta_{e,\mathrm{critical}}$:

$$\hat{B}_{b,x} = +\frac{1}{\omega}\, \frac{i}{\gamma}\, \hat{E}_{b,z} e^{i\pi/2} = +\frac{1}{\omega}\, \frac{k_e n_b}{n_a}\, i \cos\vartheta_b\, \hat{E}_{b,z} \tag{68g}$$

$$\hat{B}_{b,y} = -\frac{1}{\omega}\, \frac{k_e n_b}{n_a}\, \sin\vartheta_b \hat{E}_{b,z} \tag{68h}$$

at parallel polarization and arbitrary ϑ_e :

$$\hat{E}_{e,x} = -\frac{1}{\omega\epsilon_a\mu_a}\, k_e \cos\vartheta_e\, \hat{B}_{e,z} \tag{68i}$$

$$\hat{E}_{e,y} = +\frac{1}{\omega\epsilon_a\mu_a}\, k_e \sin\vartheta_e\, \hat{B}_{e,z} \tag{68j}$$

$$\hat{E}_{r,x} = -\frac{1}{\omega\epsilon_a\mu_a}\, k_e \cos\vartheta_e\, \hat{B}_{r,z} \tag{68k}$$

$$\hat{E}_{r,y} = -\frac{1}{\omega\epsilon_a\mu_a}\, k_e \sin\vartheta_e\, \hat{B}_{r,z} \tag{68l}$$

at parallel polarization and $\vartheta_e \le \vartheta_{e,\text{critical}}$:

$$\hat{E}_{b,x} = -\frac{1}{\omega\epsilon_b\mu_b}\,\frac{k_e n_b}{n_a}\,\cos\vartheta_b\,\hat{B}_{b,z} \tag{68m}$$

$$\hat{E}_{b,y} = +\frac{1}{\omega\epsilon_b\mu_b}\,\frac{k_e n_b}{n_a}\,\sin\vartheta_b\,\hat{B}_{b,z} \tag{68n}$$

at parallel polarization and $\vartheta_e > \vartheta_{e,\text{critical}}$:

$$\hat{E}_{b,x} = -\frac{1}{\omega\epsilon_b\mu_b}\,\frac{i}{\gamma}\,\hat{B}_{b,z}e^{i\pi/2} = -\frac{1}{\omega\epsilon_b\mu_b}\,\frac{k_e n_b}{n_a}\,i\cos\vartheta_b\,\hat{B}_{b,z} \tag{68o}$$

$$\hat{E}_{b,y} = +\frac{1}{\omega\epsilon_b\mu_b}\,\frac{k_e n_b}{n_a}\,\sin\vartheta_b\,\hat{B}_{b,z} \tag{68p}$$

We know that for plain waves the relation

$$\text{p. w. :}\quad E \overset{(22)}{=} \frac{\omega}{k}\,B = \frac{1}{\sqrt{\epsilon\mu}}\,B = \frac{k}{\omega\epsilon\mu}\,B \tag{69a}$$

holds. Considering (68), it's obviously quite reasonable to *define* the amplitudes of the evanescent fields by

$$\text{at } \vartheta_e > \vartheta_{e,\text{critical}}\text{ :}$$
$$\hat{E}_b \equiv \frac{k_e n_b}{n_a\omega\epsilon\mu}\,\hat{B}_b \quad , \quad \hat{B}_b \equiv \frac{k_e n_b}{n_a\omega}\,\hat{E}_b\ . \tag{69b}$$

Furthermore we define

$$\widetilde{\cos}\,\vartheta_b \equiv \begin{cases} \cos\vartheta_b & \text{if } \vartheta_e \le \vartheta_{e,\text{critical}} \\ i\cos\vartheta_b & \text{if } \vartheta_e > \vartheta_{e,\text{critical}} \end{cases} \quad , \quad \widetilde{\cos}\,\vartheta_b \in \mathbb{R}\ . \tag{70}$$

Inserting (69) and (70) into (68), we get for arbitrary ϑ_e

at perpendicular polarization :

$$\hat{B}_{e,x} = +\hat{B}_e\cos\vartheta_e \qquad \hat{B}_{e,y} = -\hat{B}_e\sin\vartheta_e \tag{71a}$$

$$\hat{B}_{r,x} = +\hat{B}_r\cos\vartheta_e \qquad \hat{B}_{r,y} = +\hat{B}_r\sin\vartheta_e \tag{71b}$$

$$\hat{B}_{b,x} = +\hat{B}_b \widetilde{\cos}\,\vartheta_b \qquad \hat{B}_{b,y} = -\hat{B}_b \sin\vartheta_b \tag{71c}$$

at parallel polarization :

$$\hat{E}_{e,x} = -\hat{E}_e \cos\vartheta_e \qquad \hat{E}_{e,y} = +\hat{E}_e \sin\vartheta_e \tag{71d}$$

$$\hat{E}_{r,x} = -\hat{E}_r \cos\vartheta_e \qquad \hat{E}_{r,y} = -\hat{E}_r \sin\vartheta_e \tag{71e}$$

$$\hat{E}_{b,x} = -\hat{E}_b \widetilde{\cos}\,\vartheta_b \qquad \hat{E}_{b,y} = +\hat{E}_b \sin\vartheta_b \ . \tag{71f}$$

Note that all amplitudes are real.

Now we have all necessary tools at hand, to fully exploit the relations (60). We eliminate the magnetic fields by means of (63), insert $\varphi_{e,E} \overset{(67h)}{=} 0$, insert the wave-vector components (64), and insert the amplitude components (71). Using

$$\sin^2\vartheta + \cos^2\vartheta = 1$$

$$\sin\vartheta_e = \frac{n_b}{n_a}\,\sin\vartheta_b$$

$$\text{at } \vartheta_e > \vartheta_{e,\text{critical}} : \quad \varphi_{b,B_z} \overset{(67)}{=} \varphi_{b,E_y} \overset{(67)}{=} \varphi_{b,E_x} + \pi/2 \tag{72}$$

we get

at perpendicular polarization ($\boldsymbol{E}_z = \boldsymbol{E}$) :

at $\vartheta_e \le \vartheta_{e,\text{critical}}$:

$$\hat{E}_{b,z} e^{i\varphi_{b,E}} = \hat{E}_{e,z} + \hat{E}_{r,z} e^{i\varphi_{r,E}} \tag{73a}$$

$$\cos\vartheta_b \hat{E}_{b,z} e^{i\varphi_{b,E}} = \frac{n_a}{n_b}\,\frac{\mu_b}{\mu_a}\,\cos\vartheta_e \left(\hat{E}_{e,z} - \hat{E}_{r,z} e^{i\varphi_{r,E}}\right) \tag{73b}$$

$$\hat{E}_{b,z} e^{i\varphi_{b,E}} = \hat{E}_{e,z} + \hat{E}_{r,z} e^{i\varphi_{r,E}} \tag{73c}$$

at $\vartheta_e > \vartheta_{e,\text{critical}}$:

$$\hat{E}_{b,z} e^{i\varphi_{b,E_z}} = \hat{E}_{e,z} + \hat{E}_{r,z} e^{i\varphi_{r,E}} \tag{73d}$$

$$\cos\vartheta_b \hat{E}_{b,z} e^{i\varphi_{b,E_z}} = \frac{n_a}{n_b}\,\frac{\mu_b}{\mu_a}\,\cos\vartheta_e \left(\hat{E}_{e,z} - \hat{E}_{r,z} e^{i\varphi_{r,E}}\right) \tag{73e}$$

$$\hat{E}_{b,z} e^{i\varphi_{b,E_z}} = \hat{E}_{e,z} + \hat{E}_{r,z} e^{i\varphi_{r,E}} \tag{73f}$$

at parallel polarization ($\boldsymbol{B}_z = \boldsymbol{B}$) :

at $\vartheta_e \le \vartheta_{e,\mathrm{critical}}$:

$$\hat{E}_b \cos\vartheta_b e^{i\varphi_{b,E}} = \cos\vartheta_e \left(\hat{E}_e + \hat{E}_r e^{i\varphi_{r,E}}\right) \tag{73g}$$

$$\hat{E}_b e^{i\varphi_{b,E}} = \frac{n_a}{n_b}\frac{\mu_b}{\mu_a}\left(\hat{E}_e - \hat{E}_r e^{i\varphi_{r,E}}\right) \tag{73h}$$

$$\hat{E}_b e^{i\varphi_{b,E}} = \frac{n_b}{n_a}\frac{\epsilon_a}{\epsilon_b}\left(\hat{E}_e - \hat{E}_r e^{i\varphi_{r,E}}\right) \tag{73i}$$

at $\vartheta_e > \vartheta_{e,\mathrm{critical}}$:

$$\hat{E}_b \widetilde{\cos}\,\vartheta_b e^{i\varphi_{b,E_x}} = \cos\vartheta_e \left(\hat{E}_e + \hat{E}_r e^{i\varphi_{r,E}}\right) \tag{73j}$$

$$\hat{E}_b e^{i(\varphi_{b,E_x}+\pi/2)} = \frac{n_a}{n_b}\frac{\mu_b}{\mu_a}\left(\hat{E}_e - \hat{E}_r e^{i\varphi_{r,E}}\right) \tag{73k}$$

$$\hat{E}_b e^{i\varphi_{b,E_y}} = \frac{n_b}{n_a}\frac{\epsilon_a}{\epsilon_b}\left(\hat{E}_e - \hat{E}_r e^{i\varphi_{r,E}}\right) \tag{73l}$$

The equations for under- and over-critical ϑ_e are formally identical because of (72) and because

$$\text{at perpendicular polarization } (\boldsymbol{E}_z = \boldsymbol{E}) : \ \varphi_{b,E} \equiv \varphi_{b,E_z} \tag{74a}$$

$$\text{at parallel polarization } (\boldsymbol{B}_z = \boldsymbol{B}) : \ \varphi_{b,B} \equiv \varphi_{b,B_z} \ . \tag{74b}$$

Furthermore equations (73a) and (73c) are identical. And (73h) and (73i) are identical because of

$$\frac{n_a}{n_b}\frac{\mu_b}{\mu_a} = \frac{\sqrt{\epsilon_a\mu_a}}{\sqrt{\epsilon_b\mu_b}}\frac{\mu_b}{\mu_a} = \frac{\epsilon_a}{\epsilon_b}\frac{\sqrt{\epsilon_b\mu_b}}{\sqrt{\epsilon_a\mu_a}} = \frac{n_b}{n_a}\frac{\epsilon_a}{\epsilon_b} \ . \tag{75}$$

Thus for each polarization there are two linearly independent equations, which are valid for arbitrary ϑ_e:

at perpendicular polarization ($\boldsymbol{E}_z = \boldsymbol{E}$) :

$$\hat{E}_b e^{i\varphi_{b,E}} = \hat{E}_e + \hat{E}_r e^{i\varphi_{r,E}} \tag{76a}$$

$$\cos\vartheta_b \hat{E}_b e^{i\varphi_{b,E}} = \frac{n_a}{n_b}\frac{\mu_b}{\mu_a}\cos\vartheta_e\left(\hat{E}_e - \hat{E}_r e^{i\varphi_{r,E}}\right) \tag{76b}$$

at parallel polarization ($\boldsymbol{B}_z = \boldsymbol{B}$) :

$$\hat{E}_b \cos\vartheta_b e^{i\varphi_{b,E}} = \cos\vartheta_e\left(\hat{E}_e + \hat{E}_r e^{i\varphi_{r,E}}\right) \tag{76c}$$

$$\hat{E}_b e^{i\varphi_{b,E}} = \frac{n_a}{n_b}\frac{\mu_b}{\mu_a}\left(\hat{E}_e - \hat{E}_r e^{i\varphi_{r,E}}\right) \tag{76d}$$

The phase-angles φ of the fields will turn out to be different at different polarizations. As only the phase-angles of the electrical fields are showing up in (76), we stipulate an especially simple notation for them:

$$\varphi_\perp \equiv \varphi_{r,E} \text{ at perpendicular polarization} \tag{77a}$$

$$\varphi_\parallel \equiv \varphi_{r,E} \text{ at parallel polarization} \tag{77b}$$

$$\varphi_{b\perp} \equiv \varphi_{b,E} \text{ at perpendicular polarization} \tag{77c}$$

$$\varphi_{b\parallel} \equiv \varphi_{b,E} \text{ at parallel polarization} \tag{77d}$$

Remember that we have according to (72) and (73)

at $\vartheta_e > \vartheta_{e,\text{critical}}$:

$$\varphi_{b\perp} \equiv \varphi_{b,E} = \varphi_{b,E_z} \tag{77e}$$

$$\varphi_{b\parallel} \equiv \varphi_{b,E} = \varphi_{b,E_y} = \varphi_{b,E_x} + \pi/2\ . \tag{77f}$$

Thereby we extract from (76) these Fresnel-coefficients:

at perpendicular polarization:

$$\tau_\perp \equiv \frac{\hat{E}_b e^{i\varphi_{b\perp}}}{\hat{E}_e} = \frac{2n_a\mu_b\cos\vartheta_e}{n_a\mu_b\cos\vartheta_e + n_b\mu_a\cos\vartheta_b} \tag{78a}$$

$$\rho_\perp \equiv \frac{\hat{E}_r e^{i\varphi_\perp}}{\hat{E}_e} = \frac{n_a\mu_b\cos\vartheta_e - n_b\mu_a\cos\vartheta_b}{n_a\mu_b\cos\vartheta_e + n_b\mu_a\cos\vartheta_b} \tag{78b}$$

at parallel polarization:

$$\tau_{\parallel} \equiv \frac{\hat{E}_b e^{i\varphi_{b\parallel}}}{\hat{E}_e} = \frac{2n_a\mu_b\cos\vartheta_e}{n_b\mu_a\cos\vartheta_e + n_a\mu_b\cos\vartheta_b} \tag{78c}$$

$$\rho_{\parallel} \equiv \frac{\hat{E}_r e^{i\varphi_{\parallel}}}{\hat{E}_e} = \frac{-n_b\mu_a\cos\vartheta_e + n_a\mu_b\cos\vartheta_b}{n_b\mu_a\cos\vartheta_e + n_a\mu_b\cos\vartheta_b} \tag{78d}$$

If $\boldsymbol{k}_b \in \mathbb{R}$, then all fields are plane waves. That's always the case if $n_b > n_a$, but only for $\vartheta_e \leq \vartheta_{e,\text{critical}}$ if $n_a > n_b$. For this case we now can determine all phase-angles. On the right sides of the equations (78), all factors are real at under-critical incoming angles. The amplitudes as well are real and ≥ 0 according to (61). Thus the phase angles can only be 0 or π. $\tau_{\perp} \geq 0$ and $\tau_{\parallel} \geq 0$ imply $\varphi_{b\perp} = 0$ and $\varphi_{b\parallel} = 0$. On the other hand, $\varphi_{\perp}$ and $\varphi_{\parallel}$ can be zero or π, depending on the relative magnitudes of the two terms in the numerators of $\rho_{\perp}$ and $\rho_{\parallel}$. Thus we can complete the list (67) of phase-angles:

at arbitrary ϑ_e :

$$\varphi_{e,E} \overset{(67h)}{=} 0 \overset{(67)}{=} \varphi_{e,B} \tag{79a}$$

at $\vartheta_e \leq \vartheta_{e,\text{critical}}$:

$$\varphi \overset{(77)}{=} \varphi_{r,E} = (0 \text{ OR } \pi) \quad , \quad \varphi_{r,B} \overset{(67)}{=} \varphi_{r,E} + \pi \tag{79b}$$

$$\varphi_b \overset{(77)}{=} \varphi_{b,E} = 0 \overset{(67)}{=} \varphi_{b,B} \tag{79c}$$

at $\vartheta_e > \vartheta_{e,\text{critical}}$:

$$\varphi \overset{(77)}{=} \varphi_{r,E} = \varphi_{r,B} - \pi \tag{79d}$$

$$\varphi_{b,B_x} \overset{(67)}{=} \varphi_{b,E_z} - \pi/2 \tag{79e}$$

$$\varphi_{b,B_y} \overset{(67)}{=} \varphi_{b,E_z} \tag{79f}$$

$$\varphi_{b,E_x} \overset{(67)}{=} \varphi_{b,B_z} - \pi/2 \tag{79g}$$

$$\varphi_{b,E_y} \overset{(67)}{=} \varphi_{b,B_z} \tag{79h}$$

According to (62a), the three vectors $\boldsymbol{k}, \boldsymbol{E}, \boldsymbol{B}$ respectively — after common phase factors have been canceled — the three vectors $\boldsymbol{k}, \hat{\boldsymbol{E}}e^{i\varphi_E}, \hat{\boldsymbol{B}}e^{i\varphi_B}$ must form a right-handed orthogonal system if $\boldsymbol{k} \in \mathbb{R}$. We check that by means of figures 6 and 7, in which the equations (71) are displayed graphically.

$\hat{E}_{e,z}$ in fig. 6 and $\hat{B}_{e,z}$ in fig. 7 are positive according to (67i),

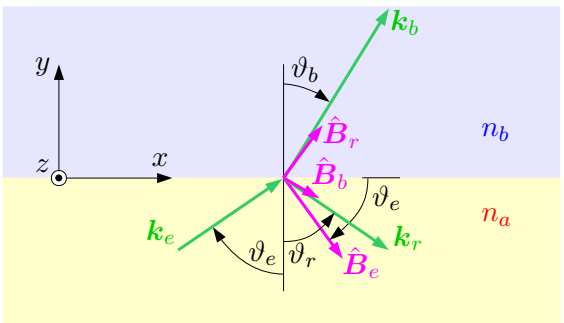

Fig. 6 : Perpendicular polarization, $\varphi_{r,E} = \pi$, $\varphi_{r,B} = 0$

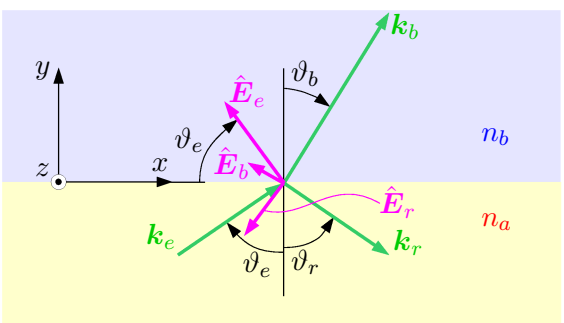

Fig. 7 : Parallel polarization, $\varphi_{r,E} = 0$, $\varphi_{r,B} = \pi$

i. e. they are pointing upwards out of the drawing plane. The three vectors $\boldsymbol{k}_e, \hat{\boldsymbol{E}}_e, \hat{\boldsymbol{B}}_e$ are forming right-handed systems in both drawings.

The three vectors $\boldsymbol{k}_b, \hat{\boldsymbol{E}}_b, \hat{\boldsymbol{B}}_b$ as well are forming right-handed systems in both drawings, in accord with our assignments $\varphi_b = \varphi_{b,E} = 0$ and $\varphi_{b,B} = 0$ in case $\vartheta_e \leq \vartheta_{e,\mathrm{critical}}$.

The three vectors $\boldsymbol{k}_r, \hat{\boldsymbol{E}}_r, \hat{\boldsymbol{B}}_r$ are forming left-handed systems in

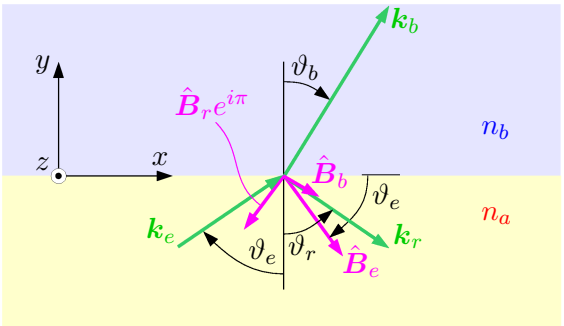

Fig. 8 : Perpendicular polarization, $\varphi_{r,E} = 0$, $\varphi_{r,B} = \pi$

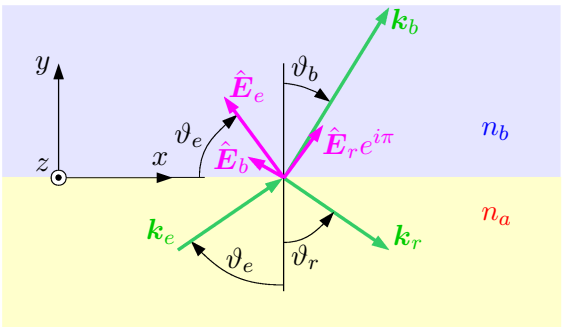

Fig. 9 : Parallel polarization, $\varphi_{r,E} = \pi$, $\varphi_{r,B} = 0$

both drawings. Thus we either must have ($\varphi_{r,E} = \pi$ AND $\varphi_{r,B} = 0$) or ($\varphi_{r,E} = 0$ AND $\varphi_{r,B} = \pi$), to achieve a right-handed system $\boldsymbol{k}_r, \boldsymbol{E}_r, \boldsymbol{B}_r$. The first alternative is drawn in figures 6 and 9, the second alternative in figures 7 and 8. Again our assignments in (79) are confirmed.

We have a closer look at $\varphi_{r,E} \equiv \varphi_\perp$ resp. $\varphi_{r,E} \equiv \varphi_\parallel$ at $\vartheta_e \leq \vartheta_{e,\text{critical}}$:

For perpendicular polarized radiation and $\boldsymbol{k}_b \in \mathbb{R}$

the phase-angle $\varphi_\perp$ must be zero if $n_b\mu_a \cos\vartheta_b < n_a\mu_b \cos\vartheta_e$. This means that the field $\boldsymbol{B}$, but not the field $\boldsymbol{E}$, makes a phase-jump of π upon reflection. (80a)

the phase-angle $\varphi_\perp$ must be π if $n_b\mu_a \cos\vartheta_b > n_a\mu_b \cos\vartheta_e$. This means that the field $\boldsymbol{E}$, but not the field $\boldsymbol{B}$, makes a phase-jump of π upon reflection. (80b)

there is no phase-jump if $n_b\mu_a \cos\vartheta_b = n_a\mu_b \cos\vartheta_e$ for the trivial reason that there is no reflected field: $\rho_\perp = 0$ and $\tau_\perp = 1$. The angle $\vartheta_{e,\text{Brewster}} = \arccos[(n_b\mu_a/n_a\mu_b)\cos\vartheta_b]$ is called Brewster-angle. (80c)

For parallel polarized radiation and $\boldsymbol{k}_b \in \mathbb{R}$

the phase-angle $\varphi_\parallel$ must be zero if $n_b\mu_a \cos\vartheta_e < n_a\mu_b \cos\vartheta_b$. This means that the field $\boldsymbol{B}$, but not the field $\boldsymbol{E}$, makes a phase-jump of π upon reflection. (81a)

the phase-angle $\varphi_\parallel$ must be π if $n_b\mu_a \cos\vartheta_e > n_a\mu_b \cos\vartheta_b$. This means that the field $\boldsymbol{E}$, but not the field $\boldsymbol{B}$, makes a phase-jump of π upon reflection. (81b)

there is no phase-jump if $n_b\mu_a \cos\vartheta_e = n_a\mu_b \cos\vartheta_b$ for the trivial reason that there is no reflected field: $\rho_\parallel = 0$ and $\tau_\parallel = 1$. The angle $\vartheta_{e,\text{Brewster}} = \arccos[(n_a\mu_b/n_b\mu_a)\cos\vartheta_b]$ is called Brewster-angle. (81c)

The condition (80c) for the Brewster-angle at perpendicular polarization can be written in the form

$$\frac{n_b \cos\vartheta_b}{n_a \cos\vartheta_e} = \frac{\mu_b}{\mu_a} \ . \tag{82a}$$

If $n_b > n_a$, then $\cos\vartheta_e$ approaches zero faster than $\cos\vartheta_b$ at increasing ϑ_e. Thus (82a) has a solution if and only if $n_b/n_a < \mu_b/\mu_a$. On the other hand, if $n_b < n_a$ then $\cos\vartheta_b$ approaches zero faster than $\cos\vartheta_e$ at increasing ϑ_e. Thus (82a) has a solution if and only if $n_b/n_a > \mu_b/\mu_a$. In total, this condition holds at perpendicular polarization:

$$\exists \text{ Brewster-angle}_\perp \iff \begin{cases} n_b > n_a \text{ AND } n_b/n_a < \mu_b/\mu_a \\ n_b < n_a \text{ AND } n_b/n_a > \mu_b/\mu_a \end{cases} \tag{82b}$$

The character $\exists$ stands for "exists".

The condition (81c) for the Brewster-angle at parallel polarization can be written in the form

$$\frac{n_b \cos\vartheta_e}{n_a \cos\vartheta_b} = \frac{\mu_b}{\mu_a} \ . \tag{82c}$$

By the same consideration as in case of perpendicular polarization, we arrive at the following conditions for the existence of a Brewster-angle at parallel polarization:

$$\exists \text{ Brewster-angle}_\parallel \iff \begin{cases} n_b > n_a \text{ AND } n_b/n_a > \mu_b/\mu_a \\ n_b < n_a \text{ AND } n_b/n_a < \mu_b/\mu_a \end{cases} \tag{82d}$$

The conditions (82b) and (82d) are mutually excluding, i. e. for any combination of materials with given ratios n_b/n_a and μ_b/μ_a there exists a Brewster-angle either *only* at perpendicular or *only* at parallel polarization. As in the frequent case $\mu_b = \mu_a$ the

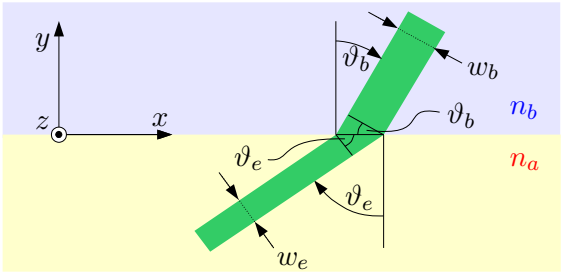

Fig. 10: The quotient w_b/w_e

condition (82d) is met, the Brewster-angle usually appears at parallel polarization, but only with exotic[2] material combinations at perpendicular polarization.

The energy-density of a plane electromagnetic wave is

$$\frac{1}{2}\Big(\epsilon|\boldsymbol{E}|^2 + |\boldsymbol{B}|^2/\mu\Big) \overset{(22)}{=} \epsilon|\boldsymbol{E}|^2 \ . \tag{83}$$

The coefficient R of reflection, and the coefficient T of transmission, are defined by

$$R = \frac{\text{reflected power}}{\text{incoming power}} = \frac{|\boldsymbol{E}_r|^2}{|\boldsymbol{E}_e|^2} \tag{84a}$$

$$T = \frac{\text{transmitted power}}{\text{incoming power}} = \frac{\epsilon_b|\boldsymbol{E}_b|^2 \cdot w_b \cdot c/n_b}{\epsilon_a|\boldsymbol{E}_e|^2 \cdot w_e \cdot c/n_a} \ . \tag{84b}$$

The definition of $w_b/w_e = \cos\vartheta_b/\cos\vartheta_e$ is explained in fig. 10. The ratio of the velocities of light in the two media is

$$\frac{c/n_b}{c/n_a} \overset{(18)}{=} \frac{\sqrt{\epsilon_a\mu_a}}{\sqrt{\epsilon_b\mu_b}} \ . \tag{85}$$

[2] I don't know whether such material combinations exist at all. Informations from readers are welcome.
mailto: gerold.gruendler@astrophys-neunhof.de

Using $|\boldsymbol{E}_r|^2/|\boldsymbol{E}_e|^2 = |\rho|^2$ and $|\boldsymbol{E}_b|^2/|\boldsymbol{E}_e|^2 = |\tau|^2$, we get

$$\text{if } \boldsymbol{k}_b \in \mathbb{R} \begin{cases} R_\perp = |\rho_\perp|^2 & \text{(86a)} \\ T_\perp = |\tau_\perp|^2 \dfrac{n_b}{n_a} \dfrac{\mu_a}{\mu_b} \dfrac{\cos\vartheta_b}{\cos\vartheta_e} & \text{(86b)} \\ R_\parallel = |\rho_\parallel|^2 & \text{(86c)} \\ T_\parallel = |\tau_\parallel|^2 \dfrac{n_b}{n_a} \dfrac{\mu_a}{\mu_b} \dfrac{\cos\vartheta_b}{\cos\vartheta_e} \,. & \text{(86d)} \end{cases}$$

All factors except of $|\rho^2|$ cancel in the coefficients of reflection.

$n = 1.5$, $\mu_r = 1$ are typical parameters of glasses used in optical instruments. $n = \mu_r = 1$ is a good approximation for air. The Fresnel-coefficients for the combination of these materials are displayed as a function of the incoming angle ϑ_e in two diagrams on page 42. The corresponding diagrams of the coefficients of reflection and transmission are displayed on page 43. In case $n_a/n_b = 1.5$ the critical angle is $\vartheta_{e,\text{critical}} = 0.23\,\pi$. The entries for over-critical incoming angles will be explained later. For the moment being we continue to consider the case $\vartheta_e \le \vartheta_{e,\text{critical}}$, i. e. $\boldsymbol{k}_b \in \mathbb{R}$.

If radiation is coming-in under the Brewster-angles $0.31\,\pi = 56°$ (at refraction from a = air into b = glass) resp. $0.19\,\pi = 34°$ (at refraction from a = glass into b = air), then $\rho_\parallel = 0$, $R_\parallel = 0$, and $T_\parallel = 1$. Consequently the radiation reflected under these angles is completely polarized perpendicular to the xy-plane (i. e. parallel to the boundary surface of the media). From (80) follows: When perpendicular polarized radiation, coming in from air, is refracted at the glass surface, then the wave's electric field gets a phase shift of π upon reflection. When perpendicular polarized radiation, coming in from glass, is refracted at the air surface, then the wave's magnetic field gets a phase shift of π upon reflection.

From (81) follows: When parallel polarized radiation, coming in from air, is refracted at the glass surface under an angle $\vartheta_e <$

$\vartheta_{\text{Brewster}}$, then the wave's electric field gets a phase shift of π upon reflection. But if the incoming angle is $\vartheta_e > \vartheta_{\text{Brewster}}$, then the wave's magnetic field gets a phase shift of π upon reflection. If parallel polarized radiation, coming in from glass, is refracted at the air surface, then in case $\vartheta_e < \vartheta_{\text{Brewster}}$ the magnetic field, but in case $\vartheta_e > \vartheta_{\text{Brewster}}$ the electric field of the wave gets a phase shift of π upon reflection.

Diagrams of the phase-angles for $n_a/n_b = 1/1.5$ resp. $n_a/n_b = 1.5$ with $\mu_a = \mu_b$ can be found on page 47. The entries for over-critical incoming angles ($\vartheta_{e,\text{critical}} = 0.23\,\pi$ in case of $n_a/n_b = 1.5$) will be explained in the sequel.

To discuss the Fresnel-coefficients at over-critical incoming angles, we insert

$$\cos\vartheta_b \overset{(52)}{=} i\,{}_{+}\sqrt{(n_a/n_b)^2\sin^2\vartheta_e - 1} \tag{87}$$

into (78), and get

if $\vartheta_e > \vartheta_{e,\text{critical}}$:

$$\tau_\perp \equiv \frac{\hat{E}_b e^{i\varphi_{b\perp}}}{\hat{E}_e} = \frac{2n_a\mu_b\cos\vartheta_e}{n_a\mu_b\cos\vartheta_e + in_b\mu_a\,{}_{+}\sqrt{(n_a/n_b)^2\sin^2\vartheta_e - 1}} \tag{88a}$$

$$\rho_\perp \equiv \frac{\hat{E}_r e^{i\varphi_\perp}}{\hat{E}_e} = \frac{n_a\mu_b\cos\vartheta_e - in_b\mu_a\,{}_{+}\sqrt{(n_a/n_b)^2\sin^2\vartheta_e - 1}}{n_a\mu_b\cos\vartheta_e + in_b\mu_a\,{}_{+}\sqrt{(n_a/n_b)^2\sin^2\vartheta_e - 1}} \tag{88b}$$

$$\tau_\parallel \equiv \frac{\hat{E}_b e^{i\varphi_{b\parallel}}}{\hat{E}_e} = \frac{2n_a\mu_b\cos\vartheta_e}{n_b\mu_a\cos\vartheta_e + in_a\mu_b\,{}_{+}\sqrt{(n_a/n_b)^2\sin^2\vartheta_e - 1}} \tag{88c}$$

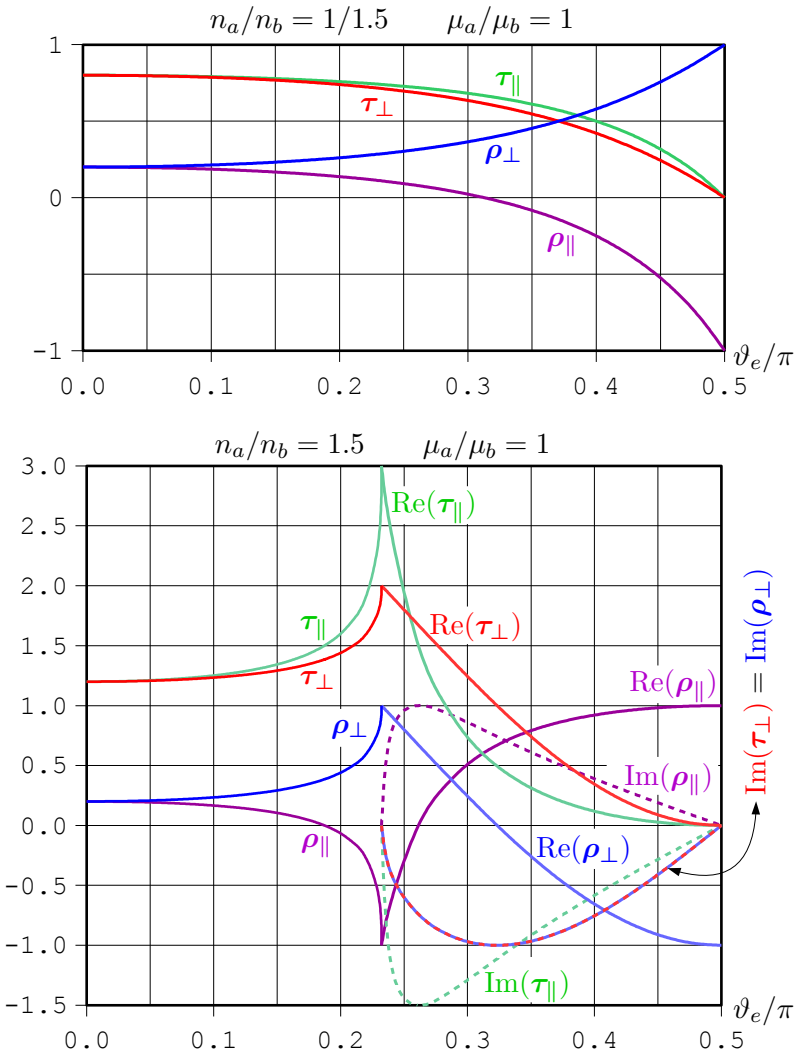

Fig. 11 : Fresnel-coefficients

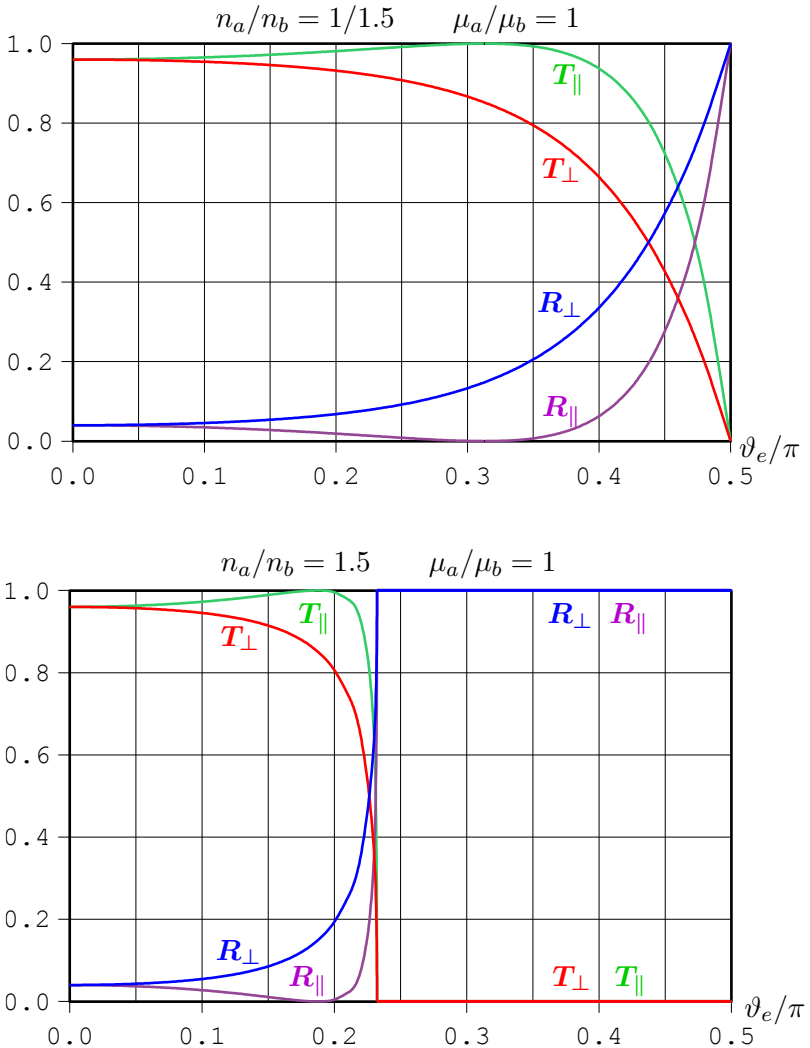

Fig. 12: Coefficients of reflection and transmission

$$\rho_{\parallel} \equiv \frac{\hat{E}_r e^{i\varphi_{\parallel}}}{\hat{E}_e} = \frac{-n_b\mu_a \cos\vartheta_e + in_a\mu_b \sqrt{(n_a/n_b)^2 \sin^2\vartheta_e - 1}}{n_b\mu_a \cos\vartheta_e + in_a\mu_b \sqrt{(n_a/n_b)^2 \sin^2\vartheta_e - 1}} \tag{88d}$$

One immediately discerns

$$\begin{aligned} &\text{if } \vartheta_e > \vartheta_{e,\text{critical}} : \\ &R_{\perp} = |\rho_{\perp}|^2 = 1 \qquad , \qquad R_{\parallel} = |\rho_{\parallel}|^2 = 1 \ . \end{aligned} \tag{89}$$

This result is confirmed by experience: Radiation, which is coming in at over-critical angles, is 100 % reflected.

The coefficients of transmission can not be computed by means of the Fresnel-coefficients τ in case of $\vartheta_e > \vartheta_{e,\text{critical}}$, because the parameter w_b, which was applied in (84b), is not defined. Therefore (84) is replaced by

$$\text{if } \vartheta_e > \vartheta_{e,\text{critical}} :$$

$$R = \frac{\text{reflected power}}{\text{incoming power}} = \frac{|\boldsymbol{E}_r|^2}{|\boldsymbol{E}_e|^2} \overset{(86)}{=} |\rho|^2 \overset{(89)}{=} 1 \tag{90a}$$

$$T = \frac{\text{transmitted power}}{\text{incoming power}} = 1 - R = 0 \ . \tag{90b}$$

"Transmitted power" in this context does mean the power, which can be measured far-off the boundary surface (strictly speaking at infinitely large distance), because nearby the boundary surface in medium b the evanescent field is different from zero. Alternatively, "transmitted power" may be interpreted as the mean value over time of the power transmitted from medium a into medium b. That mean value is zero, as the incoming power is eventually totally flowing back into medium a with the reflected wave. We will see immediately that the phase-angles $\varphi_{\perp}$ and $\varphi_{\parallel}$ are different from zero and different from π if $\vartheta_e > \vartheta_{e,\text{critical}}$. This fact is an indication

for the time-offset between the transport of energy to the boundary surface with the incoming wave, and the back-flow of energy with the reflected wave.

For the material parameters $n_a/n_b = 1.5$ and $\mu_a = \mu_b$, the coefficients (90) are displayed in the bottom diagram of fig. 12 on page 43.

We divide the Fresnel-coefficients (88) into their real and imaginary parts:

$$\text{if } \vartheta_e > \vartheta_{e,\text{critical}} :$$

$$\tau_\perp = \frac{2n_a\mu_b \cos\vartheta_e (n_a\mu_b \cos\vartheta_e - in_b\mu_a \sqrt[+]{(n_a/n_b)^2 \sin^2\vartheta_e - 1})}{n_a^2\mu_b^2 \cos^2\vartheta_e + n_b^2\mu_a^2[(n_a/n_b)^2 \sin^2\vartheta_e - 1]} \tag{91a}$$

$$\begin{aligned}\rho_\perp = {} & \frac{1}{n_a^2\mu_b^2 \cos^2\vartheta_e + n_b^2\mu_a^2[(n_a/n_b)^2 \sin^2\vartheta_e - 1]} \cdot \\ & \cdot \Big(n_a^2\mu_b^2 \cos^2\vartheta_e - n_b^2\mu_a^2[(n_a/n_b)^2 \sin^2\vartheta_e - 1] - \\ & - i2n_a\mu_b \cos\vartheta_e n_b\mu_a \sqrt[+]{(n_a/n_b)^2 \sin^2\vartheta_e - 1} \Big)\end{aligned} \tag{91b}$$

$$\tau_\parallel = \frac{2n_a\mu_b \cos\vartheta_e (n_b\mu_a \cos\vartheta_e - in_a\mu_b \sqrt[+]{(n_a/n_b)^2 \sin^2\vartheta_e - 1})}{n_b^2\mu_a^2 \cos^2\vartheta_e + n_a^2\mu_b^2[(n_a/n_b)^2 \sin^2\vartheta_e - 1]} \tag{91c}$$

$$\begin{aligned}\rho_\parallel = {} & \frac{1}{n_b^2\mu_a^2 \cos^2\vartheta_e + n_a^2\mu_b^2[(n_a/n_b)^2 \sin^2\vartheta_e - 1]} \cdot \\ & \cdot \Big(- n_b^2\mu_a^2 \cos^2\vartheta_e + n_a^2\mu_b^2[(n_a/n_b)^2 \sin^2\vartheta_e - 1] + \\ & + i2n_b\mu_a \cos\vartheta_e n_a\mu_b \sqrt[+]{(n_a/n_b)^2 \sin^2\vartheta_e - 1} \Big)\end{aligned} \tag{91d}$$

For the material combination $n_a/n_b = 1.5$ with $\mu_a = \mu_b$, the real and imaginary parts of these coefficients are displayed in the bottom diagram of fig. 11 on page 42.

Combining (91) with

$$\text{if } \vartheta_e > \vartheta_{e,\text{critical}} :$$

$$|\rho|^2 \overset{(88)}{=} 1 \quad \overset{(88)}{\Longrightarrow} \quad \hat{E}_r = \hat{E}_e \quad \overset{(88)}{\Longrightarrow} \quad \rho = \cos\varphi + i \sin\varphi \,, \tag{92}$$

we can conclude: At $\vartheta_e \gtrsim \vartheta_{e,\text{critical}}$ we have $(n_a/n_b)^2 \sin^2\vartheta_e - 1 \gtrsim 0$. Then $\cos\varphi_\perp \lesssim 1$, $\sin\varphi_\perp \lesssim 0$, $\cos\varphi_\parallel \gtrsim -1$, and $\sin\varphi_\parallel \gtrsim 0$. Consequently $\varphi_\perp \lesssim 0$ and $\varphi_\parallel \lesssim \pi$.

At $\vartheta_e \lesssim \pi/2$ we have $\cos\vartheta_e \gtrsim 0$ and $(n_a/n_b)^2 \sin^2\vartheta_e - 1 > 0$. Then $\cos\varphi_\perp \gtrsim -1$, $\sin\varphi_\perp \lesssim 0$, $\cos\varphi_\parallel \lesssim 1$, and $\sin\varphi_\parallel \gtrsim 0$. Consequently $\varphi_\perp \gtrsim \pi$ and $\varphi_\parallel \gtrsim 0$.

After we have put straight the quadrants of the respective phase-angles, we can describe them clearly by means of the ambiguous arctangent function:

$$\text{if } \vartheta_e > \vartheta_{e,\text{critical}} :$$

$$\varphi_\perp = \arctan\left(\frac{-2n_a\mu_b\cos\vartheta_e n_b\mu_a\sqrt{(n_a/n_b)^2\sin^2\vartheta_e - 1}}{n_a^2\mu_b^2\cos^2\vartheta_e - n_b^2\mu_a^2[(n_a/n_b)^2\sin^2\vartheta_e - 1]}\right) \tag{93a}$$

$$\lesssim 0 \text{ at } \vartheta_e \gtrsim \vartheta_{e,\text{critical}} \quad , \quad \gtrsim \pi \text{ at } \vartheta_e \lesssim \pi/2$$

$$\varphi_\parallel = \arctan\left(\frac{-2n_b\mu_a\cos\vartheta_e n_a\mu_b\sqrt{(n_a/n_b)^2\sin^2\vartheta_e - 1}}{n_b^2\mu_a^2\cos^2\vartheta_e - n_a^2\mu_b^2[(n_a/n_b)^2\sin^2\vartheta_e - 1]}\right) \tag{93b}$$

$$\lesssim \pi \text{ at } \vartheta_e \gtrsim \vartheta_{e,\text{critical}} \quad , \quad \gtrsim 0 \text{ at } \vartheta_e \lesssim \pi/2$$

For the material combinations $n_a/n_b = 1/1.5$ and $n_a/n_b = 1.5$ with $\mu_a = \mu_b$, the phase-shifts $\varphi_\perp$ and $\varphi_\parallel$ are displayed in fig. 13 on the next page. There also the phase-angles for $\vartheta_e \leq \vartheta_{e,\text{critical}}$ are displayed, which we have stated in (80) and (81). $\varphi_\parallel$ jumps from π to zero at the Brewster-angle $0.31\,\pi$, resp. from zero to π at the Brewster-angle $0.19\,\pi$. And at the critical angle $0.23\,\pi$ (which of course does exist only in case $n_a > n_b$) both $\varphi_\perp$ and $\varphi_\parallel$ change continuously: In the curves there is a sharp bend, but no jump.

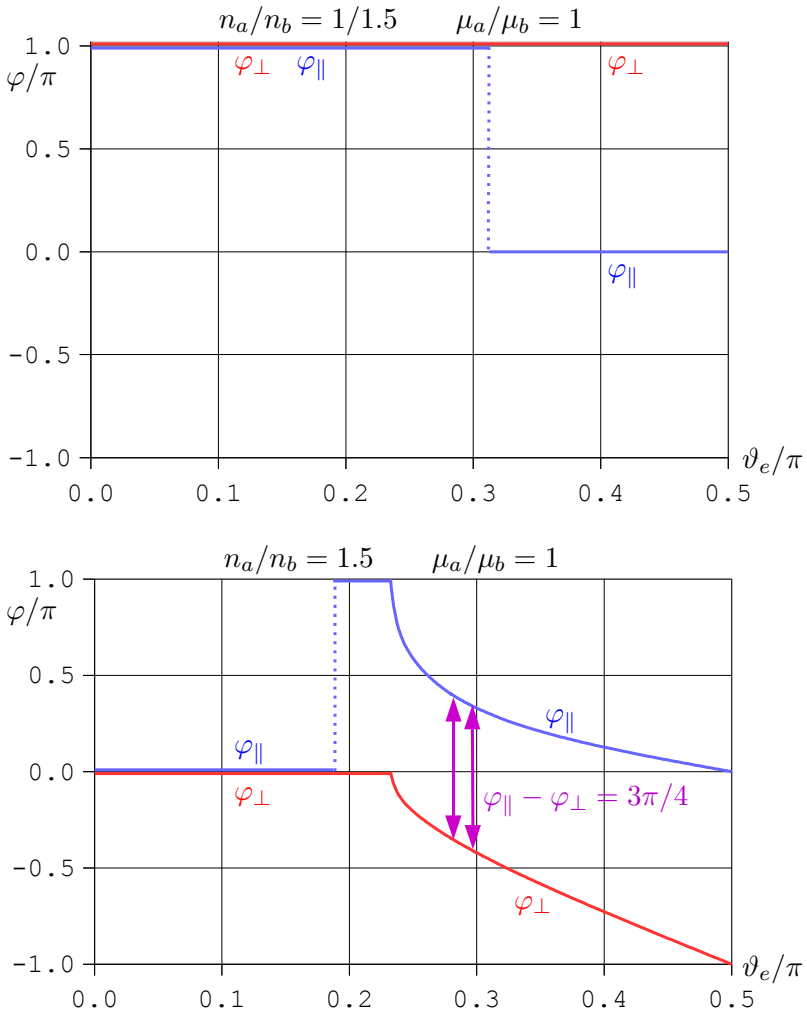

Fig. 13: The phase-shifts $\varphi_\perp$ and $\varphi_\parallel$

Sometimes the phase-angles are encountered with different signs in the literature. While $+\pi = -\pi$ modulo 2π, the sign of the phase-angle (which is a measurable quantity) is not arbitrary at $0 < |\varphi| < \pi$. The different signs are caused by different definitions: Many authors define φ as the angle, by which the phase of the reflected or the refracted field is running ahead the phase of the incoming field. According to our definition (15), however, φ is the angle by which the phase of the reflected or refracted field lags the phase of the incoming field.

The difference $\varphi_\parallel - \varphi_\perp$ is π at $\vartheta_{e,\mathrm{critical}}$, then decreases down to a minimum of $0.7487\,\pi$ at $\vartheta_e = 0.287\,\pi = 51.7°$, and then increases again up to π at $\vartheta_e = \pi/2$. Thus there exist two angles, namely $\vartheta_e = 0.279\,\pi = 50.2°$ and $\vartheta_e = 0.296\,\pi = 53.3°$, at which the difference $\varphi_\parallel - \varphi_\perp$ is exactly $0.75\,\pi$. These two angles are indicated in fig. 13 by purple arrows. In figure 14 a Fresnel-rhomb for the parameters $n_a/n_b = 1.5$, $\mu_a = \mu_b$, $\vartheta_e = 53.3°$ is drawn. If the incoming field is a linearly polarized plane wave with $\hat{E}_\perp = \hat{E}_\parallel$, then after two total reflections the phase of $\hat{E}_\parallel$ is lagging the phase of $\hat{E}_\perp$ by $3\pi/2 = -\pi/2$ modulo 2π: The linearly polarized wave has become a circularly polarized wave. If two Fresnel-rhombs are catenated, the output is again a linearly polarized wave,

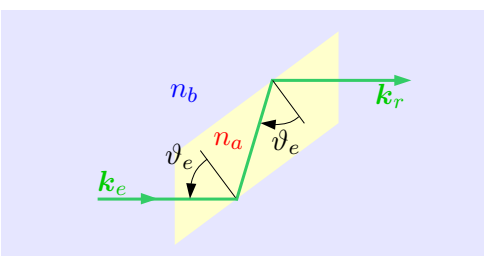

Fig. 14 : A Fresnel-rhomb

whose plane of polarization is turned 90° versus the incoming field. The functionality of Fresnel-rhombs has been checked in countless experiments, providing convincing evidence for the correctness of the reflective Fresnel-coefficients (88) and the phase-shifts (93).

Obviously $|\tau_\perp|^2 = |(88a)|^2 \neq 1$ and $|\tau_\parallel|^2 = |(88c)|^2 \neq 1$. Therefore the phase-angles can not be found by the same methods as applied in case of the reflective Fresnel-coefficients. Instead we compute the quotients $\hat{E}_b/\hat{E}_e$ of the amplitudes:

$$\text{if } \vartheta_e > \vartheta_{e,\text{critical}} :$$

$$\begin{aligned}\frac{\hat{E}_b}{\hat{E}_e} &\overset{(88a)}{=} \tau_\perp e^{-i\varphi_{b\perp}} \overset{(91a)}{=} \frac{2n_a\mu_b\cos\vartheta_e}{n_a^2\mu_b^2\cos^2\vartheta_e + n_a^2\mu_a^2\sin^2\vartheta_e - n_b^2\mu_a^2}\cdot \\ &\cdot \Big(n_a\mu_b\cos\vartheta_e\cos\varphi_{b\perp} - i\Big[n_a\mu_b\cos\vartheta_e\sin\varphi_{b\perp} + \\ &+ n_b\mu_a\,{}_+\sqrt{(n_a/n_b)^2\sin^2\vartheta_e - 1}\,\cos\varphi_{b\perp}\Big] - \\ &- n_b\mu_a\,{}_+\sqrt{(n_a/n_b)^2\sin^2\vartheta_e - 1}\,\sin\varphi_{b\perp}\Big) \end{aligned} \tag{94a}$$

$$\begin{aligned}\frac{\hat{E}_b}{\hat{E}_e} &\overset{(88c)}{=} \tau_\parallel e^{-i\varphi_{b\parallel}} \overset{(91c)}{=} \frac{2n_a\mu_b\cos\vartheta_e}{n_b^2\mu_a^2\cos^2\vartheta_e + n_a^2\mu_b^2(n_a/n_b)^2\sin^2\vartheta_e - n_a^2\mu_b^2}\cdot \\ &\cdot \Big(n_b\mu_a\cos\vartheta_e\cos\varphi_{b\parallel} - i\Big[n_b\mu_a\cos\vartheta_e\sin\varphi_{b\parallel} + \\ &+ n_a\mu_b\,{}_+\sqrt{(n_a/n_b)^2\sin^2\vartheta_e - 1}\,\cos\varphi_{b\parallel}\Big] - \\ &- n_a\mu_b\,{}_+\sqrt{(n_a/n_b)^2\sin^2\vartheta_e - 1}\,\sin\varphi_{b\parallel}\Big) \end{aligned} \tag{94b}$$

The quotients of the real amplitudes must be real. Consequently the square brackets must vanish:

$$\sin\varphi_{b\perp} = -\frac{n_b\mu_a\,{}_+\sqrt{(n_a/n_b)^2\sin^2\vartheta_e - 1}}{n_a\mu_b\cos\vartheta_e}\,\cos\varphi_{b\perp} \tag{95a}$$

$$\sin\varphi_{b\parallel} = -\frac{n_a\mu_b \,{}_+\!\sqrt{(n_a/n_b)^2\sin^2\vartheta_e - 1}}{n_b\mu_a\cos\vartheta_e}\cos\varphi_{b\parallel} \tag{95b}$$

Insertion into (94) gives

$$\text{if } \vartheta_e > \vartheta_{e,\text{critical}}:$$

$$\tau_\perp e^{-i\varphi_{b\perp}} = \frac{\hat{E}_b}{\hat{E}_e} = 2\cos\varphi_{b\perp} \tag{96a}$$

$$\tau_\parallel e^{-i\varphi_{b\parallel}} = \frac{\hat{E}_b}{\hat{E}_e} = \frac{n_a\mu_b}{n_b\mu_a}\cdot 2\cos\varphi_{b\parallel}\ . \tag{96b}$$

$\hat{E}_b$ and $\varphi_{b\perp}$ resp. $\varphi_{b\parallel}$ are two unknowns in each equations. We know, however, that the quotient of the amplitude moduli must be positive. Thus $\varphi_{b\perp}$ and $\varphi_{b\parallel}$ must be in the first or in the fourth quadrant, and they must be

$$\varphi_{b\perp} \overset{(95)}{=} \arctan\Big(-\frac{n_b\mu_a \,{}_+\!\sqrt{(n_a/n_b)^2\sin^2\vartheta_e - 1}}{n_a\mu_b\cos\vartheta_e}\Big) \tag{97a}$$

$$\varphi_{b\parallel} \overset{(95)}{=} \arctan\Big(-\frac{n_a\mu_b \,{}_+\!\sqrt{(n_a/n_b)^2\sin^2\vartheta_e - 1}}{n_b\mu_a\cos\vartheta_e}\Big) \tag{97b}$$

This is sufficient to compute the phase-angles uniquely for given values of $n_a, n_b, \mu_a, \mu_b, \vartheta_e$. For the example values $n_a/n_b = 1.5$ and $\mu_a = \mu_b$, the phase-angles are displayed in fig. 15 on the next page, together with the phase-angles (79) at under-critical incoming angles. A graphic for the case $n_a < n_b$ is superfluous, because then $\varphi_{b\perp} = \varphi_{b\parallel} = 0$ for arbitrary ϑ_e according to (79).

Concluding, we compile all phase-angles:

$$\text{at arbitrary } \vartheta_e:$$

$$\varphi_{e,E} \overset{(67h)}{=} 0 \overset{(67)}{=} \varphi_{e,B} \tag{98a}$$

at $\vartheta_e \le \vartheta_{e,\text{critical}}$:

$$\varphi \overset{(77)}{=} \varphi_{r,E} = (0 \text{ OR } \pi) \quad , \quad \varphi_{r,B} \overset{(67)}{=} \varphi_{r,E} + \pi \tag{98b}$$

$$\varphi_b \overset{(77)}{=} \varphi_{b,E} = 0 \overset{(67)}{=} \varphi_{b,B} \tag{98c}$$

at $\vartheta_e > \vartheta_{e,\text{critical}}$:

$$\varphi \overset{(77)}{=} \varphi_{r,E} = (93), \text{ siehe Abb.13} \tag{98d}$$

$$\varphi_{r,B} \overset{(67)}{=} \varphi_{r,E} + \pi \tag{98e}$$

$$\varphi_{b\perp} \equiv \varphi_{b,E} \overset{(77e)}{=} \varphi_{b,E_z} = (97a), \text{ see fig.15} \tag{98f}$$

$$\varphi_{b,B_x} \overset{(67)}{=} \varphi_{b,E_z} - \pi/2 \tag{98g}$$

$$\varphi_{b,B_y} \overset{(67)}{=} \varphi_{b,E_z} \tag{98h}$$

$$\varphi_{b\parallel} \equiv \varphi_{b,E} \overset{(77f)}{=} \varphi_{b,E_y} = (97b), \text{ see fig.15} \tag{98i}$$

$$\varphi_{b,E_x} \overset{(77f)}{=} \varphi_{b,E_y} - \pi/2 = \varphi_{b\perp} - \pi/2 \tag{98j}$$

$$\varphi_{b,B_z} \overset{(67)}{=} \varphi_{b,E_y} \overset{(67)}{=} \varphi_{b,E_x} + \pi/2 = \varphi_{b\perp} \tag{98k}$$

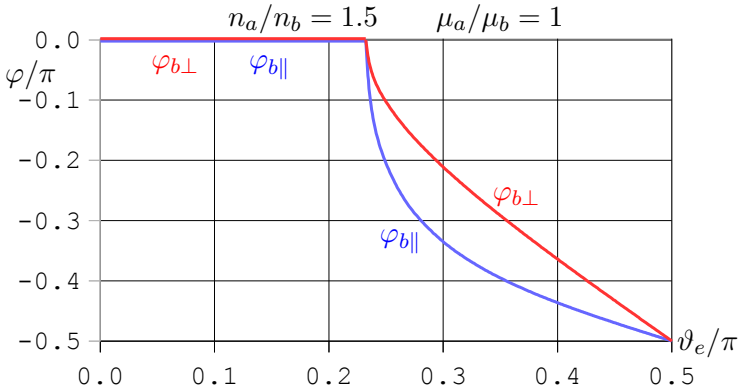

Fig. 15 : The phase-angles $\varphi_{b\perp}$ and $\varphi_{b\parallel}$

The following relations in-between the phase-angles are showing up in the numerical computations:

$$\begin{aligned} &\text{if } \vartheta_e > \vartheta_{e,\text{critical}} : \\ &\varphi_\perp = 2\varphi_{b,\perp} \quad , \quad \varphi_\parallel - \pi = 2\varphi_{b,\parallel} \end{aligned} \tag{99}$$

These relations are easy to understand. As Maxwell's equations are invariant under time inversion, and as we are assuming both materials to be perfectly transparent, the process of reflection must be invariant under time inversion as well. Consequently the phase-shift between the evanescent field and the incoming field must be equal to the phase-shift between the evanescent field and the reflected field. The additional shift of π at parallel polarization is caused by the jump of π of the reflected field's phase at $\vartheta_e > \vartheta_{e,\text{Brewster}}$.

$\hat{E}_b/\hat{E}_e \overset{(78)}{=} |\tau|$ is largest at $\vartheta_e \gtrsim \vartheta_{e,\text{critical}}$, and then decreases rapidly towards zero at larger incoming angles, as can be read off fig. 16. As furthermore the strength of the evanescent fields

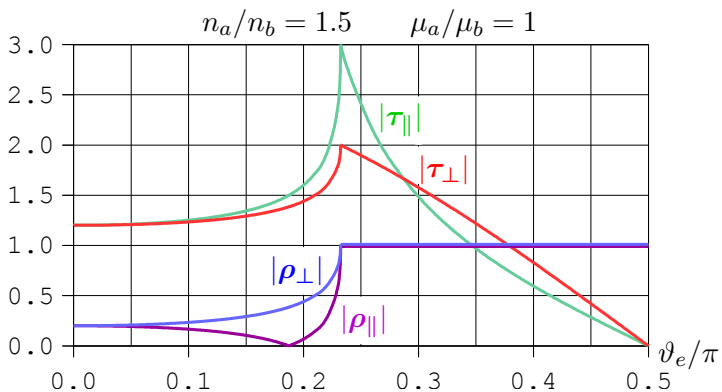

Fig. 16: Moduli of the Fresnel-coefficients

is proportional to $e^{-y/\gamma}$ with γ according to (46c) continuously decreasing for increasing ϑ_e, in experimental setups like sketched in fig. 2 the by far strongest signal is to be expected at $\vartheta_e \gtrsim \vartheta_{e,\text{critical}}$.

Now we are going to discuss the shift of the reflected beam (Goos-Hänchen shift). Artmann's [7] theory of the Goos-Hänchen shift is considered essentially correct still by today, despite various objections and alternative approaches by other authors. A concise review of the theoretical and experimental work published on the Goos-Hänchen shift has been compiled by Berman [8].

Artmann's computations are quite intricate. Therefore it's helpful to read in parallel the presentation of Ghatak et. al. [9, 10]. The result for the magnitude D of the Goos-Hänchen shift is

$$D = -\frac{1}{k_e}\frac{\mathrm{d}\varphi}{\mathrm{d}\vartheta_e} \ . \tag{100}$$

The phase-angles of the reflected radiation are indicated in (93). It's visible from the bottom diagram in fig. 13 on page 47 that $\mathrm{d}\varphi/\,\mathrm{d}\vartheta_e$ is negative at over-critical incoming angles. Thus $D =$ (100) is positive. Furthermore it's visible from that diagram, that D is largest at $\vartheta_e \gtrsim \vartheta_{e,\text{critical}}$, because there the graphs are steepest. For this reason, Goos and Hänchen evaluated the beam-shift exclusively at angles ϑ_e, which were only slightly larger than $\vartheta_{e,\text{critical}}$.

We now are going to derive (100). The fields (15) have infinite extension. If we want to discuss beam-shifts, then we must constrict the radiation to a narrow line at least in x-direction, as sketched in fig. 3 on page 6. We continue to assume a sharply defined value of

$$k = {}_{+}\sqrt{k_x^2 + k_y^2} = \frac{n\omega}{c} \ . \tag{101}$$

Thus a constriction of the radiation in x-direction (i. e. a blurred value of k_x) will imply automatically a constriction in y-direction (i. e. a blurred value of k_y) as well. As in the experiment of Goos

and Hänchen the constriction of the radiation in in x-direction was narrower by several orders of magnitude than the constriction in z-direction, it won't cause any problem if we continue to assume infinite extension of the radiation in z-direction (i. e. the sharply defined value $k_z = 0$).

Using $k_x \overset{(34)}{=} k_{e,x} \overset{(34)}{=} k_{r,x}$, we produce laterally constricted beams by means of Fourier-integrals. Thereby we get these electrical fields:

$$\boldsymbol{E}_e \overset{(15)}{=} \int_{-\infty}^{+\infty} \frac{\mathrm{d}k_x}{2\pi}\, \hat{\boldsymbol{G}}_e\, e^{i(k_x x + k_{e,y} y - \omega t)} \tag{102a}$$

$$\boldsymbol{E}_r \overset{(15)}{=} \int_{-\infty}^{+\infty} \frac{\mathrm{d}k_x}{2\pi}\, \hat{\boldsymbol{G}}_r\, e^{i(k_x x + k_{r,y} y - \omega t + \varphi)} \tag{102b}$$

The amplitudes $\hat{\boldsymbol{G}}$, the wavenumber-components k_y, and the phase-angles φ all depend on k_x. These functions can be expanded around an arbitrary central value $k_x^{(0)}$ by Taylor series. For example, the phase is

$$\varphi(k_x) = \sum_{j=0}^{\infty} \frac{(k_x - k_x^{(0)})^j}{j!}\, \frac{\mathrm{d}^j \varphi}{\mathrm{d}k_x^j}\Big|_{k_x^{(0)}} \,. \tag{103}$$

If the wave numbers, for which $\hat{\boldsymbol{E}}(k_x)$ is differing significantly from zero, are differing only slightly from $k_x^{(0)}$, then the expansions can be stopped after the linear term:

$$\varphi(k_x) \approx \varphi(k_x^{(0)}) + (k_x - k_x^{(0)})\, \frac{\mathrm{d}\varphi}{\mathrm{d}k_x}\Big|_{k_x^{(0)}} \qquad \text{if } |k_x - k_x^{(0)}| \ll |k_x^{(0)}| \tag{104}$$

In this approximation, the fields become

$$\boldsymbol{E}_e = e^{i(k_x^{(0)}x + k_{e,y}(k_x^{(0)})y - \omega t)} \cdot \int_{-\infty}^{+\infty} \frac{\mathrm{d}k_x}{2\pi}\, \hat{\boldsymbol{G}}_e(k_x)\, e^{i(k_x - k_x^{(0)})\left(x + \frac{\mathrm{d}k_{e,y}}{\mathrm{d}k_x}\Big|_{k_x^{(0)}} y\right)} \tag{105a}$$

$$\boldsymbol{E}_r = e^{i(k_x^{(0)}x + k_{r,y}(k_x^{(0)})y - \omega t + \varphi(k_x^{(0)}))} \cdot \int_{-\infty}^{+\infty} \frac{\mathrm{d}k_x}{2\pi}\, \hat{\boldsymbol{G}}_r(k_x)\, e^{i(k_x - k_x^{(0)})\left(x + \frac{\mathrm{d}k_{r,y}}{\mathrm{d}k_x}\Big|_{k_x^{(0)}} y + \frac{\mathrm{d}\varphi}{\mathrm{d}k_x}\Big|_{k_x^{(0)}}\right)} . \tag{105b}$$

The exponential functions, which have been drawn out of the integrals, are describing plane waves of infinite extension with the large wave number $k_x^{(0)}$ in x-direction. The integrands are describing the modulation of these waves' amplitudes with the small wave number $k_x - k_x^{(0)}$. The rays (105) are limited in x- and y-direction. Their maxima of intensity at the boundary surface between the two media (i. e. at $y = 0$) are located at those x values, at which the exponential functions in the integrals have their maxima, i. e. at

$$x_{e,\mathrm{peak}}(y = 0) = 0 \tag{106a}$$

$$x_{r,\mathrm{peak}}(y = 0) = -\frac{\mathrm{d}\varphi}{\mathrm{d}k_x}\Big|_{k_x^{(0)}} . \tag{106b}$$

One can read from fig. 3 on page 6:

$$D = D_x \cos\vartheta_e = \Big(x_{r,\mathrm{peak}}(y = 0) - x_{e,\mathrm{peak}}(y = 0)\Big) \cos\vartheta_e = \overset{(106)}{=} -\cos\vartheta_e \frac{\mathrm{d}\varphi}{\mathrm{d}k_x}\Big|_{k_x^{(0)}} = -\frac{\cos\vartheta_e}{k_e} \frac{\mathrm{d}\varphi}{\mathrm{d}\sin\vartheta}\Big|_{\vartheta_e} = -\frac{\cos\vartheta_e}{k_e \cos\vartheta_e} \frac{\mathrm{d}\varphi}{\mathrm{d}\vartheta}\Big|_{\vartheta_e} \tag{107}$$

This is identical to Artmann's result (100).

Corresponding to the experiments of Goos and Hänchen, Artmann restricted his treatise to angles ϑ_e, which were only slightly larger than $\vartheta_{e,\mathrm{critical}}$. This is resulting into an appreciable simplification of the formulas, because for such angles the second terms in the denominators of (93) are negligible versus the first terms respectively. Thus one gets in good approximation

$$\text{if } \vartheta_e \gtrsim \vartheta_{e,\mathrm{critical}}$$

$$\varphi_\perp \overset{(93)}{=} \arctan\left(\frac{2n_b\mu_a\sqrt{(n_a/n_b)^2\sin^2\vartheta_e - 1}}{n_a\mu_b\cos\vartheta_e}\right) \lesssim 0 \tag{108a}$$

$$\varphi_\parallel \overset{(93)}{=} \arctan\left(\frac{2n_a\mu_b\sqrt{(n_a/n_b)^2\sin^2\vartheta_e - 1}}{n_b\mu_a\cos\vartheta_e}\right) \lesssim \pi$$

$$= \pi + \left(\frac{n_a\mu_b}{n_b\mu_a}\right)^2 \cdot \varphi_\perp \ . \tag{108b}$$

The constant factor, whose order of magnitude is 1, could be pulled into the tangent function because of $|\varphi_\perp| \ll 1$. Using the formula

$$\frac{\mathrm{d}}{\mathrm{d}x}\arctan(x) = \frac{1}{1+x^2} \ , \tag{109}$$

we get

$$\frac{\mathrm{d}\varphi_\perp}{\mathrm{d}\vartheta_e} = \frac{-1}{1+\left(\frac{2n_b\mu_a\sqrt{(n_a/n_b)^2\sin^2\vartheta_e-1}}{n_a\mu_b\cos\vartheta_e}\right)^2}\,\frac{2n_b\mu_a}{n_a\mu_b}\,\frac{1}{\cos^2\vartheta_e}\cdot$$

$$\cdot\left([(n_a/n_b)^2\sin^2\vartheta_e - 1]^{-1/2}(n_a/n_b)^2\sin\vartheta_e\cos^2\vartheta_e + \right.$$

$$\left. + \sin\vartheta_e\sqrt{(n_a/n_b)^2\sin^2\vartheta_e - 1}\right) \ . \tag{110}$$

As $(n_a/n_b)^2\sin^2\vartheta_e - 1 \ll 1$ nearby the critical angle, in the numerator and in the denominator the respective second terms are

negligible versus the first terms.

$$\frac{\mathrm{d}\,\varphi_\perp}{\mathrm{d}\,\vartheta_e} = -\frac{2n_a\mu_a \sin\vartheta_e}{n_b\mu_b\sqrt{(n_a/n_b)^2\sin^2\vartheta_e - 1}} \tag{111}$$

Thus the Goos-Hänchen shift becomes

$$\begin{aligned}
&\text{if } \vartheta_e \gtrsim \vartheta_{e,\text{critical}} \\
&D_\perp \overset{(100)}{=} \frac{1}{k_e}\frac{2\mu_a\sin\vartheta_e}{\mu_b\sqrt{\sin^2\vartheta_e - (n_b/n_a)^2}} \overset{(46c)}{=} \frac{2\mu_a\sin\vartheta_e}{\mu_b}\cdot\gamma = \\
&\quad = \frac{2n_b\mu_a}{n_a\mu_b}\cdot\gamma \qquad (112a)\\
&D_\parallel = \left(\frac{n_a\mu_b}{n_b\mu_a}\right)^2 \cdot D_\perp = \frac{2n_a\mu_b}{n_b\mu_a}\cdot\gamma\,. \qquad (112b)
\end{aligned}$$

This results coincides (within the measurement accuracy) with the observations of Goos and Hänchen. The shift is proportional to the penetration depth γ, i. e. it is largest nearby $\vartheta_{e,\text{critical}}$, and decreases continuously with increasing ϑ_e.

5. Multilayer stacks and FTIR

In this section we will compute reflection and refraction by a stack of three material layers a, b, c, as displayed in fig. 17 on the next page. Let the indices of refraction of the three materials be n_a, n_b, n_c, their magnetic permeabilities μ_a, μ_b, μ_c. As there is only one relevant angle in each material layer, we now name the three angles $\vartheta_a, \vartheta_b, \vartheta_c$.

We define the notation τ_{ab} for the Fresnel-coefficient $\tau_{ab\perp}$ or $\tau_{ab\parallel}$, and the notation ρ_{ab} for the Fresnel-coefficient $\rho_{ab\perp}$ or $\rho_{ab\parallel}$. The notations ρ_{ab} and τ_{ab} are applied, if the wave comes in from medium a and impinges onto the surface of medium b. The notations ρ_{ba}

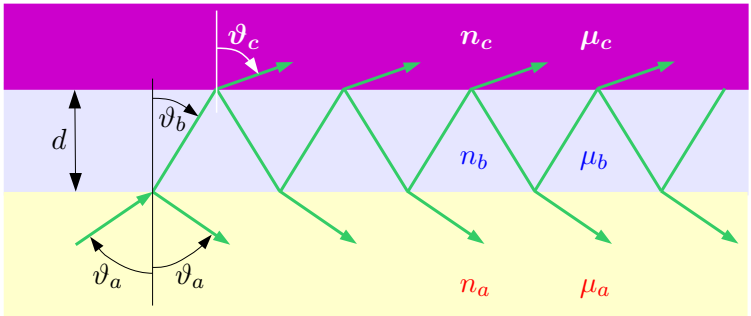

Fig. 17 : A stack of three material layers

and τ_{ba} are used if the wave is coming in from medium b and impinges onto the surface of medium a. The notations ρ_{bc} and τ_{bc} are used if the wave is coming in from medium b and impinges onto the surface of medium c. ρ_{ba} and τ_{ba} differ from ρ_{ab} and τ_{ab} by the exchange of all indices a and b, and the exchange of the angles ϑ_a and ϑ_b, see (78).

Furthermore we now apply, instead of the notations $\varphi \equiv \varphi_{r,E}$ and $\varphi_b \equiv \varphi_{b,E}$ used so far, these notations for the electric field's phase angles at reflection and refraction:

$$\varphi_{r,ab} \text{ at reflection at the boundary } ab \tag{113a}$$
$$\varphi_{r,ba} \text{ at reflection at the boundary } ba \tag{113b}$$
$$\varphi_{t,ab} \text{ at transmission through the boundary } ab \tag{113c}$$
$$\varphi_{t,ba} \text{ at transmission through the boundary } ba \tag{113d}$$
$$\varphi_{r,bc} \text{ at reflection at the boundary } bc \tag{113e}$$
$$\varphi_{t,bc} \text{ at transmission through the boundary } bc \tag{113f}$$

As before, the incoming and the reflected plane waves are assumed to have infinite extension and infinite coherence-length.

For arbitrary combinations n_a, n_b, n_c, and arbitrary under- or over-critical incoming angles, we have

$$\begin{aligned} & k_{a,x} \overset{(34)}{=} k_{b,x} \overset{(34)}{=} k_{c,x} = \\ & = k_a \sin\vartheta_a = k_b \sin\vartheta_b = k_c \sin\vartheta_c = \\ & = \frac{n_a\omega}{c} \sin\vartheta_a = \frac{n_b\omega}{c} \sin\vartheta_b = \frac{n_c\omega}{c} \sin\vartheta_c \\ & \Longrightarrow \quad n_a \sin\vartheta_a = n_b \sin\vartheta_b = n_c \sin\vartheta_c \ , \end{aligned} \tag{114}$$

with ϑ_b and/or ϑ_c possibly being complex according to (50). Thus for layer-stacks with an arbitrary numbers of layers $a, b, c, \ldots, z$ Snellius's law $n_a \sin\vartheta_a = n_z \sin\vartheta_z$ holds for the outer layers, and we don't need to consider refractions in the inner layers. But note that this is a statement on the incoming and outgoing angles only. The intensities of the transmitted and the reflected radiation will of course be strongly influenced by the properties of the inner layers.

We return to the stack of three layers. If $n_a > n_b$ and $n_c > n_b$, and if radiation is coming in under an angle $\vartheta_a < \vartheta_{a,\text{critical}}$, then the radiation in medium b must be a plane wave, and consequently $\vartheta_c < \vartheta_{c,\text{critical}}$, considering symmetry under time-inversion. If $\vartheta_a > \vartheta_{a,\text{critical}}$, then the radiation in medium b must be evanescent, and the outgoing angle must be $\vartheta_c > \vartheta_{c,\text{critical}}$, again due to invariance under time inversion. Consequently, if $n_a > n_b < n_c$, then the transmitted part of the radiation will go out under the angle $\vartheta_c = \vartheta_{c,\text{critical}}$ if $\vartheta_a = \vartheta_{a,\text{critical}}$.

The "Stokes-relations"

$$\rho_{ab}^2 + \tau_{ba}\tau_{ab} = 1 \tag{115a}$$

$$\rho_{ab} + \rho_{ba} = 0 \tag{115b}$$

will turn out to be most useful in the following discussion. They are easily proved due to direct insertion of the Fresnel-coefficients

(78). As the Fresnel-coefficients (78) are valid for arbitrary under- and overcritical incoming angles, the Stokes-relations (115) are as well valid for arbitrary incoming angles $0 \leq \vartheta_a \leq \pi/2$.

The Stokes-relations can be made plausible as a consequence of invariance under time inversion. The process of reflection and refraction must be invariant under time inversion, because we are always assuming lossless media (no energy is absorbed by either of the media). In the left drawing of figure 18, the process is sketched as we considered it up to now. Due to inversion of the direction of time it changes to the process displayed in the right sketch:

A wave with wave-number $\boldsymbol{k}'_e = -\boldsymbol{k}_r$, coming in from medium a, impinges under the angle ϑ_a onto the surface of medium b, and is partially reflected into medium a and partially refracted into medium b. At the same time a wave with wave-number $\boldsymbol{k}''_e = -\boldsymbol{k}_b$, coming in from medium b, impinges under the angle ϑ_b onto the surface of medium a, and is partially reflected into medium b and partially refracted into medium a. Clearly the two incoming waves must have the same phase relations as the two outgoing waves in the process of the left sketch.

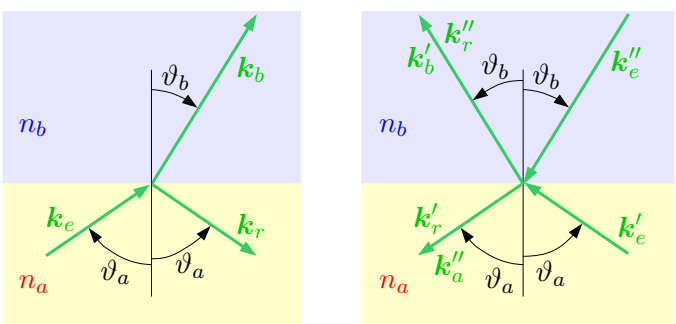

Fig. 18 : Time inversion

While the waves, which are reflected and refracted into the medium a, add up to the outgoing wave with wave-number $\boldsymbol{k}'_r = \boldsymbol{k}''_a = -\boldsymbol{k}_e$, those waves, which are reflected and refracted into medium b with wave-numbers $\boldsymbol{k}'_b = \boldsymbol{k}''_r$ must mutually annihilate due to destructive interference.

The Fresnel-relations

$$\hat{E}_b e^{i\varphi_{t,ab}} \overset{(78)}{=} \tau_{ab}\hat{E}_e \quad , \quad \hat{E}_r e^{i\varphi_{r,ab}} \overset{(78)}{=} \rho_{ab}\hat{E}_e \tag{116}$$

apply to the left sketch in fig. (18). For the right sketch in that figure, the relations

$$\hat{E}'_b e^{i\varphi_{t,ab}+\varphi_{r,ab}} = \tau_{ab}\hat{E}'_e e^{i\varphi_{r,ab}} = \tau_{ab}\hat{E}_r e^{i\varphi_{r,ab}} = \tau_{ab}\rho_{ab}\hat{E}_e \tag{117a}$$

$$\hat{E}'_r e^{i2\varphi_{r,ab}} = \rho_{ab}\hat{E}'_e e^{i\varphi_{r,ab}} = \rho_{ab}\hat{E}_r e^{i\varphi_{r,ab}} = \rho_{ab}^2\hat{E}_e \tag{117b}$$

$$\hat{E}''_a e^{i\varphi_{t,ba}+\varphi_{t,ab}} = \tau_{ba}\hat{E}''_e e^{i\varphi_{t,ab}} = \tau_{ba}\hat{E}_b e^{i\varphi_{t,ab}} = \tau_{ba}\tau_{ab}\hat{E}_e \tag{117c}$$

$$\hat{E}''_r e^{i\varphi_{r,ba}+\varphi_{t,ab}} = \rho_{ba}\hat{E}''_e e^{i\varphi_{t,ab}} = \rho_{ba}\hat{E}_b e^{i\varphi_{t,ab}} = \rho_{ba}\tau_{ab}\hat{E}_e \tag{117d}$$

apply. Invariance under time inversion implies

$$\hat{E}'_r e^{i2\varphi_{r,ab}} + \hat{E}''_a e^{i\varphi_{t,ba}+\varphi_{t,ab}} = \hat{E}_e = \rho_{ab}^2\hat{E}_e + \tau_{ba}\tau_{ab}\hat{E}_e \tag{118a}$$

$$\hat{E}'_b e^{i\varphi_{t,ab}+\varphi_{r,ab}} + \hat{E}''_r e^{i\varphi_{r,ba}+\varphi_{t,ab}} = 0 = \tau_{ab}\rho_{ab}\hat{E}_e + \rho_{ba}\tau_{ab}\hat{E}_e \ . \tag{118b}$$

Canceling $\hat{E}_e$ and τ_{ab}, the Stokes-relations (115) follow immediately. τ_{ab} can be canceled only if $\tau_{ab} \neq 0$, i. e. according to (78) at arbitrary $\vartheta_a < \pi/2$. Thus we have explained the Stokes-relations by the invariance under time inversion at arbitrary $\vartheta_a < \pi/2$. (Only from (78) it's visible, that the Stokes relations hold as well at $\vartheta_a = \pi/2$.) While figure 18 can only illustrate the case $\vartheta_a \leq \vartheta_{a,\text{critical}}$, the interference condition (118) is valid even at over-critical incoming angles, at which the y-components of the wave vectors $\boldsymbol{k}_b, \boldsymbol{k}''_e, \boldsymbol{k}'_b, \boldsymbol{k}''_r$ are imaginary.

5.1. Under-critical angles

We evaluate the three-layer stack sketched in fig. 17 on page 58 with arbitrary refractive indices n_a, n_b, n_c, assuming either $n_a < n_b < n_c$, or $\vartheta_a \leq \vartheta_{a,\text{critical}}$ and $\vartheta_c \leq \vartheta_{c,\text{critical}}$. In this case, the fields are plain waves in all three media. The phase-difference between the wave, which one-times is reflected at the surface bc and then transmitted into the medium a, relative to that wave which is immediately reflected at the surface ab, is

$$\varphi_{t,ab} + \varphi_{r,bc} + \varphi_{t,ba} + \eta - \varphi_{r,ab} \ , \tag{119}$$

with η being the geometric phase-difference

$$\begin{aligned} \eta &= k_b \frac{2d}{\cos\vartheta_b} - k_a \sin\vartheta_a \frac{2d\sin\vartheta_b}{\cos\vartheta_b} = 2dk_b\cos\vartheta_b \ = \\ &= 2d|k_{b,y}| \overset{(53b)}{=} 2d\,\frac{k_a n_b}{n_a}\,\cos\vartheta_b \ \in \mathbb{R} \ . \end{aligned} \tag{120}$$

Radiation, which is directly reflected at the boundary surface ab, is described by

$$\hat{E}_r^{(1)} e^{i\chi_{(1)}} \equiv \hat{E}_r^{(1)} e^{i\varphi_{r,ab}} \overset{(78)}{=} \rho_{ab}\hat{E}_e \ . \tag{121}$$

Radiation, which is transmitted into the medium b, once reflected at the surface bc, and then transmitted into the medium a, is described by

$$\hat{E}_r^{(2)} e^{i\chi_{(2)}} \equiv \hat{E}_r^{(2)} e^{i(\eta+\varphi_{t,ba}+\varphi_{r,bc}+\varphi_{t,ab})} \overset{(78)}{=} e^{i\eta}\tau_{ba}\rho_{bc}\tau_{ab}\hat{E}_e \ . \tag{122}$$

Radiation, which is reflected a second time between the boundaries, is described by

$$\begin{aligned} \hat{E}_r^{(3)} e^{i\chi_{(3)}} &\equiv \hat{E}_r^{(3)} e^{i(2\eta+\varphi_{t,ba}+\varphi_{r,bc}+\varphi_{r,ba}+\varphi_{r,bc}+\varphi_{t,ab})} \overset{(78)}{=} \\ &= e^{i2\eta}\tau_{ba}\rho_{bc}\rho_{ba}\rho_{bc}\tau_{ab}\hat{E}_e \ . \end{aligned} \tag{123}$$

The total electrical field reflected into medium a is

$$\hat{E}_r e^{i\alpha} \equiv \sum_{m=1}^{\infty} \hat{E}_r^{(m)} e^{i\chi_{(m)}} = \rho_{ab}\hat{E}_e + e^{i\eta}\tau_{ba}\rho_{bc}\tau_{ab}\hat{E}_e + \\ + e^{i2\eta}\tau_{ba}\rho_{bc}\rho_{ba}\rho_{bc}\tau_{ab}\hat{E}_e + \dots \quad (124)$$

As usual, we define the amplitude $\hat{E}_r$ real and ≥ 0. The reflective three-layer Fresnel coefficient is defined by

$$\rho_{abc} \equiv \frac{\hat{E}_r e^{i\alpha}}{\hat{E}_e} = \rho_{ab} + \tau_{ba}\tau_{ab}\rho_{bc}e^{i\eta}\sum_{j=0}^{\infty}(\rho_{ba}\rho_{bc}e^{i\eta})^j \ . \quad (125)$$

$\vartheta_b = \pi/2$ at $\vartheta_a = \vartheta_{a,\text{critical}}$, and consequently $\tau_{ba} \overset{(78)}{=} 0$. Thus

$$\rho_{abc} = \rho_{ab} \overset{(78)}{=} \pm 1 \quad \text{at } \vartheta_a = \vartheta_{a,\text{critical}} \ . \quad (126)$$

If $\vartheta_a < \vartheta_{a,\text{critical}}$, then $|\rho_{ba}\rho_{bc}e^{i\eta}| < 1$, and the geometric series (125) is converging. In this case we get

$$\text{if } \vartheta_a \leq \vartheta_{a,\text{critical}}: \\ \rho_{abc} = \frac{\rho_{ab} - \rho_{ab}\rho_{ba}\rho_{bc}e^{i\eta} + \tau_{ba}\tau_{ab}\rho_{bc}e^{i\eta}}{1 - \rho_{ba}\rho_{bc}e^{i\eta}} \overset{(115)}{=} \frac{\rho_{ab} + \rho_{bc}e^{i\eta}}{1 + \rho_{ab}\rho_{bc}e^{i\eta}} \quad (127)$$

While $\vartheta_{a,\text{critical}}$ had to be excluded in course of the derivation, this result is identical to (126) at the critical angle. Thus (127) is valid for arbitrary angles $\leq \vartheta_{a,\text{critical}}$.

Transmission through the layer stack can be computed by the same method. Radiation, which is transmitted without multiple reflections through both surfaces, is described by

$$\hat{E}_t^{(1)} e^{i\xi_{(1)}} \equiv \hat{E}_t^{(1)} e^{i(\eta/2+\varphi_{t,bc}+\varphi_{t,ab})} \overset{(78)}{=} e^{i\eta/2}\tau_{bc}\tau_{ab}\hat{E}_e \ . \quad (128a)$$

Radiation, which is transmitted into medium b, once reflected at the surface bc, once reflected at the surface ba, and then transmitted into medium c, is described by

$$\hat{E}_t^{(2)} e^{i\xi_{(2)}} \equiv \hat{E}_t^{(2)} e^{i(3\eta/2+\varphi_{t,bc}+\varphi_{r,ba}+\varphi_{r,bc}+\varphi_{t,ab})} = \overset{(78)}{=} e^{i3\eta/2} \tau_{bc}\rho_{ba}\rho_{bc}\tau_{ab}\hat{E}_e \ . \tag{128b}$$

Radiation, which is reflected another time between the surfaces, is described by

$$\hat{E}_t^{(3)} e^{i\xi_{(3)}} \equiv \hat{E}_t^{(3)} e^{i(5\eta/2+\varphi_{t,bc}+\varphi_{r,ba}+\varphi_{r,bc}+\varphi_{r,ba}+\varphi_{r,bc}+\varphi_{t,ab})} = \overset{(78)}{=} e^{i5\eta/2} \tau_{bc}\rho_{ba}\rho_{bc}\rho_{ba}\rho_{bc}\tau_{ab}\hat{E}_e \ . \tag{128c}$$

The total electrical field transmitted into medium c is

$$\hat{E}_t e^{i\beta} \equiv \sum_{m=1}^{\infty} \hat{E}_t^{(m)} e^{i\xi_{(m)}} = e^{i\eta/2}\tau_{bc}\tau_{ab}\hat{E}_e + e^{i3\eta/2}\tau_{bc}\rho_{ba}\rho_{bc}\tau_{ab}\hat{E}_e + \\ + e^{i5\eta/2}\tau_{bc}\rho_{ba}\rho_{bc}\rho_{ba}\rho_{bc}\tau_{ab}\hat{E}_e + \dots \tag{129}$$

As usual we define the amplitude $\hat{E}_t$ real and ≥ 0. The three-layer-stack Fresnel-coefficient of transmission is defined by

$$\tau_{abc} \equiv \frac{\hat{E}_t e^{i\beta}}{\hat{E}_e} = \tau_{bc}\tau_{ab} e^{i\eta/2} \sum_{j=0}^{\infty} (\rho_{ba}\rho_{bc} e^{i\eta})^j \ . \tag{130}$$

$\vartheta_b = \pi/2$ at $\vartheta_a = \vartheta_{a,\mathrm{critical}}$, and consequently $\tau_{bc} \overset{(78)}{=} 0$. Thus

$$\tau_{abc} = 0 \quad \text{at } \vartheta_a = \vartheta_{a,\mathrm{critical}} \ . \tag{131}$$

If $\vartheta_a < \vartheta_{a,\mathrm{critical}}$, then $|\rho_{ba}\rho_{bc}e^{i\eta}| < 1$, and the geometric series (130) is converging:

$$\text{if } \vartheta_a \leq \vartheta_{a,\mathrm{critical}} : \\ \tau_{abc} \equiv \frac{\hat{E}_t e^{i\beta}}{\hat{E}_e} = \frac{\tau_{bc}\tau_{ab} e^{i\eta/2}}{1 - \rho_{ba}\rho_{bc} e^{i\eta}} \tag{132}$$

While $\vartheta_{a,\text{critical}}$ had to be excluded in course of the derivation, this result is identical to (131) at the critical angle. Therefore (132) is valid at arbitrary angles $\leq \vartheta_{a,\text{critical}}$.

The coefficients of reflection and transmission of the layer-stack fig. 17 are

$$\text{if } \vartheta_a \leq \vartheta_{a,\text{critical}} :$$

$$R = |r_{abc}|^2 \overset{(127)}{=} \left| \frac{\rho_{ab} + \rho_{bc} e^{i\eta}}{1 + \rho_{ab}\rho_{bc} e^{i\eta}} \right|^2 \tag{133a}$$

$$T = 1 - R \ . \tag{133b}$$

In case of a symmetric layer-stack $a = c \neq b$ these formulas simplify to

$$\text{if } \vartheta_a \leq \vartheta_{a,\text{critical}} :$$

$$R = |r_{aba}|^2 = \left| \frac{\rho_{ab} + \rho_{ba} e^{i\eta}}{1 + \rho_{ab}\rho_{ba} e^{i\eta}} \right|^2 \overset{(115)}{=} \left| \frac{\rho_{ab} - \rho_{ab} e^{i\eta}}{1 - \rho_{ab}^2 e^{i\eta}} \right|^2 \tag{134a}$$

$$T = 1 - R \ . \tag{134b}$$

Alternatively we may write

$$T = |t_{aba}|^2 \overset{(132)}{=} \left| \frac{\tau_{ba}\tau_{ab} e^{i\eta/2}}{1 - \rho_{ba}^2 e^{i\eta}} \right|^2 \overset{(115)}{=} \left| \frac{(1 - \rho_{ab}^2) e^{i\eta/2}}{1 - \rho_{ab}^2 e^{i\eta}} \right|^2 \ . \tag{134c}$$

In (86) we needed to consider the widening of the refracted radiation, as sketched in fig. 10, when we described T as a function of τ_{ab}. But for a symmetric layer stack, $\vartheta_c = \vartheta_a$ holds. Therefore no widening factor is showing up in (134c). We double-check the consistency of (134c) and (134b). If $\vartheta_a \leq \vartheta_{a,\text{critical}}$, then both $\rho_{ab} \in \mathbb{R}$ and $\eta \in \mathbb{R}$ are real:

$$R+T=(134a)+(134c)\ =$$
$$=\frac{(\rho_{ab}-\rho_{ab}e^{i\eta})(\rho_{ab}-\rho_{ab}e^{-i\eta})+(1-\rho_{ab}^2)e^{i\eta/2}(1-\rho_{ab}^2)e^{-i\eta/2}}{(1-\rho_{ab}^2e^{i\eta})(1-\rho_{ab}^2e^{-i\eta})}$$
$$=\frac{\rho_{ab}^2-\rho_{ab}^2e^{-i\eta}-\rho_{ab}^2e^{i\eta}+\rho_{ab}^2+1-\rho_{ab}^2-\rho_{ab}^2+\rho_{ab}^4}{1-\rho_{ab}^2e^{-i\eta}-\rho_{ab}^2e^{i\eta}+\rho_{ab}^4}=1 \quad (135)$$

This is proofing the consistency of (134c) and (134b).

It's clearly visible from (134), how at $\vartheta_a<\vartheta_{a,\mathrm{critical}}$ the reflective properties of the layer stack can be tuned due to variation of d and consequently of $\eta=$ (120). If $e^{i\eta}=1$ (and consequently $e^{i\eta/2}=-1$), then $R=0$ and $T=1$. If $e^{i\eta}=-1$, then R is maximized and T is minimized.

5.2. Over-critical angles

We will discuss the case $\vartheta_a>\vartheta_{a,\mathrm{critical}}$ exclusively for layer-stacks with $n_a>n_b<n_c$, but not for layer-stacks with $n_a>n_b>n_c$. At $n_a>n_b<n_c$ and $\vartheta_a>\vartheta_{a,\mathrm{critical}}$, the evanescent fields in medium b are described by

$$\boldsymbol{E}_b \overset{(46)}{=} \hat{\boldsymbol{E}}_b e^{-y/\gamma+i(xk_{e,x}-\omega t+\varphi_{b,E})} \quad (136a)$$
$$\boldsymbol{B}_b \overset{(46)}{=} \hat{\boldsymbol{B}}_b e^{-y/\gamma+i(xk_{e,x}-\omega t+\varphi_{b,B})}\ . \quad (136b)$$

At multiple reflections, the geometric phase-angle η is replaced by a damping factor $e^{-d/\gamma}$ for each transition in either direction through the layer b. Thus we get instead of (129)

$$\tau_{abc}\equiv\frac{\hat{E}_te^{i\beta}}{\hat{E}_e}=e^{-d/\gamma}\tau_{bc}\tau_{ab}+e^{-3d/\gamma}\tau_{bc}\rho_{ba}\rho_{bc}\tau_{ab}+$$
$$+e^{-5d/\gamma}\tau_{bc}\rho_{ba}\rho_{bc}\rho_{ba}\rho_{bc}\tau_{ab}+\ldots \quad (137)$$

Due to the exponential damping, we always have $|\rho_{ba}\rho_{bc}e^{-2d/\gamma}| < 1$. Thus the geometric series is converging.

$$\text{if } \vartheta_a > \vartheta_{a,\text{critical}} :$$

$$\tau_{abc} = \tau_{bc}\tau_{ab}e^{-d/\gamma}\sum_{j=0}^{\infty}(\rho_{ba}\rho_{bc}e^{-2d/\gamma})^j = \frac{\tau_{bc}\tau_{ab}e^{-d/\gamma}}{1-\rho_{ba}\rho_{bc}e^{-2d/\gamma}} \tag{138}$$

The reflective coefficient (124) is replaced by

$$\begin{aligned}\rho_{abc} \equiv \frac{\hat{E}_r e^{i\alpha}}{\hat{E}_e} &= \rho_{ab} + e^{-2d/\gamma}\tau_{ba}\rho_{bc}\tau_{ab} + e^{-4d/\gamma}\tau_{ba}\rho_{bc}\rho_{ba}\rho_{bc}\tau_{ab} + \dots \\ &= \rho_{ab} + \tau_{ba}\tau_{ab}\rho_{bc}e^{-2d/\gamma}\sum_{j=1}^{\infty}(\rho_{ba}\rho_{bc}e^{-2d/\gamma})^j \ .\end{aligned} \tag{139}$$

Due to the exponential damping, we always have $|\rho_{ba}\rho_{bc}e^{-2d/\gamma}| < 1$. Thus the geometric series is converging.

$$\text{if } \vartheta_a > \vartheta_{a,\text{critical}} :$$

$$\begin{aligned}\rho_{abc} &= \frac{\rho_{ab} - \rho_{ab}\rho_{ba}\rho_{bc}e^{-2d/\gamma} + \tau_{ba}\tau_{ab}\rho_{bc}e^{-2d/\gamma}}{1-\rho_{ba}\rho_{bc}e^{-2d/\gamma}} \\ &\overset{(115)}{=} \frac{\rho_{ab} + \rho_{bc}e^{-2d/\gamma}}{1-\rho_{ba}\rho_{bc}e^{-2d/\gamma}}\end{aligned} \tag{140}$$

Obviously we could have arrived much simpler at (138) and (140) due to replacing $i\eta$ by $-2d/\gamma$ in (132) and (127).

The coefficients of reflection and transmission of the layer-stack fig. 17 are

$$\text{if } \vartheta_a > \vartheta_{a,\text{critical}} :$$

$$R = |r_{abc}|^2 \overset{(140)}{=} \left|\frac{\rho_{ab} + \rho_{bc}e^{-2d/\gamma}}{1-\rho_{ba}\rho_{bc}e^{-2d/\gamma}}\right|^2 \tag{141a}$$

$$T = 1 - R \ . \tag{141b}$$

In case of a symmetric layer stack $a = c \neq b$, these formulas simplify to

if $\vartheta_a > \vartheta_{a,\text{critical}}$:

$$R = |\rho_{aba}|^2 = \left|\frac{\rho_{ab} - \rho_{ab}e^{-2d/\gamma}}{1 - \rho_{ab}^2 e^{-2d/\gamma}}\right|^2 \tag{142a}$$

$$T = 1 - R\ . \tag{142b}$$

Alternatively we may write

$$T = |\tau_{aba}|^2 \overset{(138)}{=} \left|\frac{\tau_{ba}\tau_{ab}e^{-d/\gamma}}{1 - \rho_{ab}^2 e^{-2d/\gamma}}\right|^2 \overset{(115)}{=} \left|\frac{(1 - \rho_{ab}^2)e^{-d/\gamma}}{1 - \rho_{ab}^2 e^{-2d/\gamma}}\right|^2 . \tag{142c}$$

In (86) we needed to consider the widening of the refracted radiation as sketched in fig. 10, when we displayed T as a function of τ_{ab}. But for a symmetric layer stack $\vartheta_c = \vartheta_a$ holds, and therefore no widening factor is showing up in (142c). We double-check the consistency of (142c) and (142b). In case $\vartheta_a > \vartheta_{a,\text{critical}}$, the coefficient $\rho_{ab} \in \mathbb{C}$ in general is complex, with $|\rho_{ab}|^2 = 1$:

$$\begin{aligned} R + T &= (142a) + (142c) \ = \\ &= \frac{(\rho_{ab} - \rho_{ab}e^{-2d/\gamma})(\rho_{ab}^* - \rho_{ab}^* e^{-2d/\gamma}) + \\ &\qquad (1 - \rho_{ab}^2 e^{-2d/\gamma})(1 - [\rho_{ab}^2]^* e^{-2d/\gamma}) \\ &\qquad \underline{+(1 - \rho_{ab}^2)e^{-d/\gamma}(1 - [\rho_{ab}^2]^*)e^{-d/\gamma}} \ = \\ &= \frac{1 - e^{-2d/\gamma} - e^{-2d/\gamma} + e^{-4d/\gamma} + }{1 - [\rho_{ab}^2]^* e^{-2d/\gamma} - \rho_{ab}^2 e^{-2d/\gamma} + e^{-4d/\gamma}} \\ &\qquad \underline{+e^{-2d/\gamma} - [\rho_{ab}^2]^* e^{-2d/\gamma} - \rho_{ab}^2 e^{-2d/\gamma} + e^{-2d/\gamma}} = 1 \end{aligned} \tag{143}$$

This is proofing the consistency of (142c) and (142b).

If $\vartheta_a > \vartheta_{a,\text{critical}}$, then $R = (141a) \approx 1$ at $d \gg \gamma$, and $R \approx 0$ at $d \ll \gamma$. Only at $d = \infty$, R is exactly 1 and T is exactly zero. At finite d, the equations (141) (resp. (142) for a symmetric layer-stack) are a quantitative description of the intensities, which can be observed at frustrated total internal reflection (FTIR).

$$T \overset{(142c)}{=} \left|\frac{(1-\rho_{ab}^2)e^{-d/\gamma}}{1-\rho_{ab}^2 e^{-2d/\gamma}}\right|^2 \approx \left|1-\rho_{ab}^2\right|^2 e^{-2d/\gamma} \quad \text{if } d > \gamma \qquad (144)$$

is a fair approximation at $d > \gamma$, which becomes an excellent approximation at $d \gg \gamma$. This is the exponential decrease of T with increasing d, which Meixner et. al. [4] found for large d, see equation (58) on page 23. They found a significantly lower decrease at small d. They did not, however, explain that observation with our formula (142c), because this formula is based on the assumption of infinitely extended surfaces, between which the FTIR is happening. In contrast, Meixner et. al. used in their experiment as second surface a tip with only 80 nm effective aperture, i. e. an aperture which was much smaller than the applied wavelength of 514.5 nm. Therefore they correctly did not fit their results to (142c), but to a special correction factor which they computed with respect to the limited aperture of their detector.

We close this article with the evaluation of the FTIR of a wave-packet, whose extension is limited in time and space (at least in xy-direction). Coming in from medium a, it's peak is impinging at time $t_e = 0$ under the angle $\vartheta_a > \vartheta_{a,\text{critical}}$ at $x_e = 0$ onto the boundary surface of medium b. We are assuming a symmetric layer stack aba with $n_c = n_a > n_b$. d is the thickness of layer b. The situation is sketched in fig. 19 on the next page. We are looking for the answers to four questions:

* At which point x_r of the surface ($y = 0$) will the peak of the reflected wave packet show up?
* At which point x_t of the surface ($y = d$) will the peak of the

transmitted wave packet show up?

* At which time t_r will the peak of the reflected wave packet show up at point $(x = x_r, y = 0)$?
* At which time t_t will the peak of the transmitted wave packet show up at point $(x = x_t, y = d)$?

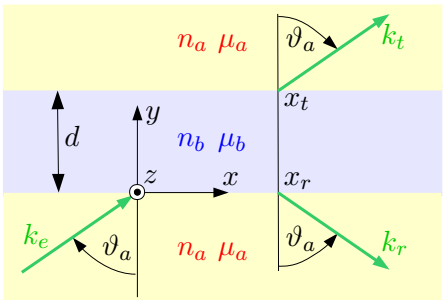

Fig. 19 : Frustrated total internal reflection (FTIR)

We define the scalar instantaneous values

$$\widetilde{E}_e(t,\boldsymbol{r}) = \hat{E}_e e^{i(\boldsymbol{r}\cdot\boldsymbol{k}_e-\omega t)} \tag{145a}$$

$$\widetilde{E}_r(t,\boldsymbol{r}) \overset{(139)}{=} \hat{E}_r e^{i(\boldsymbol{r}\cdot\boldsymbol{k}_r-\omega t+\alpha)} = \rho_{aba}\widetilde{E}_e(t,\boldsymbol{r}) \tag{145b}$$

$$\widetilde{E}_t(t,\boldsymbol{r}) \overset{(137)}{=} \hat{E}_t e^{i(\boldsymbol{r}\cdot\boldsymbol{k}_t-\omega t+\beta)} = \tau_{aba}\widetilde{E}_e(t,\boldsymbol{r}) \tag{145c}$$

$$\boldsymbol{k}_t = \boldsymbol{k}_e \ , \ |\boldsymbol{k}_r| = |\boldsymbol{k}_e| \ , \ k_{r,y} = -k_{e,y} \ ,$$

which must not be confused with the moduli E_e, E_r, E_t. The moduli always are ≥ 0, while the scalar instantaneous values are oscillating around zero, and thereby are assuming positive and negative values.

We can read off (145):

$$\rho_{aba} = |\rho_{aba}|\, e^{i\alpha} \tag{146a}$$

$$\tau_{aba} = |\tau_{aba}|\, e^{i\beta} \tag{146b}$$

Following the delineation by Ghatak et. al. [9, 10], we form wave packets, which are limited in space and time, due to Fourier-transformations of the fields (145). With $k_x \overset{(34)}{=} k_{e,x} \overset{(34)}{=} k_{r,x} \overset{(34)}{=} k_{t,x}$, we get:

$$\widetilde{E}_e = \int_{-\infty}^{+\infty} \frac{\mathrm{d}k_x}{2\pi} \int_{-\infty}^{+\infty} \frac{\mathrm{d}\omega}{2\pi}\, \hat{G}_e\, e^{i(k_x x + k_{e,y} y - \omega t)} \tag{147a}$$

$$\widetilde{E}_r = \int_{-\infty}^{+\infty} \frac{\mathrm{d}k_x}{2\pi} \int_{-\infty}^{+\infty} \frac{\mathrm{d}\omega}{2\pi}\, |\rho_{aba}|\, \hat{G}_e e^{i(k_x x + k_{r,y} y - \omega t + \alpha)} \tag{147b}$$

$$\widetilde{E}_t = \int_{-\infty}^{+\infty} \frac{\mathrm{d}k_x}{2\pi} \int_{-\infty}^{+\infty} \frac{\mathrm{d}\omega}{2\pi}\, |\tau_{aba}|\, \hat{G}_e e^{i(k_x x + k_{e,y} (y-d) - \omega t + \beta)} \tag{147c}$$

Note the factor $(y - d)$ in the exponent of the last function, instead of the factor y in the first and second function. The fields are evanescent in the range between $y = 0$ and $y = d$. There is the phase-jump β on the way from $y = 0$ to $y = d$, but no additional change of phase due to the product $k_{e,y} y$.

The Fourier-amplitude $\hat{G}_e$, the wave-number-components $k_{e,y}$ and $k_{r,y} = -k_{e,y}$, the moduli $|\rho_{aba}|$ and $|\tau_{aba}|$ of the Fresnel coefficients, and the phase angles α and β, all are functions of the two variables of integration k_x and ω. Note that $k_a \equiv k_e = k_r$ and $k_{a,y}^2 \equiv k_{e,y}^2 = k_{r,y}^2$. We consider k_x and ω as two mutually independent variables. That means: While k_x is being varied,

$$k_a = \frac{\omega n_a}{c} = \sqrt{k_x^2 + k_{a,y}^2} = \tag{148a}$$
$$= \text{constant at integration over and derivative to } k_x$$

is kept constant. Thereby the Fourier-amplitude $\hat{G}_e$ does not only fix the spectrum of the wave-packet's k_x-values, but indirectly

also the spectrum of it's k_y-values. Due to integration over k_x, the infinitely extended wave fields are restricted to a ray which is limited in x- and y-direction. Only in z-direction the fields stay extended infinitely.

While ω is being varied,

$$k_x = \sqrt{k_a^2 - k_{a,y}^2} = \sqrt{\omega^2 n_a^2 c^{-2} - k_{a,y}^2} = \tag{148b}$$
$$= \text{constant at integration over and derivative to } \omega$$

is kept constant. Due to the integration over ω, the ray becomes a wave-packet, which is limited in time, and moving along the path of the ray.

The four variables $k_{e,y}$, $k_{r,y} = -k_{e,y}$, α, and β are showing up in the exponents of (147). We expand these four quantities in Taylor-series around central values $k_x^{(0)}$ and $\omega^{(0)}$. We assume that the Fourier-amplitude $\hat{G}_e$ is differing significantly from zero only in such a small neighborhood of $k_x^{(0)}$ and $\omega^{(0)}$, that the Taylor-series may be truncated in good approximation after the linear term. Thus we get e. g. for $k_{e,y}$:

$$k_{e,y}(k_x,\omega) = k_{e,y}(k_x^{(0)},\omega^{(0)}) + (k_x - k_x^{(0)})\left.\frac{\mathrm{d}\,k_{e,y}}{\mathrm{d}\,k_x}\right|_{k_x^{(0)}} +$$
$$+ (\omega - \omega^{(0)})\left.\frac{\mathrm{d}\,k_{e,y}}{\mathrm{d}\,\omega}\right|_{\omega^{(0)}} \tag{149}$$

In this approximation, the equations (147) become:

$$\widetilde{E}_e = e^{i\left(k_x^{(0)}x + k_{e,y}^{(0)}y - \omega^{(0)}t\right)} \int_{-\infty}^{+\infty}\frac{\mathrm{d}k_x}{2\pi}\int_{-\infty}^{+\infty}\frac{\mathrm{d}\omega}{2\pi}\,\hat{G}_e\,\cdot$$
$$\cdot\, e^{i\left(\left[k_x - k_x^{(0)}\right]\left[x + y\,\frac{\mathrm{d}\,k_{e,y}}{\mathrm{d}\,k_x}\right] - \left[\omega - \omega^{(0)}\right]\left[t - y\,\frac{\mathrm{d}\,k_{e,y}}{\mathrm{d}\,\omega}\right]\right)} \tag{150a}$$

$$\widetilde{E}_r = e^{i\left(k_x^{(0)}x + k_{e,y}^{(0)}y - \omega^{(0)}t + \alpha^{(0)}\right)} \int_{-\infty}^{+\infty} \frac{\mathrm{d}k_x}{2\pi} \int_{-\infty}^{+\infty} \frac{\mathrm{d}\omega}{2\pi}\, \hat{G}_e \cdot$$

$$\cdot\, e^{i\left(\left[k_x - k_x^{(0)}\right]\left[x + y\,\frac{\mathrm{d}\,k_{e,y}}{\mathrm{d}\,k_x} + \frac{\mathrm{d}\,\alpha}{\mathrm{d}\,k_x}\right] - \left[\omega - \omega^{(0)}\right]\left[t - y\,\frac{\mathrm{d}\,k_{e,y}}{\mathrm{d}\,\omega} - \frac{\mathrm{d}\,\alpha}{\mathrm{d}\,\omega}\right]\right)} \tag{150b}$$

$$\widetilde{E}_t = e^{i\left(k_x^{(0)}x + (y-d)k_{e,y}^{(0)} - \omega^{(0)}t + \beta^{(0)}\right)} \int_{-\infty}^{+\infty} \frac{\mathrm{d}k_x}{2\pi} \int_{-\infty}^{+\infty} \frac{\mathrm{d}\omega}{2\pi}\, \hat{G}_e \cdot$$

$$\cdot\, e^{i\left(\left[k_x - k_x^{(0)}\right]\left[x + (y-d)\,\frac{\mathrm{d}\,k_{e,y}}{\mathrm{d}\,k_x} + \frac{\mathrm{d}\,\beta}{\mathrm{d}\,k_x}\right] - \left[\omega - \omega^{(0)}\right]\left[t - (y-d)\,\frac{\mathrm{d}\,k_{e,y}}{\mathrm{d}\,\omega} - \frac{\mathrm{d}\,\beta}{\mathrm{d}\,\omega}\right]\right)} \tag{150c}$$

It is understood that the derivatives with respect to k_x and ω shall be taken at $k_x^{(0)}$ and $\omega^{(0)}$, respectively. The exponential functions, which are shifted out of the integrals, are describing infinitely extended plain waves with the high wave-number $k_x^{(0)}, k_{e,y}^{(0)}$ and the high frequency $\omega^{(0)}$. The integrals are describing the amplitude modulation of these waves with the low wave-number $k_x - k_x^{(0)}$ and the low frequency $\omega - \omega^{(0)}$, thus defining wave-packets which are limited in space and time. At the boundary surfaces of the materials (i. e. at $y = 0$ and $y = d$) the wave-packets have their maxima at those x-values and at those t-values, at which the exponential functions under the integrals assume their maximum values (i. e. one). The exponential functions assume the value one, when the red emphasized brackets in (150) are zero.

The peak of the incoming wave-packet arrives at time $t = t_{e,\mathrm{peak}}$ the point $x = x_{e,\mathrm{peak}}$ of the boundary surface $y = 0$. From the exponential function of the integrand of (150a) we can read off:

$$x_{e,\mathrm{peak}} = 0 \tag{151a}$$

$$t_{e,\mathrm{peak}} = 0 \tag{151b}$$

At time $t = t_{r,\mathrm{peak}}$ the peak of the reflected wave-packet shows up at the point $x = x_{r,\mathrm{peak}}, y = 0$ of the boundary surface. From

(150b) we can read off:

$$x_{r,\text{peak}} = -\frac{\mathrm{d}\,\alpha}{\mathrm{d}\,k_x}\Big|_{k_x^{(0)}} \tag{151c}$$

$$t_{r,\text{peak}} = +\frac{\mathrm{d}\,\alpha}{\mathrm{d}\,\omega}\Big|_{\omega^{(0)}} \tag{151d}$$

The peak of the transmitted wave-packet shows up at time $t_{t,\text{peak}}$ at the point $x = x_{t,\text{peak}}, y = d$ of the other surface. From (150c) we can read off:

$$x_{t,\text{peak}} = -\frac{\mathrm{d}\,\beta}{\mathrm{d}\,k_x}\Big|_{k_x^{(0)}} \tag{151e}$$

$$t_{t,\text{peak}} = +\frac{\mathrm{d}\,\beta}{\mathrm{d}\,\omega}\Big|_{\omega^{(0)}} \tag{151f}$$

The phase angles α and β can be computed, using

$$k_e = \frac{\omega n_a}{c} \tag{152a}$$

$$k_x = k_e \sin\vartheta_a = \frac{\omega n_a}{c}\,\sin\vartheta_a \tag{152b}$$

$$-k_{r,y} = k_{e,y} = k_e\cos\vartheta_a = \frac{\omega n_a}{c}\,\cos\vartheta_a \tag{152c}$$

$$\gamma \overset{(46c)}{=} \frac{1}{k_e\,{}_+\!\sqrt{\sin^2\vartheta_a - (n_b/n_a)^2}} = \frac{1}{{}_+\!\sqrt{k_x^2 - (\omega n_b/c)^2}} = \\ = \frac{c}{\omega n_a\,{}_+\!\sqrt{\sin^2\vartheta_a - \sin^2\vartheta_{a,\text{critical}}}} \tag{152d}$$

and the definitions

$$K_a \equiv n_a\mu_b\cos\vartheta_a \overset{(152c)}{=} \frac{k_{e,y}c\mu_b}{\omega} \tag{153a}$$

$$K_b \equiv n_b\mu_a\cos\vartheta_a \overset{(152c)}{=} \frac{n_b k_{e,y}c\mu_a}{n_a\omega} \tag{153b}$$

$$W_a \equiv n_a\mu_b \sqrt[+]{(n_a/n_b)^2 \sin^2\vartheta_a - 1} \overset{(152d)}{=} \frac{n_a\mu_b c}{n_b\gamma\omega} \tag{153c}$$

$$W_b \equiv n_b\mu_a \sqrt[+]{(n_a/n_b)^2 \sin^2\vartheta_a - 1} \overset{(152d)}{=} \frac{\mu_a c}{\gamma\omega} \,. \tag{153d}$$

We continue to consider a symmetric layer stack $n_a = n_c > n_b$ at over-critical incoming angles $\vartheta_a > \vartheta_{a,\text{critical}}$. Using the abbreviations (153), the Fresnel-coefficients (88) become

$$\rho_{ab\perp} = \frac{K_a - iW_b}{K_a + iW_b} \tag{154a}$$

$$\rho_{ab\parallel} = \frac{-K_b + iW_a}{K_b + iW_a} \,. \tag{154b}$$

Inserting these coefficients into

$$\rho_{aba} \overset{(142a)}{=} \frac{\rho_{ab}(1 - e^{-2d/\gamma})}{1 - \rho_{ab}^2 e^{-2d/\gamma}} \tag{155a}$$

$$\tau_{aba} \overset{(142c)}{=} \frac{(1 - \rho_{ab}^2)e^{-d/\gamma}}{1 - \rho_{ab}^2 e^{-2d/\gamma}} \,, \tag{155b}$$

we get

$$\begin{aligned}
\tau_{aba\perp} &= \frac{([K_a + iW_b]^2 - [K_a - iW_b]^2)e^{-d/\gamma}}{[K_a + iW_b]^2 - [K_a - iW_b]^2 e^{-2d/\gamma}} \\
&= \frac{i4K_aW_b}{(K_a^2 - W_b^2)(e^{+d/\gamma} - e^{-d/\gamma}) + i2K_aW_b(e^{+d/\gamma} + e^{-d/\gamma})} \\
&= \frac{i2K_aW_b \operatorname{csch}(d/\gamma)}{K_a^2 - W_b^2 + i2K_aW_b \operatorname{cth}(d/\gamma)} \\
&\overset{(153)}{=} \frac{i2k_{e,y}\mu_b\mu_a\gamma^{-1} \operatorname{csch}(d/\gamma)}{(k_{e,y}\mu_b)^2 - (\mu_a\gamma^{-1})^2 + i2k_{e,y}\mu_b\mu_a\gamma^{-1} \operatorname{cth}(d/\gamma)}
\end{aligned} \tag{156a}$$

$$\begin{aligned}
\rho_{aba\perp} &\overset{(142a)}{=} \frac{(K_a - iW_b)(K_a + iW_b)(1 - e^{-2d/\gamma})}{(K_a + iW_b)^2 - (K_a - iW_b)^2 e^{-2d/\gamma}} \\
&= \frac{(K_a^2 + W_b^2)(e^{+d/\gamma} - e^{-d/\gamma})}{(K_a^2 - W_b^2)(e^{+d/\gamma} - e^{-d/\gamma}) + i2K_aW_b(e^{+d/\gamma} + e^{-d/\gamma})} \\
&= \frac{K_a^2 + W_b^2}{K_a^2 - W_b^2 + i2K_aW_b \operatorname{cth}(d/\gamma)} \\
&\overset{(153)}{=} \frac{(k_{e,y}\mu_b)^2 + (\mu_a\gamma^{-1})^2}{(k_{e,y}\mu_b)^2 - (\mu_a\gamma^{-1})^2 + i2k_{e,y}\mu_b\mu_a\gamma^{-1} \operatorname{cth}(d/\gamma)}
\end{aligned} \tag{156b}$$

$$\begin{aligned}
\tau_{aba\parallel} &= \frac{[(K_b + iW_a)^2 - (K_b - iW_a)^2]e^{-d/\gamma}}{(K_b + iW_a)^2 - (K_b - iW_a)^2 e^{-2d/\gamma}} \\
&= \frac{i4K_bW_a}{(K_b^2 - W_a^2)(e^{+d/\gamma} - e^{-d/\gamma}) + i2K_bW_a(e^{+d/\gamma} + e^{-d/\gamma})} \\
&= \frac{i2K_bW_a \operatorname{csch}(d/\gamma)}{K_b^2 - W_a^2 + i2K_bW_a \operatorname{cth}(d/\gamma)} \\
&\overset{(153)}{=} \frac{i2k_{e,y}\mu_a\mu_b\gamma^{-1} \operatorname{csch}(d/\gamma)}{(n_b/n_a)^2(k_{e,y}\mu_a)^2 - (n_a/n_b)^2(\mu_b\gamma^{-1})^2 + \\
&\qquad + i2k_{e,y}\mu_a\mu_b\gamma^{-1} \operatorname{cth}(d/\gamma)}
\end{aligned} \tag{156c}$$

$$\begin{aligned}
\rho_{aba\parallel} &\overset{(142a)}{=} -\frac{(K_b + iW_a)(K_b - iW_a)(1 - e^{-2d/\gamma})}{(K_b + iW_a)^2 - (K_b - iW_a)^2 e^{-2d/\gamma}} \\
&= -\frac{(K_b^2 + W_a^2)(e^{+d/\gamma} - e^{-d/\gamma})}{(K_b^2 - W_a^2)(e^{+d/\gamma} - e^{-d/\gamma}) + i2K_bW_a(e^{+d/\gamma} + e^{-d/\gamma})} \\
&= -\frac{K_b^2 + W_a^2}{K_b^2 - W_a^2 + i2K_bW_a \operatorname{cth}(d/\gamma)} \\
&\overset{(153)}{=} -\frac{(n_b/n_a)^2(k_{e,y}\mu_a)^2 + (n_a/n_b)^2(\mu_b\gamma^{-1})^2}{(n_b/n_a)^2(k_{e,y}\mu_a)^2 - (n_a/n_b)^2(\mu_b\gamma^{-1})^2 + \\
&\qquad + i2k_{e,y}\mu_a\mu_b\gamma^{-1} \operatorname{cth}(d/\gamma)} \ .
\end{aligned} \tag{156d}$$

We define the abbreviations

$$k_{e,y\perp} \equiv \frac{\mu_b}{\mu_a}\, k_{e,y} \qquad , \qquad k_{e,y\parallel} \equiv \frac{n_b^2 \mu_a}{n_a^2 \mu_b}\, k_{e,y} \ , \tag{157}$$

and compute the phase angles β and α:

$$\tau_{aba\perp} \overset{(156a)}{=} \frac{2K_a W_b \,\mathrm{csch}(d/\gamma)\,[2K_a W_b \,\mathrm{cth}(d/\gamma) + i(K_a^2 - W_b^2)]}{|K_a^2 - W_b^2 + i2K_a W_b \,\mathrm{cth}(d/\gamma)|^2} =$$

$$= |\tau_{aba\perp}|\, e^{i\beta_\perp} \quad \Longrightarrow \quad \beta_\perp = \arctan\Big(\frac{K_a^2 - W_b^2}{2K_a W_b \,\mathrm{cth}(d/\gamma)}\Big)$$

$$\beta_\perp \overset{(153),(157)}{=} \frac{\pi}{2} - \arctan\Big(\frac{2\gamma k_{e,y\perp} \,\mathrm{cth}(d/\gamma)}{\gamma^2 k_{e,y\perp}^2 - 1}\Big) \tag{158a}$$

$$\rho_{aba\perp} \overset{(156b)}{=} \frac{K_a^4 - W_b^4 - i2(K_a^3 W_b + K_a W_b^3)\,\mathrm{cth}(d/\gamma)}{|K_a^2 - W_b^2 + i2K_a W_b \,\mathrm{cth}(d/\gamma)|^2} =$$

$$= |\rho_{aba\perp}|\, e^{i\alpha_\perp} \Longrightarrow \alpha_\perp = \arctan\Big(\frac{-2(K_a^3 W_b + K_a W_b^3)\,\mathrm{cth}(d/\gamma)}{K_a^4 - W_b^4}\Big)$$

$$\alpha_\perp \overset{(153),(157)}{=} -\arctan\Big(\frac{2\gamma k_{e,y\perp} \,\mathrm{cth}(d/\gamma)}{\gamma^2 k_{e,y\perp}^2 - 1}\Big) \tag{158b}$$

$$\tau_{aba\parallel} \overset{(156c)}{=} \frac{2K_b W_a \,\mathrm{csch}(d/\gamma)[2K_b W_a \,\mathrm{cth}(d/\gamma) + i(K_b^2 - W_a^2)]}{|(K_b^2 - W_a^2) + i2K_b W_a \,\mathrm{cth}(d/\gamma)|^2} =$$

$$= |\tau_{aba\parallel}|\, e^{i\beta_\parallel} \quad \Longrightarrow \quad \beta_\parallel = \arctan\Big(\frac{K_b^2 - W_a^2}{2K_b W_a \,\mathrm{cth}(d/\gamma)}\Big)$$

$$\beta_\parallel \overset{(153),(157)}{=} \frac{\pi}{2} - \arctan\Big(\frac{2\gamma k_{e,y\parallel} \,\mathrm{cth}(d/\gamma)}{\gamma^2 k_{e,y\parallel}^2 - 1}\Big) \tag{158c}$$

$$\rho_{aba\parallel} \overset{(156d)}{=} \frac{-K_b^4 + W_a^4 + i2(K_b^3 W_a + K_b W_a^3)\,\mathrm{cth}(d/\gamma)}{|K_b^2 - W_a^2 + i2K_b W_a \,\mathrm{cth}(d/\gamma)|^2} =$$

$$= |\rho_{aba\parallel}|\, e^{i\alpha_\parallel} \Longrightarrow \alpha_\parallel = \arctan\Big(\frac{2(K_b^3 W_a + K_b W_a^3)\,\mathrm{cth}(d/\gamma)}{-K_b^4 + W_a^4}\Big)$$

$$\alpha_{\parallel} \overset{(153),(157)}{=} -\arctan\left(\frac{2\gamma k_{e,y\parallel}\,\mathrm{cth}(d/\gamma)}{\gamma^2 k_{e,y\parallel}^2 - 1}\right) \tag{158d}$$

As the phase angles have the same form at perpendicular and at parallel polarization, the computations can be done with the general parameters α, β, and $k_{e,y}$. As α and β are differing only by a constant term, we conclude from (151)

$$x_{r,\mathrm{peak}} = x_{t,\mathrm{peak}} \qquad \text{and} \qquad t_{r,\mathrm{peak}} = t_{t,\mathrm{peak}}\ . \tag{159}$$

The derivative of α with respect to k_x is

$$\begin{aligned}
\frac{\mathrm{d}\alpha}{\mathrm{d}k_x} &= -\frac{1}{1+\left(\frac{2\gamma k_{e,y}\,\mathrm{cth}(d/\gamma)}{\gamma^2 k_{e,y}^2-1}\right)^2}\cdot 2\left[\frac{(\gamma^2 k_{e,y}^2-1)\cdot}{}\right.\\
&\cdot\left(\frac{\mathrm{d}\gamma}{\mathrm{d}k_x}\,k_{e,y}\,\mathrm{cth}(d/\gamma)+\gamma\,\frac{\mathrm{d}k_{e,y}}{\mathrm{d}k_x}\,\mathrm{cth}(d/\gamma)+\gamma k_{e,y}\,\frac{\mathrm{d}\,\mathrm{cth}(d/\gamma)}{\mathrm{d}k_x}\right)-\\
&\left.\frac{-2\left(\gamma\,\frac{\mathrm{d}\gamma}{\mathrm{d}k_x}\,k_{e,y}^2+\gamma^2 k_{e,y}\frac{\mathrm{d}k_{e,y}}{\mathrm{d}k_x}\right)\gamma k_{e,y}\,\mathrm{cth}(d/\gamma)}{(\gamma^2 k_{e,y}^2-1)^2}\right] =\\
&= -\frac{2}{(\gamma^2 k_{e,y}^2-1)^2+\left(2\gamma k_{e,y}\,\mathrm{cth}(d/\gamma)\right)^2}\cdot\Big[\\
&-(\gamma^2 k_{e,y}^2+1)\,k_{e,y}\,\mathrm{cth}(d/\gamma)\,\frac{\mathrm{d}\gamma}{\mathrm{d}k_x}-\\
&-(\gamma^2 k_{e,y}^2+1)\,\gamma\,\mathrm{cth}(d/\gamma)\,\frac{\mathrm{d}k_{e,y}}{\mathrm{d}k_x}+\\
&+(\gamma^2 k_{e,y}^2-1)\,\gamma k_{e,y}\frac{\mathrm{d}\,\mathrm{cth}(d/\gamma)}{\mathrm{d}k_x}\Big]\ .
\end{aligned} \tag{160}$$

Inserting the differential quotients

$$\frac{\mathrm{d}\gamma}{\mathrm{d}k_x} \overset{(152d)}{=} -k_x\cdot[k_x^2-(\omega n_b/c)^2]^{-3/2} = -k_x\gamma^3 \tag{161a}$$

$$\frac{\mathrm{d}\,k_{e,y}}{\mathrm{d}\,k_x} \overset{(148b)}{=} -k_x[\omega^2 n_a^2 c^{-2} - k_x^2]^{-1/2} = -\frac{k_x}{k_{e,y}} \tag{161b}$$

$$\frac{\mathrm{d}\ \mathrm{cth}(d/\gamma)}{\mathrm{d}\,k_x} = \Big(\frac{d/\gamma}{\sinh(d/\gamma)}\Big)^2 \cdot \frac{(-1)}{d} \cdot (-k_x\gamma^3) \tag{161c}$$

into (160) gives

$$\begin{aligned} x_{r,\mathrm{peak}} &\overset{(151c)}{=} -\frac{\mathrm{d}\,\alpha}{\mathrm{d}\,k_x} \overset{(158)}{=} -\frac{\mathrm{d}\,\beta}{\mathrm{d}\,k_x} \overset{(151e)}{=} x_{t,\mathrm{peak}} = \\ &= +\frac{2}{(\gamma^2 k_{e,y}^2 - 1)^2 + \big(2\gamma k_{e,y}\,\mathrm{cth}(d/\gamma)\big)^2} \cdot \Big[\\ &\quad + (\gamma^2 k_{e,y}^2 + 1)\, k_x \gamma^3 k_{e,y}\,\mathrm{cth}(d/\gamma) + \\ &\quad + (\gamma^2 k_{e,y}^2 + 1)\,\gamma\,\frac{k_x}{k_{e,y}}\ \mathrm{cth}(d/\gamma) + \\ &\quad + (\gamma^2 k_{e,y}^2 - 1)\,\gamma k_{e,y}\,\frac{\gamma^3 k_x}{d} \cdot \Big(\frac{d/\gamma}{\sinh(d/\gamma)}\Big)^2 \Big] \\ &\overset{d\ll\gamma}{=} 0 \quad \text{due to } \mathrm{cth}^{-2} \\ &\overset{d\gg\gamma}{=} \frac{2(\gamma^2 k_{e,y}^2 + 1)(\gamma^3 k_{e,y} k_x + \gamma k_x k_{e,y}^{-1})}{(\gamma^2 k_{e,y}^2 - 1)^2 + \big(2\gamma k_{e,y}\big)^2} \end{aligned} \tag{162}$$

Remarkably this result is strictly independent of d, and finite, at $d \gg \gamma$. Thus there is a saturation effect.

At $\vartheta_a = \vartheta_{a,\mathrm{critical}}$ we have $d \ll \gamma$ for any finite d, because $\gamma =$ (152d) is diverging at $\vartheta_a = \vartheta_{a,\mathrm{critical}}$. The factor $\mathrm{cth}(d/\gamma)$ in the denominator can not compensate the high powers of γ in the numerator. A further divergence, which is of no interest for our present evaluation, is encountered at $\vartheta_a = \pi/2$ due to the factor $k_{e,y}$ in the denominator.

For a numeric analysis of (162) we choose $n_a = 1.5$ (glass), $n_b = 1$ (air), $\omega = 3 \cdot 10^{15}\,\mathrm{Hz}$ (red light with wavelength $= 633\,\mathrm{nm}$ in air). We assume that the light is perpendicular polarized. In this case

$k_{e,y\perp} \overset{(157)}{=} k_{e,y}$ due to $\mu_a = \mu_b$. The bottom diagram of fig. 20 on the following page is showing the dependency of $x_{r,\text{peak}} = x_{t,\text{peak}}$ from the angle ϑ_a at constant $d = 1\,\mu\text{m}$. The critical angle is $\vartheta_{a,\text{critical}} = 0.23228\,\pi$, and the smallest angle displayed in the diagram is $\vartheta_a = 0.23230\,\pi$. The largest angle displayed in the diagram is $\vartheta_a = 0.49656\,\pi$. Note the logarithmic scale of the y-axis.

The top diagram in fig. 20 is showing $x_{r,\text{peak}} = x_{t,\text{peak}}$ at constant $\vartheta_a = 0.23228\,\pi$ for some values of the distance d. Note the logarithmic scale of the x-axis. At $d \approx 10\,\mu\text{m}$ the saturation value of $x_{\text{peak}} \approx 9\,\mu\text{m}$ is reached.

Inserting the derivatives

$$\frac{\mathrm{d}\gamma}{\mathrm{d}\omega} \overset{(152d)}{=} [k_x^2 - (\omega n_b/c)^2]^{-3/2} \frac{\omega n_b^2}{c^2} = \frac{\gamma^3 \omega n_b^2}{c^2} \tag{163a}$$

$$\frac{\mathrm{d}\,k_{e,y}}{\mathrm{d}\omega} \overset{(148b)}{=} \frac{\omega n_a^2}{c^2 k_{e,y}} \tag{163b}$$

$$\frac{\mathrm{d}\ \mathrm{cth}(d/\gamma)}{\mathrm{d}\omega} = -\Big(\frac{d/\gamma}{\sinh(d/\gamma)}\Big)^2 \cdot \frac{\gamma^3 \omega n_b^2}{dc^2} \tag{163c}$$

instead of the derivatives with respect to k_x into (160), we find

$$\begin{aligned} t_{r,\text{peak}} &\overset{(151d)}{=} +\frac{\mathrm{d}\alpha}{\mathrm{d}\omega}\Big|_{\omega^{(0)}} \overset{(158)}{=} +\frac{\mathrm{d}\beta}{\mathrm{d}\omega}\Big|_{\omega^{(0)}} \overset{(151f)}{=} t_{t,\text{peak}} = \\ &= \frac{2}{(\gamma^2 k_{e,y}^2 - 1)^2 + \big(2\gamma k_{e,y}\,\mathrm{cth}(d/\gamma)\big)^2} \cdot \Big[\\ &\quad (\gamma^2 k_{e,y}^2 + 1)\, k_{e,y} \frac{\gamma^3 \omega n_b^2}{c^2}\,\mathrm{cth}(d/\gamma) + \\ &\quad + (\gamma^2 k_{e,y}^2 + 1)\,\gamma \frac{\omega n_a^2}{c^2 k_{e,y}}\,\mathrm{cth}(d/\gamma) + \\ &\quad + (\gamma^2 k_{e,y}^2 - 1)\,\gamma^4 k_{e,y} \frac{\omega n_b^2}{dc^2} \Big(\frac{d/\gamma}{\sinh(d/\gamma)}\Big)^2 \Big] \end{aligned} \tag{164}$$

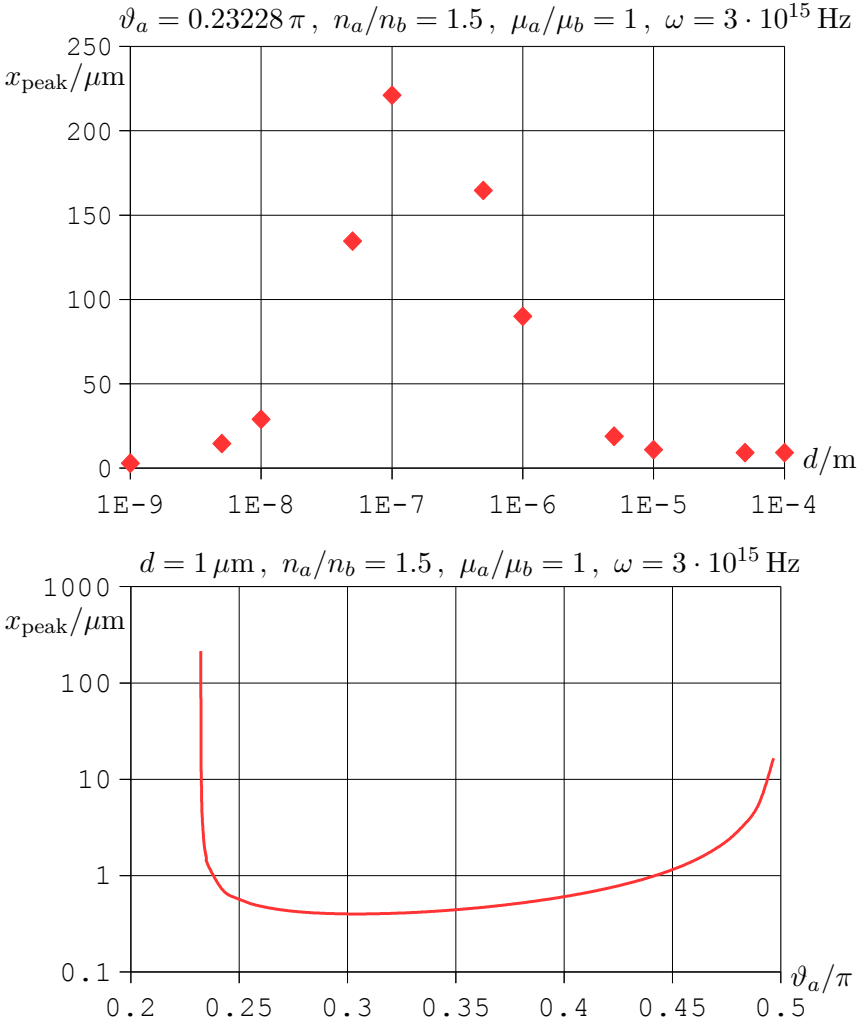

Fig. 20: The shift $x_{r,\rm peak} = x_{t,\rm peak}$

$$\overset{d\ll\gamma}{=} 0 \quad \text{due to } \operatorname{cth}^{-2}$$

This result has the same form as the formula for $x_{r,\text{peak}} = x_{t,\text{peak}}$. Again there is the divergence of γ at the critical angle $\vartheta_{a,\text{critical}}$, and again there is a saturation effect at $d \gg \gamma$.

The result (164) is displayed in fig. 21 on the next page for the parameters $n_a = 1.5$ (glass), $n_b = 1$ (air), $\omega = 3 \cdot 10^{15}\,\text{Hz}$ (red light with wavelength = 633 nm in air) and perpendicular polarization. The bottom diagram is displaying the dependency of $t_{r,\text{peak}} = t_{t,\text{peak}}$ on the angle ϑ_a at constant $d = 1\,\mu\text{m}$. The critical angle is $\vartheta_{a,\text{critical}} = 0.23228\,\pi$, the smallest angle displayed in the diagram is $\vartheta_a = 0.23230\,\pi$. The largest angle displayed in the diagram is $\vartheta_a = 0.49656\,\pi$. Note the logarithmic scale of the y-axis.

The top diagram of fig. 21 is showing $t_{r,\text{peak}} = t_{t,\text{peak}}$ at constant $\vartheta_a = 0.23228\,\pi$ for some values of the distance d. Note the logarithmic scale of the x-axis. At $d \approx 15\,\mu\text{m}$ the saturation value of $t_{\text{peak}} \approx 30 \cdot 10^{-15}\text{s}$ is reached. This is the strangest result of our whole evaluation. Messages could be forwarded due to certain sequences of light pulses. For each pulse emitted at $y = 0$, the receiver could detect a pulse at $y = d$ about 30 fs later, no matter how large d may be! Of course the received light-pulses would be only tiny (i. e. exponentially damped) as compared to the sent pulses. But the sender could apply extremely huge signal levels. There is a not yet settled dispute, whether really messages could be transmitted by means of evanescent pulses at a speed exceeding the speed of light in vacuum. A worth reading review on this issue can be found in [11].

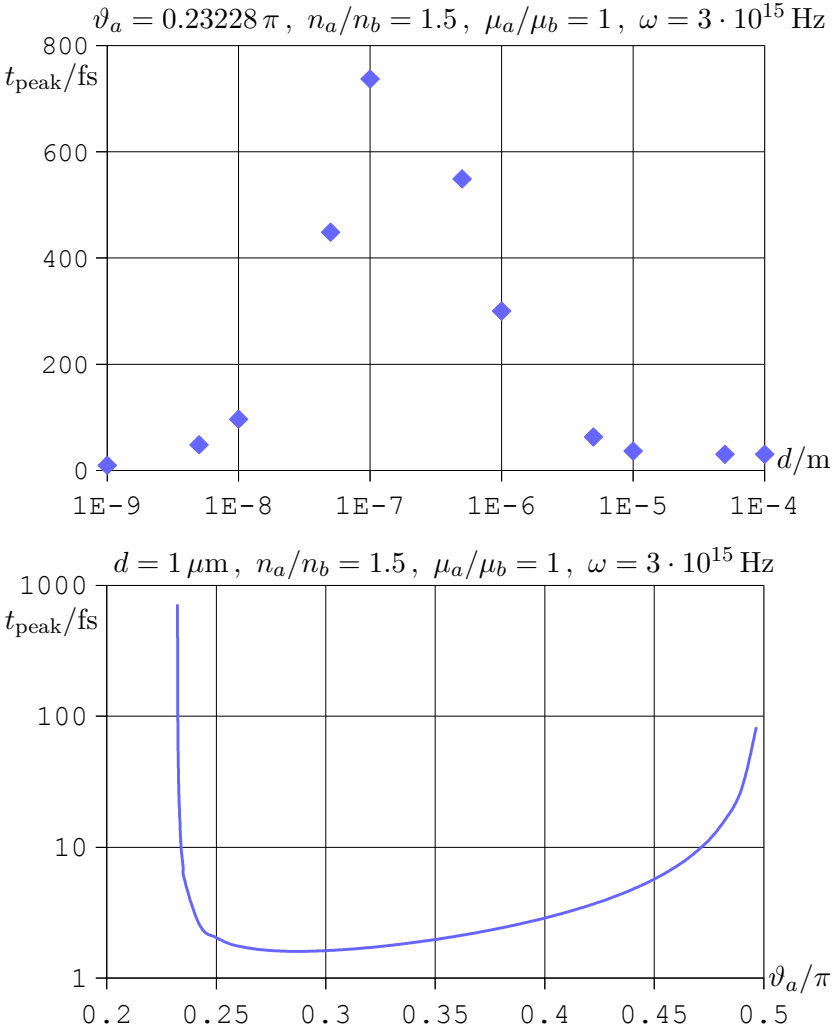

Fig. 21 : The delay $t_{r,\mathrm{peak}} = t_{t,\mathrm{peak}}$

References

[1] M. Born, E. Wolf: *Principles of Optics* (Pergamon Press, Oxford, 2nd ed. 1964)

[2] John David Jackson: *Classical Electrodynamics* (John Wiley, New York, USA, 3rd ed. 2001)

[3] Isaac Newton: *Opticks* (W. Innys, 4th ed., London, 1730) https://archive.org/details/opticksortreatis1730newt

[4] A. J. Meixner, M. A. Bopp, G. Tarrach: *Direct measurement of standing evanescent waves with a photon-scanning tunneling microscope*, App. Opt. **33**, 7995-8000 (1994)

[5] F. Goos, H. Hänchen: *Ein neuer und fundamentaler Versuch zur Totalreflektion*, Ann. Phys. (Leipzig) VI **1**, 333-346 (1947)

[6] F. Goos, H. Lindberg-Hänchen: *Neumessung des Strahlversetzungseffektes bei Totalreflektion*, Ann. Phys. (Leipzig) VI **5**, 251-252 (1949)

[7] K. Artmann: *Berechnung der Seitenversetzung des totalreflektierten Strahles*, Ann. Phys. (Leipzig) VI **2**, 87-102 (1948)

[8] Paul R. Berman: *Goos-Hänchen effect*, Scholarpedia **7**, 11584 (2012) doi:10.4249/scholarpedia.11584

[9] A. K. Ghatak, M. R. Shenoy, I. C. Goyal, K. Thyagarajan: *Beam Propagation under frustrated total Reflection*, Opt. Com. **56**, 313-317 (1986)

[10] A. Ghatak, S. Banerjee : *Temporal delay of a pulse undergoing frustrated total internal reflection*
Appl. Opt. **28**, 1960-1961 (1989)

[11] H. G. Winful : *Tunneling time, the Hartman effect, and superluminality: A proposed resolution of an old paradox*,
Phys. Rep. **436**, 1-69 (2006)